RHODES UNIVERSITY
*Where leaders learn*

# The role of northwest striking structures in controlling high-grade ore shoots at the Syama Gold Mine, Mali, West Africa

By

**Ali Soro**

Dissertation submitted in partial fulfilment of the requirements for the degree of

**Master of Science**

**(Exploration Geology)**

Exploration Geology MSc Program
Department of geology
Rhodes University
Grahamstown, South Africa

October 2019

## Declaration

I, Ali Soro, hereby declare that, except for references to other people's work, which has been referenced, this dissertation consists of my own original work and has not been previously, entirely or partially submitted for any degree in any other University or Institution.

Signature: 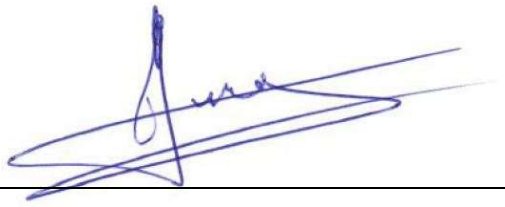

Ali Soro

Date: 22 October 2019

# Abstract

This study intended to investigate the relationship between the NW striking structures and the high-grade ore shoots at the Syama gold mine in Mali, West Africa.

All structural data collected since 1987 from drill core have been integrated to allow the interpretation and modelling of these NW-SE structures. The structures collected were grouped into three main groups; foliations/shears/faults, veins and joints/contacts/fractures. Micromine software was used to plot the structures, printed out on A3 paper and interpreted manually using tracing paper.

Analysis and interpretation of stereographic plots has shown that the majority of the high-grade zones are generally located at the intersection of the NNE structures and the NW structures. The observed cross-cutting relationship between the NNE and the NW structures suggests two different generation of faults. It is suggested that the NW structures were active during the D4 deformation event (Standing, 2007) and have played a role in reactivating earlier (D3) NNE structures, allowing greater fluid flow and enhancing the gold grade. These zones are mainly defined by brecciation and stockwork veining. The E-W structures are believed to be the latest and are attributed to the D5 event.

Although gold mineralisation is grossly controlled by the NNE structures, the NW structures need to be considered as major gold enrichment upgrading factors at Syama. It is therefore strongly recommended that ongoing exploration at Syama specifically target the intersection of the NW and NNE structures as favourable zones for high-grade mineralisation.

# Acknowledgement

I would like to take this opportunity to express my gratitude to anyone who has contributed to help me complete this Master's program at Rhodes University.

First my employer, Resolute Mining Limited, through its General Manager – Exploration, Bruce Mowat for granting me the opportunity to attend this course. Patrick Manouge, Exploration Manager Resolute Mali, Syama Gold Mine, who has identified this project and has been my internal supervisor by reviewing all my work. Roger Speers, Exploration Manager Resolute Cote d'Ivoire, by accepting the reschedule of my break and leaves time to match up with the Master's program schedule over the two years. My colleagues from Resolute Cote d'Ivoire and Resolute Mali (Syama Gold Mine), for their support during my study time.

Second, Rhodes University through Professor Jock Harmer, director of the Exploration Geology Master's Program, who has reviewed and commented on my work as my co-supervisor. I would like to show my gratitude and my appreciation to Dr Lynnette Greyling, University of Cape Town, who has been my day to day supervisor and assisted me, step by step during this work. I will never thank you enough Lynnette. Thanks to all the geology department staff of Rhodes University for your lectures delivered and assistance. Special thanks to the program's Office Administrator, Ms Ashley Goddard, for your assistance from my application time through my study period with all administrative issues. You have been greatly helpful.

Finally, my lovely family. Thank you for your prayers, your support and your sacrifice during these two years of study.

# Table of contents

# List of figures

# Chapter 1. Introduction

## 1.1 Locality

The Syama gold mine is located in West Africa, 280km southeast of Bamako, the capital of Mali, and 30km from Côte d'Ivoire's border (**Figure 1**). Sikasso, the second largest city in Mali is located 85km to the northeast of Syama. Kadiolo, the capital of the regional circle is 35km to the south of Syama. Fourou, the nearest town to the mine site, is located 15km to the south. Syama village, from which Syama Gold Mine was named, is located 2km to the south of the mine. Access to the mine site is by the Bamako-Sikasso-Zégoua main road to Côte d'Ivoire and then by gravel road to Fourou via Kadiolo. During the dry season, an alternative short road is used through Farakala and Bananso, from the Bamako-Sikasso road.

Climatically, the project area is described as subtropical with two main seasons: a hot dry season from October to June and a warm rainy season from July to September. The annual rainfall is about 1200mm and the temperatures range from 21°C to 42°C with an average temperature of approximately 27°C. The vegetation falls within the Sahelian transition zone (Sudanian), which is savannah and cleared forests. The mains crops of the area are, cotton, maize, millet and sorghum.

Syama lies within the catchment of two major rivers; the Bagoe and Banifing. The Bagoe is a north-flowing river to the west of the project, part of which forms the border with Côte d'Ivoire, while the Banifing is a west-flowing river which passes through the village of Bananso approximately 11km northeast of the Syama mine site. The regional topography is tabular with lateritic plateau spread out between the tributaries of the Bagoe River.

The area is dominated by lateritic plateau, with elevations varying between 328m and 482m above sea level. Isolated hills form a series of high points along a north-east to south-west trend. On the higher ground, the soil is composed of laterite with occasional crevassing of detrital sands. On the lower ground, the soil is predominantly sandy clay.

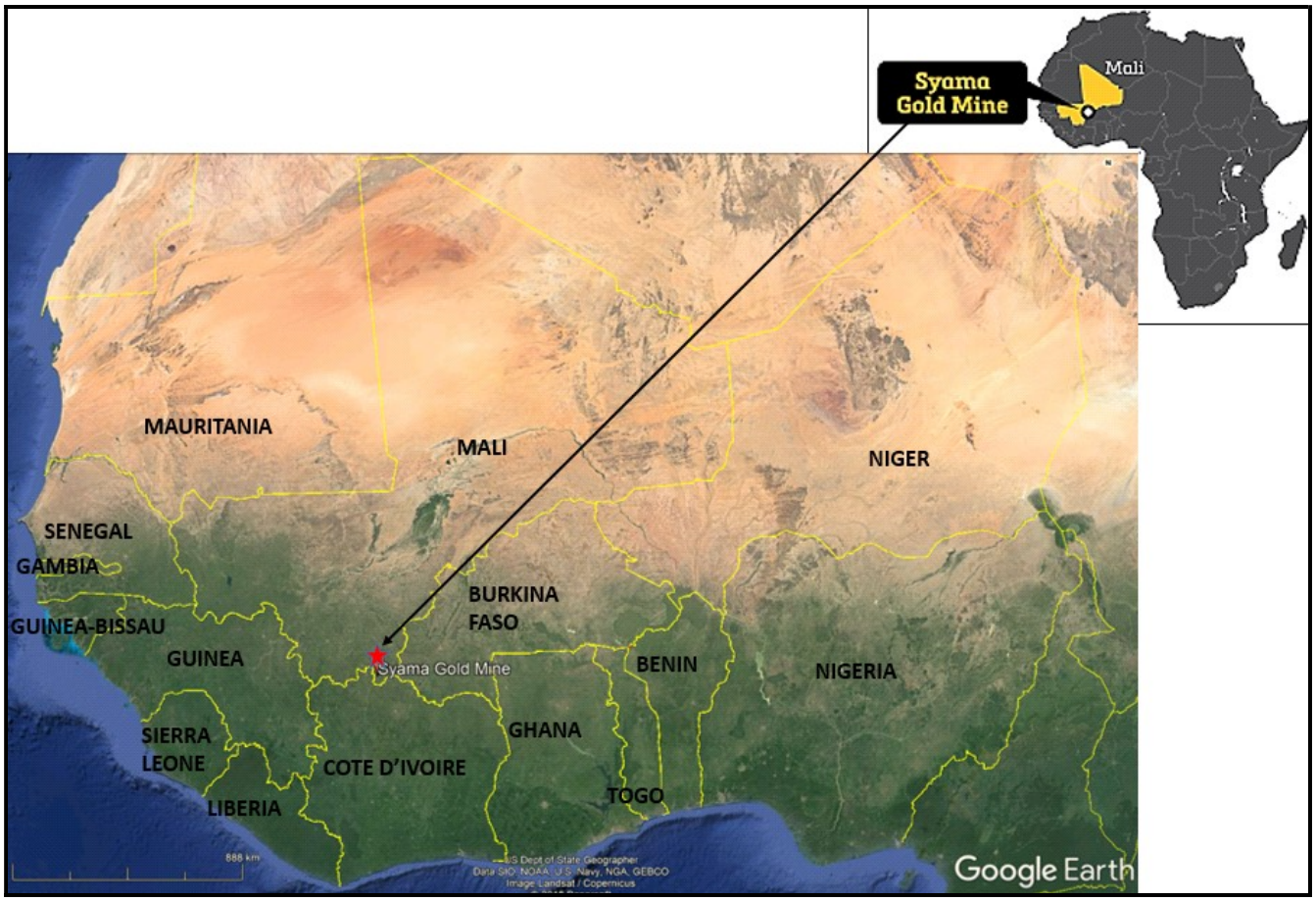


Figure 1. **Location of Syama Gold Mine (after Google Earth, 2018)**

## 1.2 Exploration and Mining History

The Syama gold deposit was first identified in 1984 by a regional geochemical survey undertaken by la Direction Nationale de Géologie et des Mines (DNGM) of Mali with assistance from the United Nations Development Program (UNDP).

BHP Minerals acquired the Syama gold project in 1987 and commenced open pit mining operations in January 1990, after the completion of mining feasibility studies.

In August 1996, Randgold Resources agreed to acquire the asset from BHP Minerals and resumed operations in October of that year. However, metallurgical issues, coupled with difficulties in grinding the ore and an unreliable power supply led Randgold Resources to suspend mining and milling operations at Syama and place the mine on care and maintenance in early 2001.

In June 2004, Resolute Mining Limited acquired the project from Randgold. After a positive pre-feasibility study, with reserves estimated at 1.6Moz @ 3.93g/t Au and resources estimated

at 3.0Moz @ 2.47g/t Au, Resolute resumed operations at Syama with a planned 7 years open pit operation and potential underground extension.

Resolute recommenced open pit mining in 2007, eventually utilising parallel sulphide and oxide processing plants. In June 2015, Resolute completed the open pit mining operation at Syama main pit and commenced mining the satellite deposits. The satellites pits are providing ore to the oxide plant while the sulphide plant is processing stockpiles and sulphide ore from the Syama underground development. To optimize the production by using the two plants and extend the Mine life, Resolute has undertaken some deep drilling beneath Syama main pit in 2015. The aim of this drilling is to expand and convert the underground resources into reserves and provide long term ore for the sulphide plant.

In the updated definitive feasibility study for Syama, underground reserves (Resolute, 2018) are estimated at 3.0Moz at 2.7g/t Au, equivalent to 14 years of mine life at a production rate of ~200,000oz Au per annum.

Syama underground operations are now operational and represent the first fully mechanised automated underground operations in the world. The automation is expected to increase production and performance by reducing the number of machines and personnel to be used, which will in turn lead to capital and maintenance savings and better safety control. The underground mine is expected to achieve full production rates at the low All-In Sustaining Cost (AISC) of US$746/oz.

The Syama gold mine, orebody is a shear zone hosted deposit type, grossly controlled by a NNE striking structural system, steeply dipping to WNW and moderately plunging at 30°-40° to the north. Deep drilling beneath the Syama open pit has intersected significant high-grade ore shoots which are believed to coincide with NW-SE striking cross faults. The southern extension of the Syama underground orebody remains relatively untested and could yield additional resources (**Figure 2**). Evidence of the NW-SE structures being associated with high-grade ore shoots could be critical in driving a more efficient exploration strategy for targeting of the high-grade ore shoots to expand mineral resources and ore reserves.

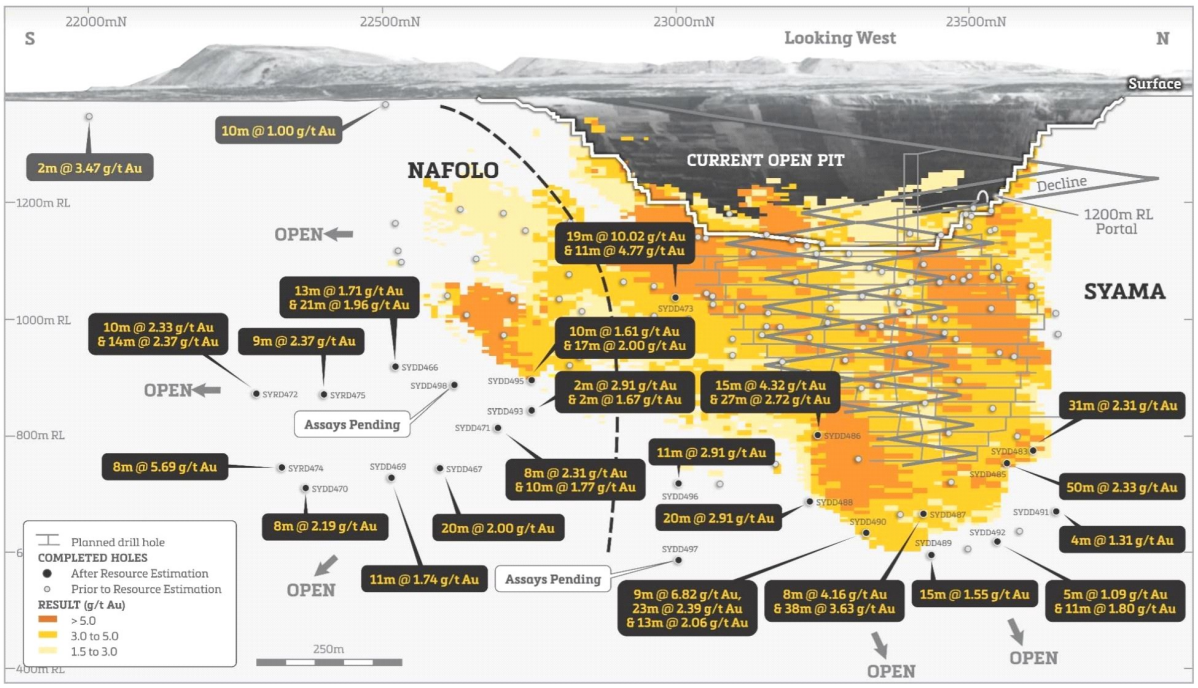


Figure 2. **Syama extension potential, looking West (Courtesy of Resolute, 2018).**

## 1.3 Aims of study

This project has been designed to identify and define the relationship between the NW structures and the high-grade ore shoots. It is hoped that these findings will aid in more effective drill targeting of the high-grade shoots and potentially lead to significantly increased ore reserves.

Some limitations that may have affected this study were met, including:

- The structures were collected by various geologists and companies, which may has affected the consistency of the data collected.
- Little of the core could be considered reliably oriented and as such only alpha measurements were collected. This limitation has reduced the number of structures data available for this study.
- The mineralised zones at Syama are often highly broken (strongly sheared zones), so orientations are often poor, making it difficult to collect reliable structural measurements.

- The Syama open pit walls are disrupted by the current underground mining work, making it impossible to collect pit wall structural measurements that could help to confirm some structures seen in the drill cores,
- The underground mining has not advanced enough to allow for underground wall and backs mapping, which could help to crosscheck some structures from the drill cores.

## 1.4 Methodology

Structural data collected by BHP (1987-1996), Randgold (1996-2001) and Resolute (2003-2017) over the Syama deposit have been used in this study. The structural data collected included bedding, foliation, shears, faults, veins, lithologic contacts, joints and fractures. To conduct this study, the structures have been selected and grouped into three, across three levels of the mine grid elevation from 1200mRL to 1000mRL of the orebody spaced of 100mRL intervals. The selection was based on the density and availability of structures and grade data. The main reason for selecting these structure types, and the 100mRL level intervals, is to cover a representative range of structure types across the orebody which ranges over 600m depth from 1300mRL to 600mRL. The three levels selected are likely to be the most representative of the structure across the ore body. Note that the Syama local grid used is 15 degrees (15º) rotated to the east and the RL used is the mine pit one. Each group of structures at each level will help for structural understanding. This selection will allow determination of each structure type's behaviours at each level and will help to establish the relationship between structures and gold high-grade envelop. The structures used are:

- **Foliation, Shear and Fault structures**
- **Veins measurement structures**
- **Joints, contacts and fractures structures**

The relationship between the interpreted structures and the high-grade ore zone was done by superimposing the interpreted structures on the identified high-grade ore zone. When necessary the interpreted structures have been extrapolated to cover the high-grade ore zone as at Syama the ore zones are often dominated by completely broken rocks and no structural data can be collected in these zones. The logging of structures has been done using standard Resolute

coding and this coding and the associated legend used in Micromine on the plots for this study are shown in **(Appendix I)**.

Because the mineralisation is believed to be linked mainly to shears with higher grade intersections associated with increased carbonate and quartz-carbonate veining, the two main potentially mineralised structural groups of foliations, shears and faults and veins were used for this study. The joints, contacts and fractures were found to be too erratic as they do not follow any preferential trends, so they were not used in this study.

The structural measurements were done using, rocket, kenometer and protractor wrap instruments. To allow better structural interpretation, all data collected were converted into Dip and Dip-Direction as they were collected in three different ways, Dip and Strike (Azimuth), Alpha and Beta, or Dip and Dip-Direction. The structures were plotted using Micromine software and printed out on A3 paper. Flitch sections in plan view at different levels of the orebody are shown in this study and relevant structures have been identified and interpreted against the high-grade ore shoot zones.

Structural measurement checking was done during this study, using a wooden "rocket launcher" logging device on half core. Ten (10) holes were used to identify the NW structures on the cores. The NW trending foliations, shears and veins are seen on the rocket launcher in **Figures 3, 4** and **5** respectively.

Figure 3. **Photo of NW trending Foliation on half cores.**

Figure 4. **Photo of NW trending Shears on half cores.**

Figure 5. **Photo of NW trending Veins on half cores.**

# Chapter 2. Geological Setting

## 2.1 Tectonic Setting

The West African Craton, is made up of two main parts, known as the Man-Leo Rise to the south and the Requibat Rise to the north, separated by the Taoudeni Basin (**Figure 6**). The Man-Leo Rise consist of two domains, the Kenema-Man Archean domain (3.5Ga) to the west and the Paleoproterozoic Baoule-Mossi domain of Birimian age (2.3-2.00Ga) to the east (Feybesse et al., 2006).The Syama Gold Mine is located in the central part of the Paleoproterozoic Baoule-Mossi domain , the world's largest Paleoproterozoic gold province (Goldfarb et al., 2017). The deposit is an orogenic gold deposit type occurring along or proximal to shear zones in metamorphosed volcanic and sedimentary units of the Birimian Supergroup sequences (Feybesse et al., 2006).

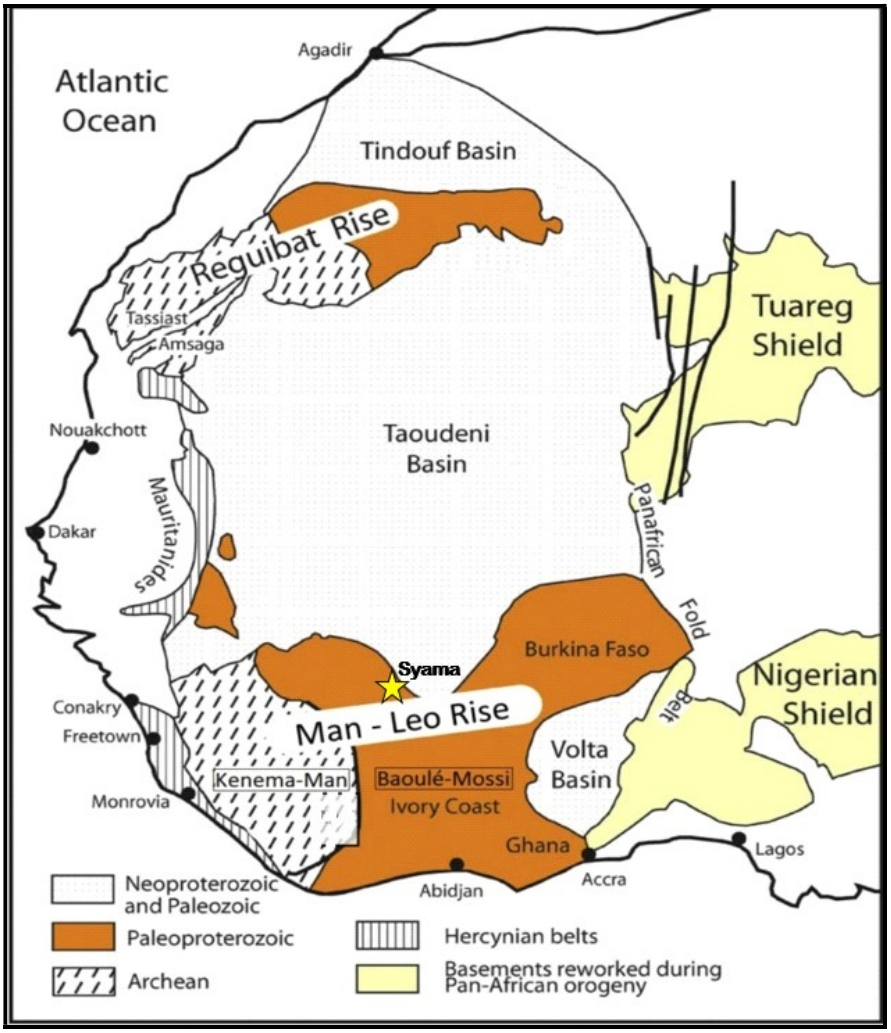


Figure 6. **Geological map of West African Craton (after Peucat et al., 2005).**

The Kenema-Man Archean domain is composed of gneiss, migmatite, granitoids and schists. The Paleoproterozoic Baoule-Mossi domain, referred to as the Birimian Supergroup, is composed of elongated belts of sediments, mafic igneous and volcanic units intruded by granitic plutons (Andre et al., 2006).

During the Eburnean Orogeny the Birimian greenstones belts were first affected by regional penetrative foliation (D1) of NE-SW to N-S which was followed by the formation of high strain shear zones (D2), of NW-SE along the basin and belt contacts, (Feybesse et al., 2006; Allibone et al., 2002). The isoclinal folds due to compression are regionally well developed and resulted in formation of the NE-SW trending greenstone belts bounded by granite-gneiss terrains.

The Birimian greenstone belts extend over ten countries in West Africa including Mali, Cote d'Ivoire, Niger, Burkina Faso, Benin, Togo, Ghana, Guinea, Liberia and Senegal, and contain the bulk of West African Gold deposits (**Figure 7**). The gold resources are concentrated within the 2250Ma to 2000Ma greenstone belts of the Leo-Man Rise. Most of the major deposits are classified as orogenic gold style (Goldfarb et al., 2017), although there are paleoplacer, porphyry (Gaoua: Le Mignot et al., 2017) and skarn (Tongon: Lawrence et al., 2017; Ity: Beziat et al., 2016) deposits within some of the greenstone belts, and perhaps local intrusion related gold systems (Gara, Yalea: Lawrence et al. (2013a, 2013b, 2016), and Massawa: Treloar et al. (2015)).

Gold is dominantly hosted in the greenstone belt rocks, mainly of greenschist metamorphic facies dominantly in tholeiitic volcanic rocks and sediments, in strongly sheared, ductile to brittle-ductile environments. The main styles of mineralisation are breccia, quartz or quartz-carbonate veins, hydrothermally altered in all types of lithology. The gold bearing zones are mainly occurring along NNE trending, narrow, linear greenstone belts in shear zones and focussed principally on second or third order structures developed in proximity to the dominant first order structures (Goldfarb et al., 2017).

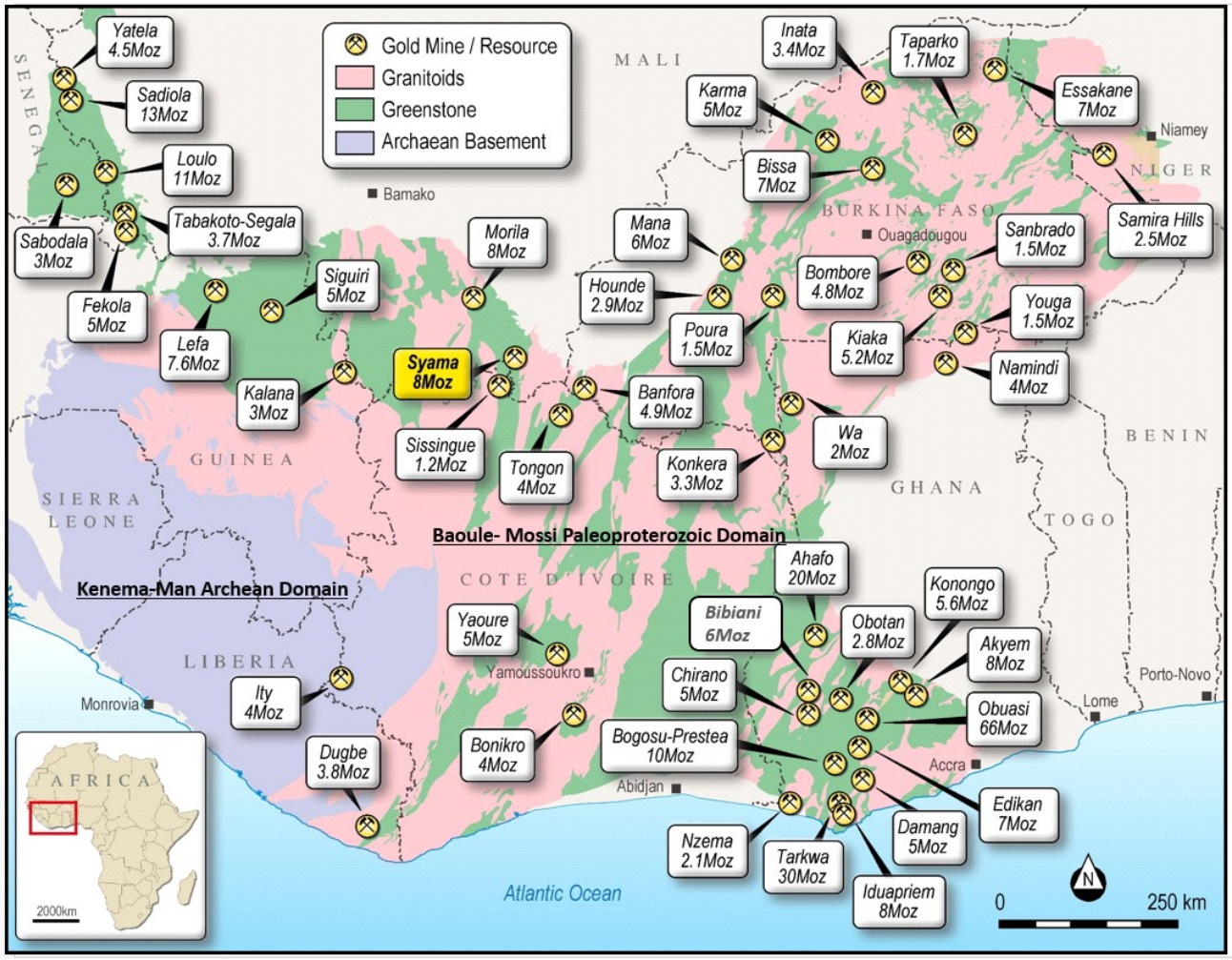


Figure 7. **Simplified geological map of West African craton showing settings of main gold deposits (after Le Mignot et al., 2017).**

## 2.2 Regional Geology

The northern margin of the Paleoproterozoic Baoule-Mossi domain covers southern Mali, with four greenstone belts identified (Kusnir, 1999). The most eastern Bagoe belt, most recently referred to as the Syama-Boundiali belt or simply Syama greenstone belt, contains the Syama gold mine and the Tabakoroni gold mine (0.3Moz at 2.9g/t Au of reserves and 0.8Moz at 2.3g/t Au of resources), (Resolute Mining Limited, 2018), in Mali, both operated by Resolute Mining (**Figure 8**). In addition to the deposits in Mali, the belt hosts the Sissingue gold Mine (0.4Moz at 2.1g/t Au of reserves and 0.5Moz at 1.8g/t Au of resources), (Perseus Mining Limited, 2018), situated in northern Cote d'Ivoire and operated by Perseus Mining Limited.

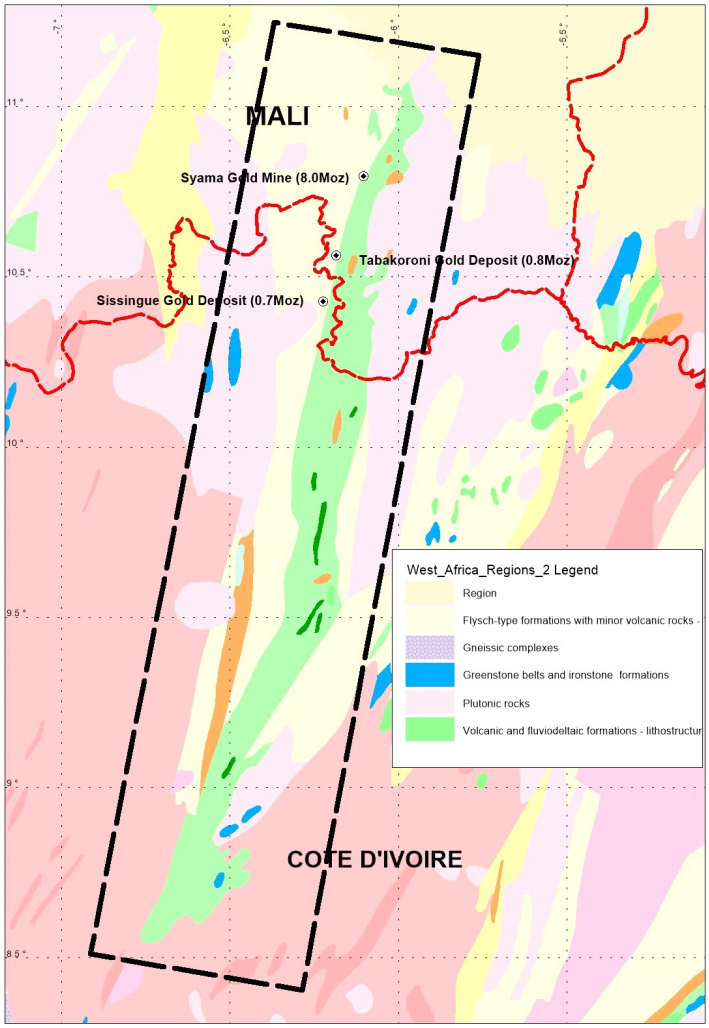


Figure 8. **Syama greenstone belt (adapted from West African eXploration Initiative Team, 2016).**

The Syama gold deposit (>8Moz), is located on the Syama greenstone belt at the boundary of the Kadiana-Madinani terrane to the west and the Kadiolo terrane to the east (Bentley et al., 2000; Standing, 2005). The Kadiana-Madinani terrane is dominated by sediments of the Sikoro Formation and a narrow belt of interbedded basalts and sediments; called the Syama Formation. The Kadiolo terrane comprises polymictic conglomerate and sandstone of N'Golopene formation that were sourced from the Kadiana-Madinani terrane (**Figure 9**).

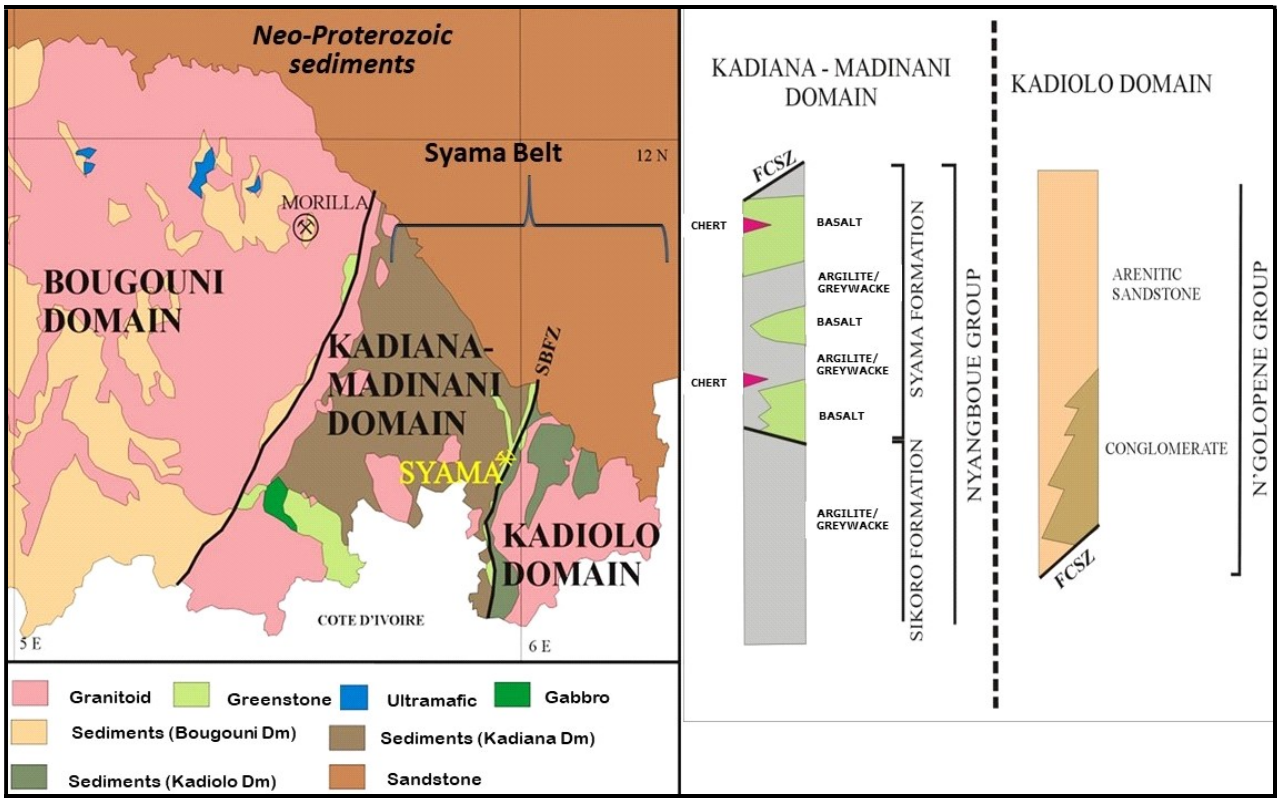


Figure 9. **Regional geology of southern Mali (after Bentley et al., 2000).**

The Syama deposit is hosted in the NNE striking, west dipping, Syama formation, which is part of the Kadiana-Madinani terrane (**Figure 10**). The Syama formation consists of a hangingwall sequence of strongly, deformed and altered basalts, with interbedded greywacke and argillite. The sequence is intruded by a swarm of lamprophyre dykes. The general geological sequence dips moderately to the west and is interpreted to be overturned to the east in the vicinity of Syama. The structural footwall of the Syama deposit is interpreted as the Kadiana-Madinani/Kadiolo terrane boundary and consists of a less deformed/altered conglomerate containing clasts of hangingwall lithologies. The conglomerate is therefore younger than the hangingwall mine sequence at Syama. Conglomerates in the footwall of the ore body are considered to be part of the Kadiolo terrane.

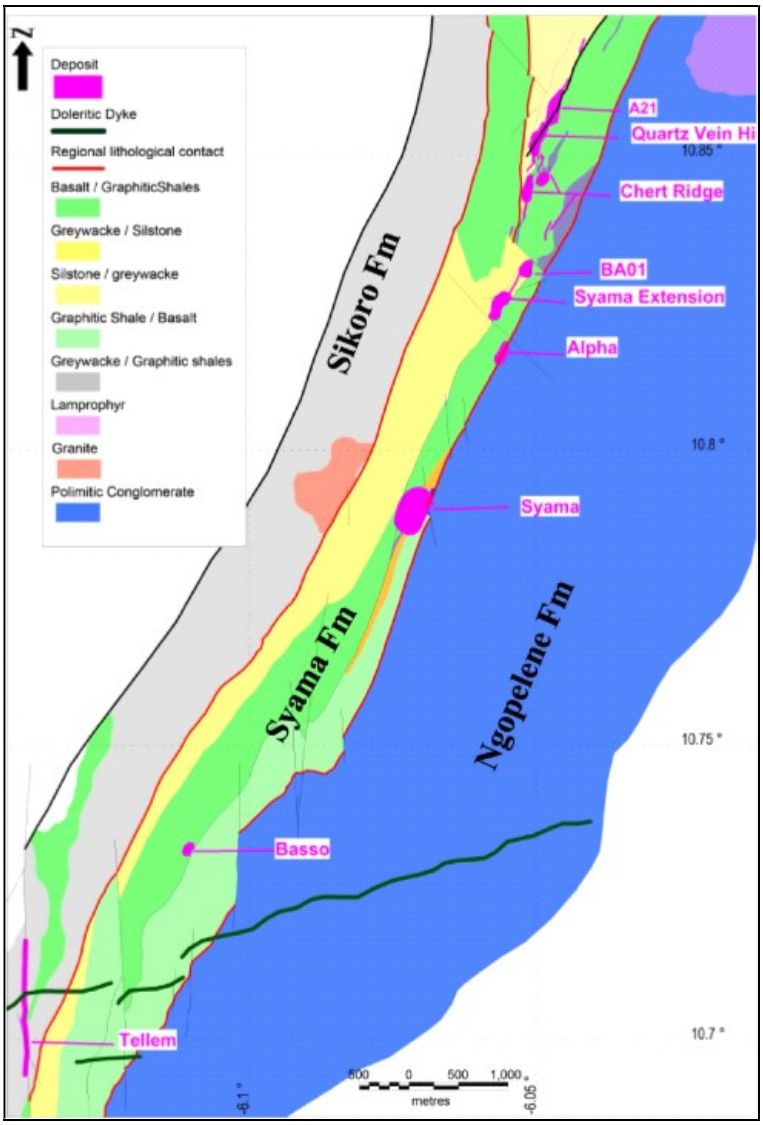


Figure 10. **Geology of the Syama area (after Standing, 2005).**

The structural setting of the Syama deposit is NNE trending and is cross-cut by a series of E-W and NW structures. The deposit is marked by a complex zone of faulting, thrusting and shearing located at the boundary of the Kadiana-Madinani Domain in the west and the Kadiolo Domain to the east, called Syama-Bananso Shear Zone (SBSZ). The Syama-Bananso Shear Zone is the principal structure in the Syama pit (**Figure 11**) and can be observed for over 200m in the Syama open pit. The diversity of shear senses in the Syama-Bananso Fault Zone (SBFZ), attests to the long and repeated movement along this structure (Standing, 2005).

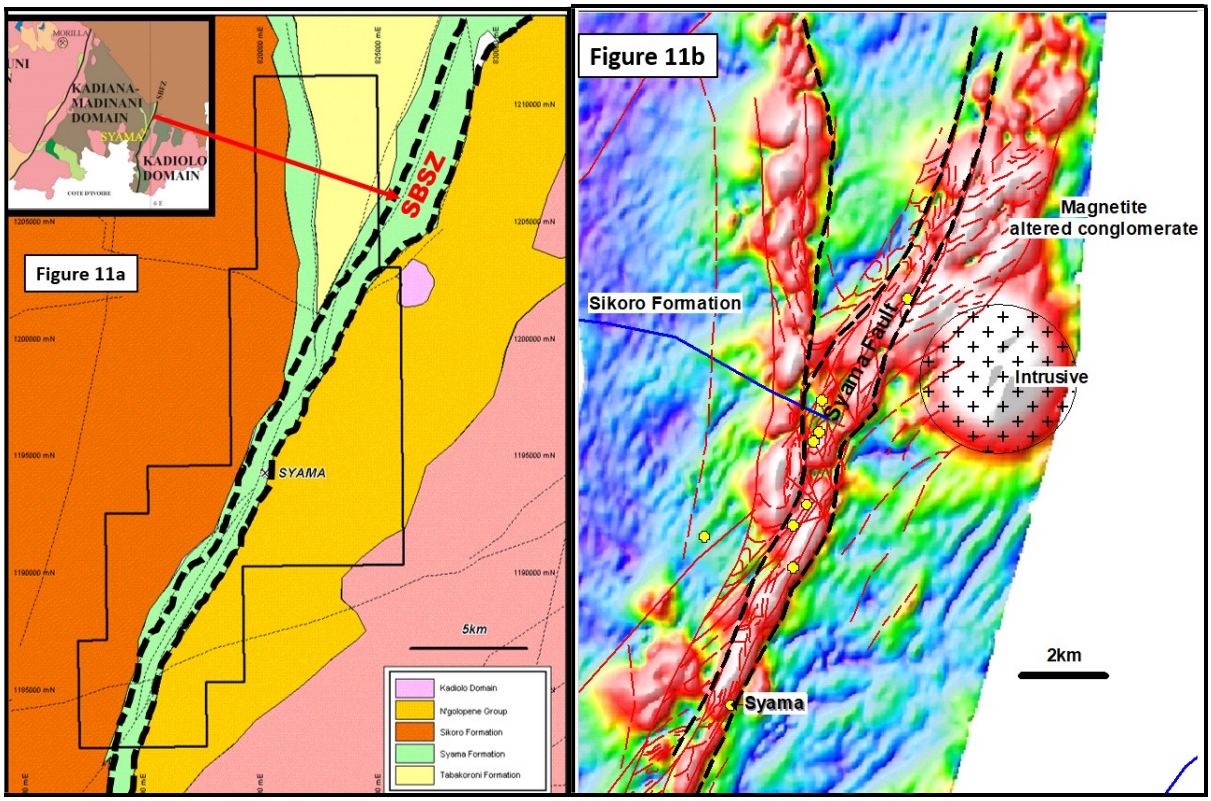


Figure 11. **Syama-Bananso Fault Zone. (a). shown on Geology map. (b). shown on aeromagnetic image (Courtesy of Resolute, 2017).**

The mineralisation at Syama is inferred to have occurred during the middle to late stage of the Eburnean orogeny. The hydrothermal activity at Syama has been dated at 2100 ± 40Ma (Hanssen et al., 1997). Syama mineralisation is hosted within mafic volcanics and volcaniclastic sediments. The volcanic rocks were originally deposited in a narrow rift or graben in an intra-arc setting (Olsen et al., 1992). Gold mineralisation overlapped with compressional deformation and intrusive activity, which may have played an important role as a heat source and increasing hydrothermal fluid flow. The deposit style is of Low-T, high level brittle breccia associated with disseminated sulphide (Olsen et al., 1992).

## 2.3 Previous work

A number of structural studies have been undertaken or committed on the Syama gold deposit by the three mining companies that have conducted mining operations at Syama. The various studies highlight the structural complexities of the Syama deposit.

Olson et al., (1992), during their time with BHP, undertook a study on the regional setting, structures and descriptive geology of Syama gold deposit. They interpreted the NNE and NW structures as a conjugate set of faults.

McCuaig (2004), commissioned by Resolute Mining to review the Syama gold deposit's structures, suspected that the zones of massive silica pyrite locally follow the NNW striking faults and control significant high-grade shoots away from the main ore body into the footwall. He suggested that there is the potential for more ore in the footwall of the main ore zone behind the east wall of the pit along NNW trending structures. He also reported the isoclinal folding to have been overprinted by moderate NW and SW dipping oblique dextral and sinistral thrusts that cross-cut and reactivate earlier compressional fabrics.

McCuaig (2005), emphasised the fact that the NNW trending lodes seemed to be favoured for high-grade gold mineralisation and they should be tested to confirm that.

Standing et al., (2007), reported that the ore shoots are controlled by the influence of isoclinal folding on a preferential lithology, late faulting and possible duplexing within the orebody by vertical link faults.

# Chapter 3. Local Geology

## 3.1 Host Rocks

The Syama deposit is hosted entirely by Syama Formation rocks associated with the regionally extensive Syama-Bananso Shear Zone (SBSZ), which forms the contact between the Syama Formation and N'Golopene Group rocks. Olsen et al., 1992, divided the lithological sequence at Syama into Hangingwall and Footwall domains, represented by the Syama Formation and N'Golopene Group respectively, (**Figure 12**).

- ***Hangingwall (Syama Formation):*** consists predominantly of basalt interbedded with sedimentary units comprising carbonaceous shale, siltstone, sandstone, greywacke, argillite and chert. These rocks are intruded by dolerite, lamprophyre, andesite, feldspar porphyry, quartz-feldspar porphyry, diorite and granodiorite dykes.

- ***Footwall (N'Golopene Group):*** dominated by polymict conglomerates, containing clasts of all Hangingwall rock types, including basalt, sediments and intrusive. Mineralisation in the Footwall appears restricted to occasional mineralised clasts within the conglomerate and rare late structures immediately adjacent to the SBSZ. The presence of mineralised Syama Formation clasts within the conglomerate suggests deposition post-dated the mineralising events.

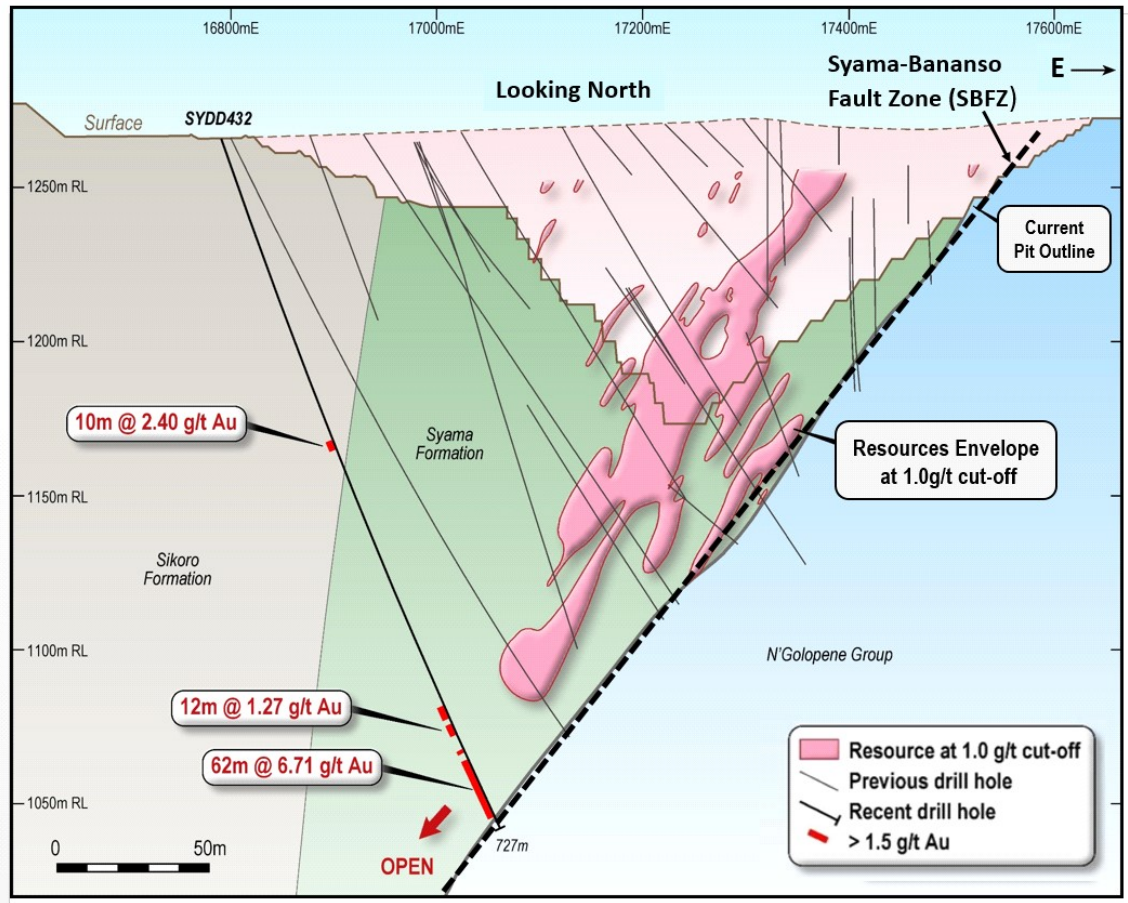


Figure 12. **Syama geology and mineralisation, striking NNE and dip to WNW (Courtesy of Resolute, 2017).**

The different rocks encountered at Syama are as follow:

- ***Basalt*** - Basaltic units are typically tholeiitic in composition and metamorphosed to greenschist facies. Where mineralised, the basalt is bleached, carbonated, veined, brecciated and silicified. Gold mineralisation is associated with more intensely altered basalt and in particular where it is brecciated with disseminated pyrite (Olson et al., 1992; Beeson et al., 2007). Where not mineralised, they are massive, chlorite-rich basalts (**Figure 13**).

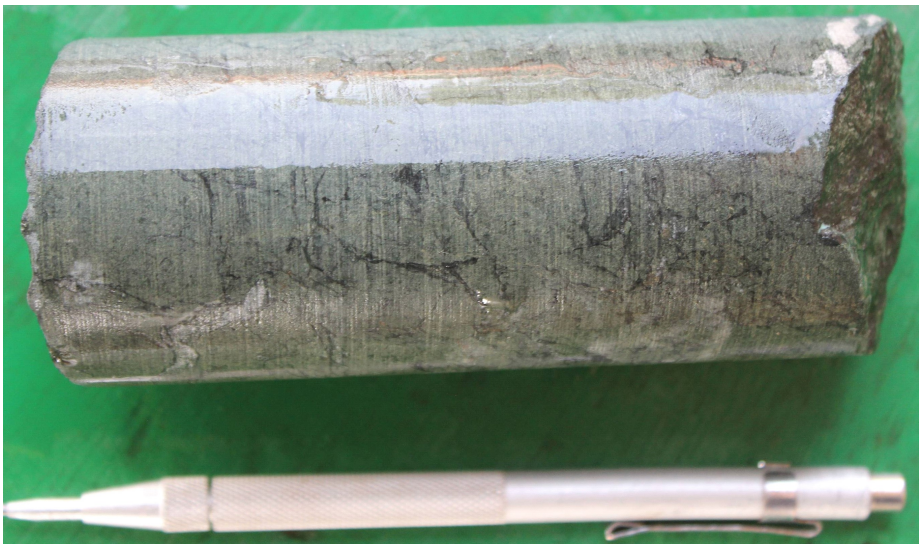

Figure 13. **Basalt unit with chlorite-calcite alteration. Photo taken from Syama core library.**

- ***Greywacke – Argillite – Carbonaceous Shale sediments*** - The sediment units are typically fine to coarse grained and comprise quartz, feldspar and chlorite with volcanic lithic fragments (**Figure 14**). Sediments comprise thin-bedded to laminated, fine-grained greywacke, graphitic shale and siliceous argillite. Massive thick-bedded medium to coarse grained greywacke units are shaly to silty in composition and commonly contain graphitic layers. Some graphitic argillaceous horizons contain up to 5% disseminated cubic diagenetic or metamorphic pyrite (Olson et al., 1992; Beeson et al., 2007)

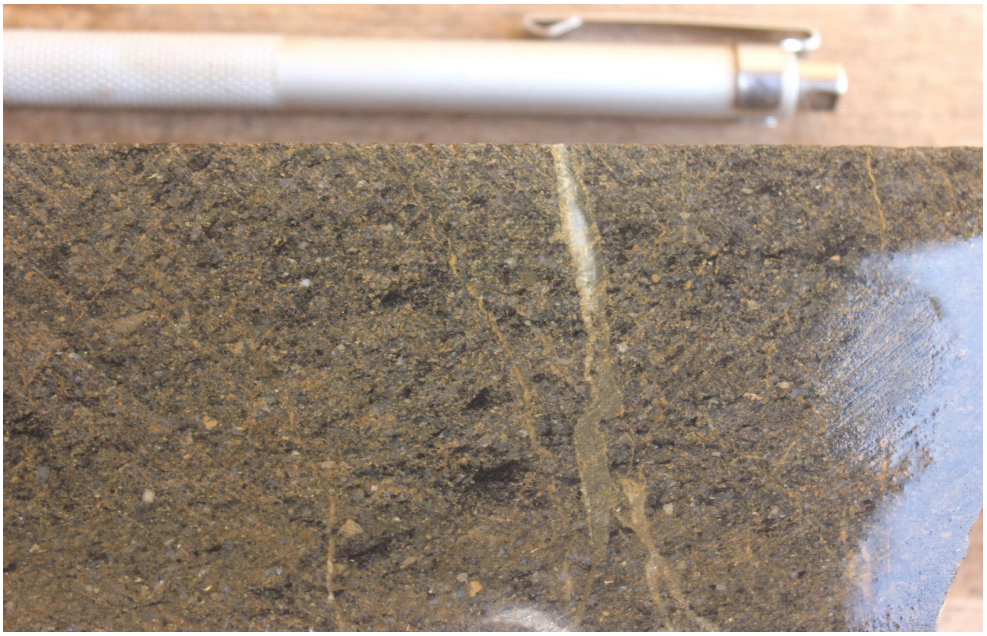

Figure 14. **Greywacke unit. Photo taken from Syama core library.**

❖ ***Conglomerate*** - Massive conglomerate forms the footwall to the mineralised sequence. Clasts within the conglomerate comprise basalt, andesite and sediments with minor porphyritic intrusive rocks (**Figure 15**). The matrix-supported conglomerate appears to have been principally derived from the hangingwall lithologies, and is therefore interpreted to be younger (Olson et al., 1992; Beeson et al., 2007).

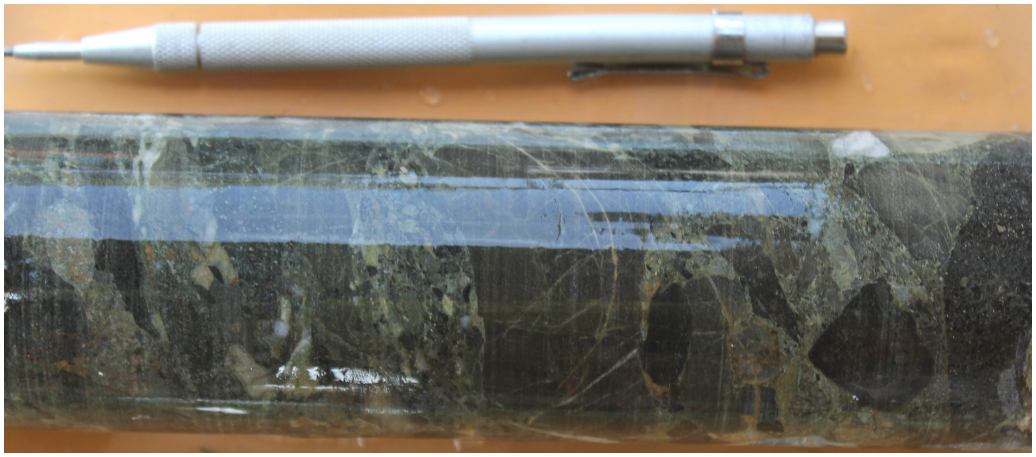

Figure 15. **Conglomerate unit. Photo taken from Syama core library.**

❖ ***Lamprophyre intrusive rocks*** - Intrusive units comprise fine grained amphibole-porphyritic rocks that in part forms a component of mineralised zones (**Figure 16**), (Olson et al., 1992; Beeson et al., 2007). The lamprophyres can be difficult to distinguish from altered basalt in hand specimen. They are generally distinguished by the presence of green fuchsite (chrome-bearing sericite) phenocrysts after olivine and an order of magnitude higher chrome, which can be shown by pXRF.

Figure 16. **Lamprophyre unit. Photo taken from Syama core library.**

## 3.2 Structure

### 3.2.1 Syama deformation history

The deformation history of Syama deposit area is interpreted to have five (5) phases (Standing, 2007) as follows (**Figure 17**):

**DE1:** deposition of the stratigraphy with regional volcanics emplacement.

**D1:** Development of layer-parallel fabric with compression and isoclinal folding of the Syama stratigraphy.

**D2:** refolding of early developed isoclinal folds in a dextral system of NE and N faults.

**DE2:** hydrothermal activity, lamprophyre intrusion and conglomerate development.

**D3:** formation of dextral NNE shears subparallel to stratigraphy and is potentially the most important for gold mineralisation.

**D4:** transgression, dominantly sinistral shearing along pre-existing structures, formation of quartz veins with sericite+carbonate+pyrite within the shear zones formed during D3. McCuaig (2004), attributes the NW structures to the D4 event and states that they often merge into and reactivate the earlier D3 structures, effectively warping the ore zone at these intersections points

and potentially causing high-grade breccia zones. He also cites evidence of offsets (several meters to 10's meters maximum) in both the NNE structures and the conglomerate contact in the pit, further confirming these structures are later than the NNE structures.

**D5:** relates to normal fault movement, is considered to be reflecting the late conjugate faults, east-west quartz veins setting.

**$D_E$3:** extensional collapse along the Syama-Bananso Shear Zone.

All subsequent references to deformation events in this thesis correspond with the above Standing (2007) structural synthesis.

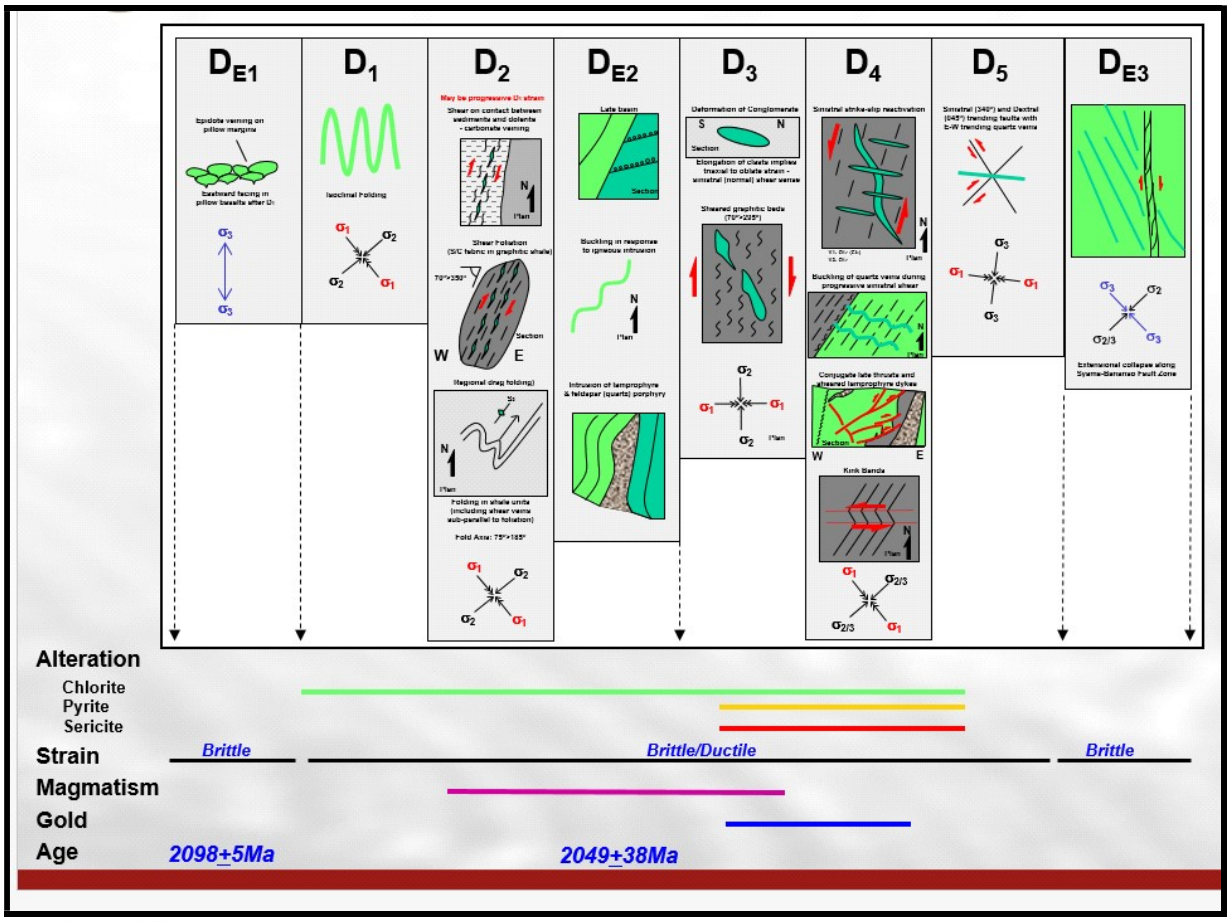


Figure 17. **Syama - Schematic deformation history (after Standing, 2007).**

### 3.2.2 Bedding and Primary fabrics

The rocks at Syama generally show very little evidence of strain in drill core and outcrop. Primary volcanic textures are well preserved and display minimal distortion. The primary textures are also well preserved in sedimentary units.

### 3.2.3 Foliations, Shears and Faults

The mafic, ultramafic and sedimentary rocks rarely display penetrative ductile deformation fabrics. Foliation development is generally limited to shear foliation in narrow shear zones (**Figure 18**). Shear zones are commonly best developed in the carbonaceous siltstone and shale units interbedded between basalt units (**Figure 19**). Brittle fault and breccia zones are best developed within the more competent basalt and greywacke units or the more brittle silicified carbonaceous shale units. (**Figure 20**). Lamprophyre intrusions are often present within these structural zones and are variably affected by deformation. This suggests that there are several generations of lamprophyre intrusion.


Figure 18. **Foliated Carbonaceous Siltstone (Hole ID: SYDD432). Photo taken on half core.**


Figure 19. **Sheared Carbonaceous Shale (Hole ID: SYDD432). Photo taken on half core.**


Figure 20. **Brittle fault zone affecting more competent basalt, lamprophyre and silicified carbonaceous shale, (Hole ID: SYDD432). Photo taken on half core.**

### 3.2.4 Folds

Folds are difficult to see at the scale of hand specimen or core at Syama, although historical mapping in the pit has described megascopic fold structures (Craig et al., 2014).

## 3.3 Gold Mineralisation

Economic gold mineralisation at Syama is restricted to the Syama Formation rocks. All rock types in the Syama Formation can be mineralised, although basalt is perhaps the preferred host rock as it is competent nature makes it more susceptible to brittle deformation. Highest gold grades are associated with brecciation of the more competent lithologies, carbonate/quartz-carbonate stockwork veining and increased pyrite content. The pyrite occurs as two phases, a very fine-grained disseminated phase and an apparently later coarser-grained blebby phase. Both pyrite phases are associated with gold mineralisation (Olson et al., 1992) and may be indicative of two gold mineralising events. Ongoing internal Resolute geochemical studies tend to support the theory of two mineralising events at Syama – an early event associated with lamprophyre intrusion (D1 or earlier?), and a later, structurally controlled event (D2/D3) (P. Manouge, 2019, pers. comm., 31 July).

Minor, uneconomic gold mineralisation within the footwall conglomerates appears limited to mineralised clasts of Syama Formation rocks and rare late structures immediately adjacent to the SBSZ. Mineralised clasts within the conglomerate suggest that deposition potentially postdates at least an early mineralising event.

### 3.3.1 Mineralisation style and ore texture

There are four types of mineralisation associated with the sulphide orebody: intense stockwork ore, breccia ore, intense sheeted veinlets ore, and greywacke ore (Olson et al., 1992).

- ***Stockwork ore*** consists of a strong alteration pattern of dolomite-ankerite-quartz-albite veinlets with disseminated gold-bearing pyrite (**Figure 21**). The original host rock is usually basalt with magnetite and ilmenite phenocrysts altered to leucoxene (Olson et al., 1992; Beeson et al., 2007).

Figure 21. **Stockwork ore in Basalt (after Standing, 2007).**

- ***Breccia ore*** consists of fragments of all lithologies, including basalt, sediments and various intrusive (generally lamprophyres, but also dolerite and rarely felsic porphyry). A sample of brecciated basalt is shown below (**Figure 22**). High gold grades are associated with intense sulphidation of the breccia matrix (Olson et al., 1992; Beeson et al., 2007).

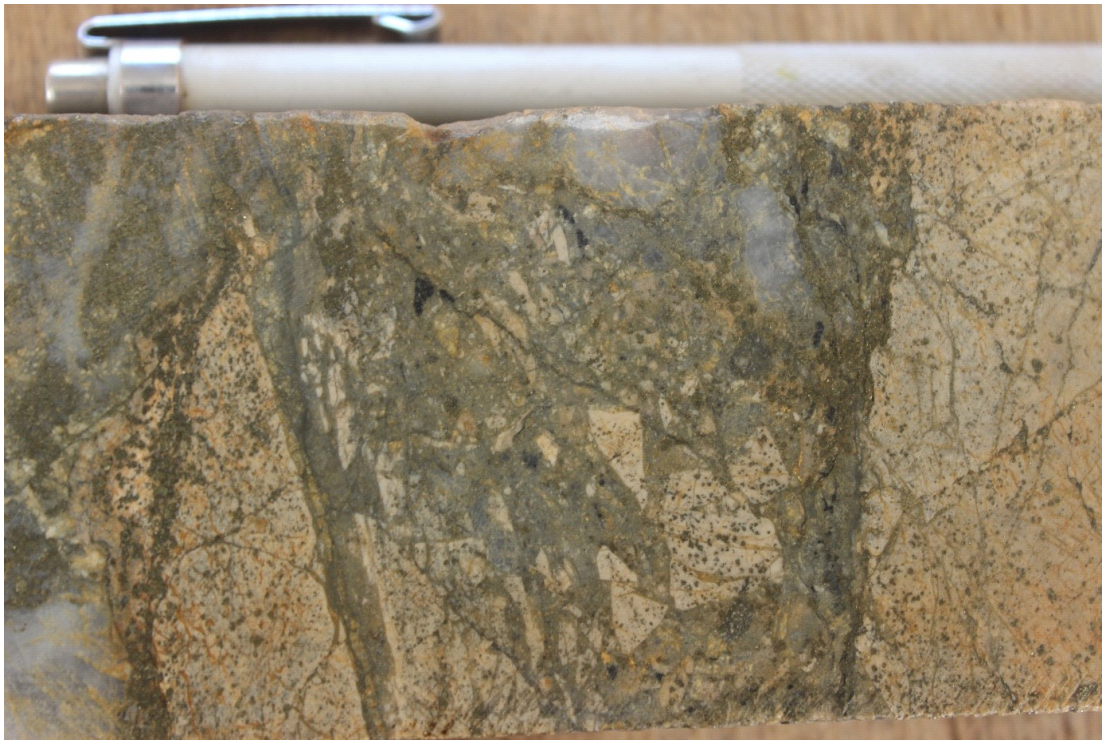
Figure 22. **Breccia ore zone. Photo taken from Syama core library.**

- ***Sheeted veinlet ore*** is best developed in the basalt and consists of relatively dense sets of thin (1-2cm) dolomite veinlets with minor pyrite and albite (**Figure 23**). The veinlets

are often surrounded by a strongly bleached and pyrite-rich alteration halo, with associated high gold grades (Olson et al., 1992; Beeson et al., 2007).

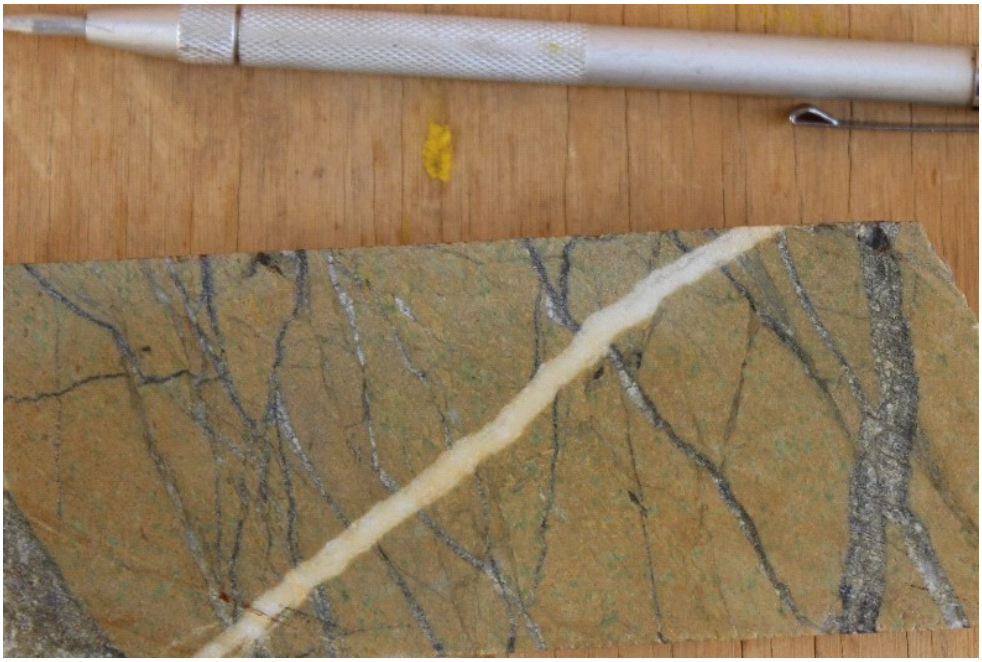

Figure 23. **Sheeted veinlet ore. Photo taken from Syama core library.**

- ***Greywacke ore*** occurs as disseminated pyrite in coarse-grained greywacke and locally of dolomite-quartz-ankerite vein stockwork (**Figure 24**).

Figure 24. **Disseminated pyrite in altered greywacke. Photo taken from Syama core library.**

### 3.3.2 Alteration and ore mineralogy

The alteration assemblage at Syama has been divided into several domains (courtesy of Resolute, 2016), from the hangingwall to the footwall as follows (**Figure 25**).

- ***Hangingwall_1 (HW1***): is distal alteration dominated by chlorite-calcite alteration, essentially regional metamorphism at greenschist facies. The calcite veins are barren and primary textures are preserved.

- ***Hangingwall_1a (HW1a):*** same as HW1 but weakly mineralised, generally associated with narrow, discontinuous graphitic shears +/- lamprophyre dykes.

- ***Hangingwall_2 (HW2):*** is transitional to proximal alteration, composed of chlorite-sericite alteration, which results in (often) patchy bleaching, outer hydrothermal alteration halo. It is associated with minor quartz–carbonate and graphite veining. The primary textures are still preserved here.

- ***Hangingwall_2a (HW2a):*** as for HW2, this alteration is weakly mineralised around narrow, discontinuous hangingwall shears.

- ***Hangingwall_3 (HW3):*** is proximal alteration, of sericite-ankerite-(silica)-(fuchsite) alteration. Fuchsite alteration is of olivine in the lamprophyres. Dolomite, graphite and quartz-carbonate veining increasing, mostly sheeted or weak stockwork. Primary texture becoming obscured by alteration.

- ***Hangingwall_3a (HW3a):*** As for HW3 except variably mineralised. Stronger mineralisation in brecciated zones or zones with increased vein density.

- ***Ore Zone***: Sericite-ankerite-albite-silica-(fuchsite) alteration. Increased dolomite (sparry), graphite and quartz-carbonate veining – complex stockwork or high density sheeted veins. Increased brecciation and texture destruction. Increased sulphide content. Pyrite is the dominant sulphide, occurring in two distinct phases – the first is finely disseminated throughout the host rock and in dolomite vein selvages (early phase?). The second is coarse clusters/aggregates of ragged pyrite that overprints the first phase (D2/3). Both phases carry gold mineralisation. There is no arsenopyrite and chalcopyrite and visible gold are rare. The gold is almost entirely locked up in pyrite (refractory).

- ***Footwall (FW):*** Chlorite-calcite alteration in the footwall conglomerate.

The HW1 through Ore Zone domains are all within the Syama Formation and FW is the N'Golopene Group Banmbere conglomerate. Note that HW2 & HW3 can occur either side of the ore zone.

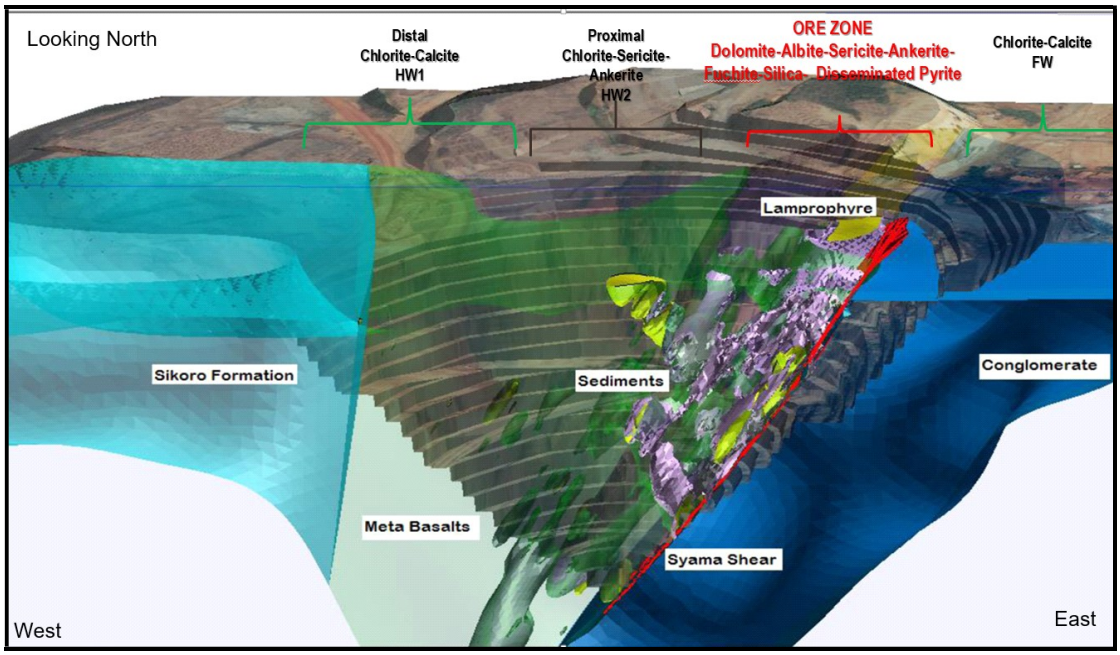


Figure 25. **Alteration halos in the Syama pit (Courtesy of Resolute, 2016).**

All lithologies at Syama can be mineralised as show below (**Figure 26**).

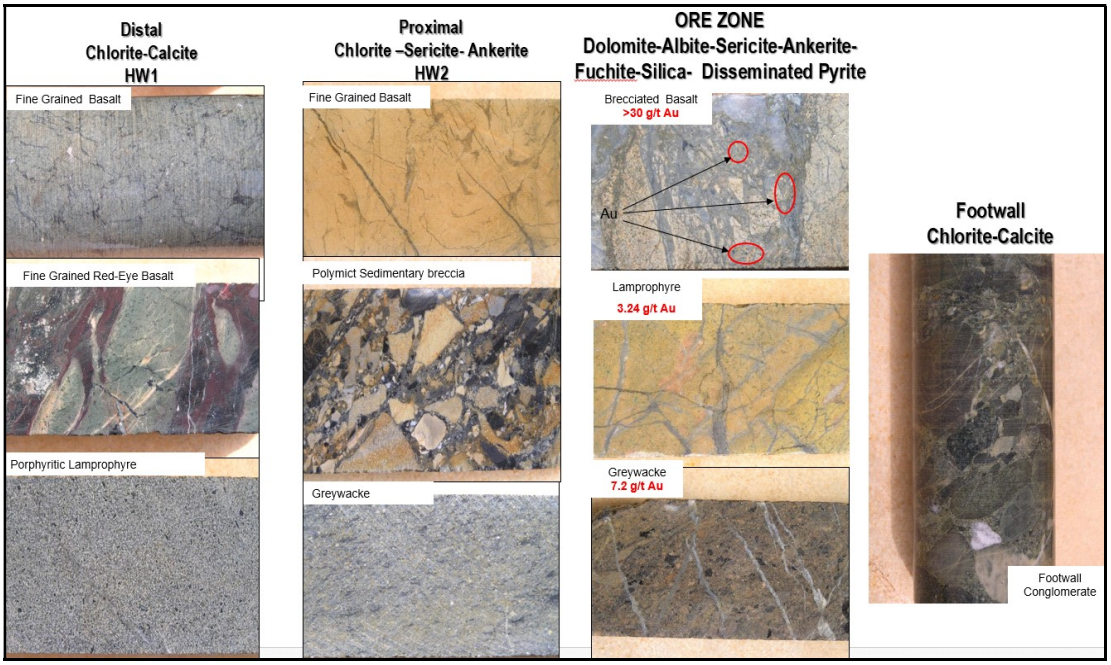


Figure 26. **Syama alteration styles in different rocks (Resolute, 2016).**

# Chapter 4. NW Structures and their relation to high grade ore shoots

## 4.1 Introduction

All hydrothermal ore deposits require transport of large quantities of relatively insoluble metals in solution from source region to the site of deposition (Goldfarb et al., 2005). Faults and shears are the most likely conduits for large volumes of fluid and metal through the rocks (Cox, 2001). In order to transport the required metal volumes in fluid, the permeability of the fault zones must be continuously regenerated. The ore deposits are generally localised, on irregularities (i.e. bends, jogs, bumps and branches) in fault zones (Cox, 2001, Goldfarb et al., 2005). The fact that irregularities commonly extend beyond or sit off the main fault strand explains why deposits commonly occur on second or third order structures rather than on the main fault (Goldfarb et al., 2005). The mineralisation and veining are localised at dilatational jogs on fault zones, therefore, to understand any hydrothermal mineralisation system it is important to understand the structural setting of the geological environment where you are working.

This project was designed to understand the relationship between the NW structures and the high-grade ore shoots at Syama and aid in more effective targeting of these high-grade mineralisation zones. The main focus of current exploration at Syama is the southern extension prospect, called Nafolo (**Figure 27**).

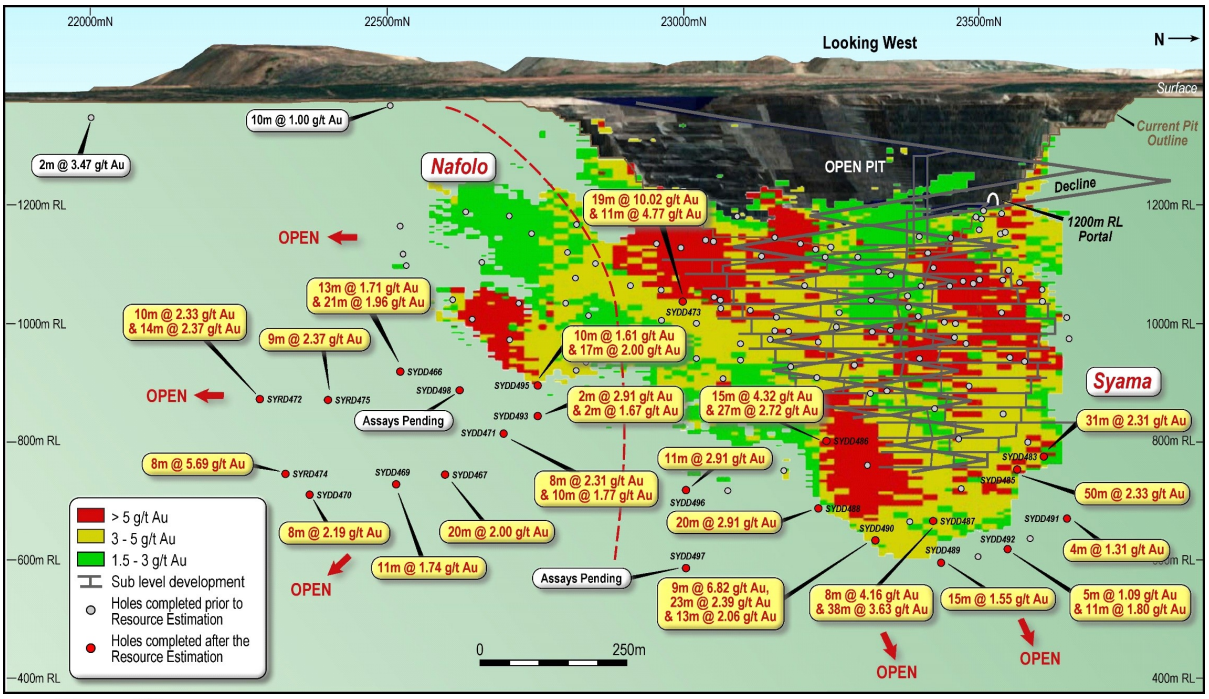


Figure 27. **Syama long section looking west (Courtesy of Resolute, 2018).**

## 4.2 Definitions

The structures assessed to conduct this study are:

❖ **Foliation, Shear and Fault structures:**

- **Foliations** are planar fabrics formed by tabular or platy minerals or other flat objects with a preferred orientation. **Primary foliations** are formed during deposition of sediments and the formation of magmatic rocks, and **secondary foliation or tectonic foliation** are produced from stress and strain and include cleavage, schistosity and mylonitic foliations

- **Shears** are faults that are associated with ductile deformation.

- **Faults** are surfaces or narrow zones along which two blocks of rock have moved relative to each other in a direction parallel to the surface or zone in response to induced stresses. They are associated with brittle deformation. They are integral in the transport of fluid and the localisation of sites of structurally controlled mineral deposits.

❖ **Vein structures:**

- **Veins** are tabular bodies of minerals which have been precipitated into a fracture or other structures within rocks from hydrothermal fluid. They are common components of greenstone gold deposits and can give information regarding the sequence of structural events leading to the determination of controls on mineralisation and ore-forming processes (Robert and Poulsen, 2001). They form in or adjacent to both brittle and ductile fault zones and are generally formed oblique to their related fault. The major gold bearing features at Syama are carbonate and quartz-carbonate veins with mineralisation generally hosted within zones of intense brecciation and/or stockwork and sheeted vein sets.

❖ **Joints, contacts and fractures structures:**

- **Joints** (also termed extensional fractures) are planes of separation on which no or undetectable shear displacement has taken place. The two walls of the resulting tiny opening typically remain in tight (matching) contact. Joints may result from regional tectonics (i.e. the compressive stresses in front of a mountain belt), folding (due to curvature of bedding), faulting, or internal stress release during uplift or cooling. They often form under high fluid pressure (i.e. low effective stress), perpendicular to the smallest principal stress.

- **Contacts** are boundaries which separates one rock units from another. There are two main types of contact; **primary contacts** are depositional and conformable within a sedimentary sequence, and **secondary contacts** are unconformable and include intrusive contacts and those induced by tectonic activity, such as faults and shears.

- **Fractures** are surfaces along which rocks have broken; they are therefore surfaces across which the rock has lost cohesion.

## 4.3 Structural analysis and interpretation at various levels in the mine.

### 4.3.1 Structural analysis and interpretation at mine level 1200mRL

Structural analysis and interpretation of foliations, shears and faults (**Appendix II**) at the 1200mRL mine level (**Figure 28**), highlights the dominant NNE to NE trend attributed to the D3

event, crosscut by several NW striking structures, corresponding to the D4 event. Very few E-W structures are observed, which are related to the late D5 event.

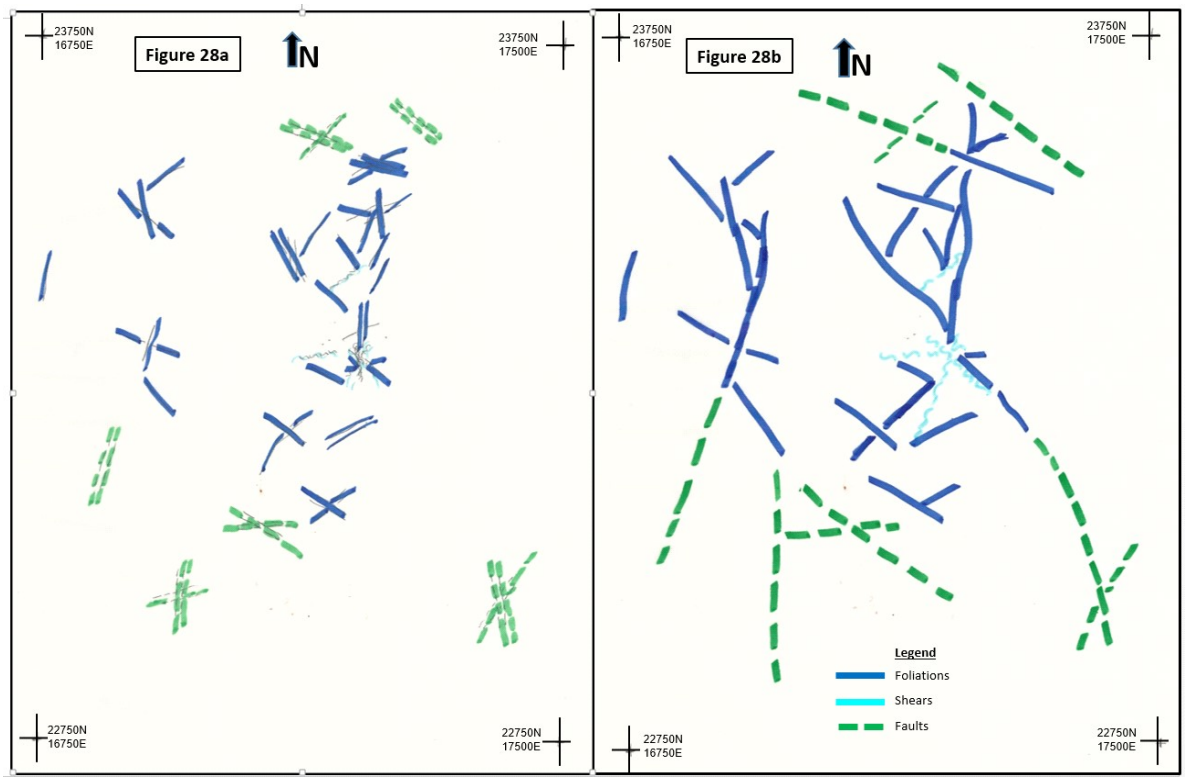


Figure 28. **Foliations/Shears/Faults interpretation at mine level 1200mRL. (a). showing the main trends identified from measurement. (b). showing the interpretation form lines.**

The stereographic projection of foliations (**Figure 29**), shears (**Figure 30**), and faults (**Figure 31**) at mine level 1200mRL, plotted on lower projection of an equal-area stereonet (Schmidt projection) indicate dominantly NNE to NE trending and W to NW dipping structures (D3).

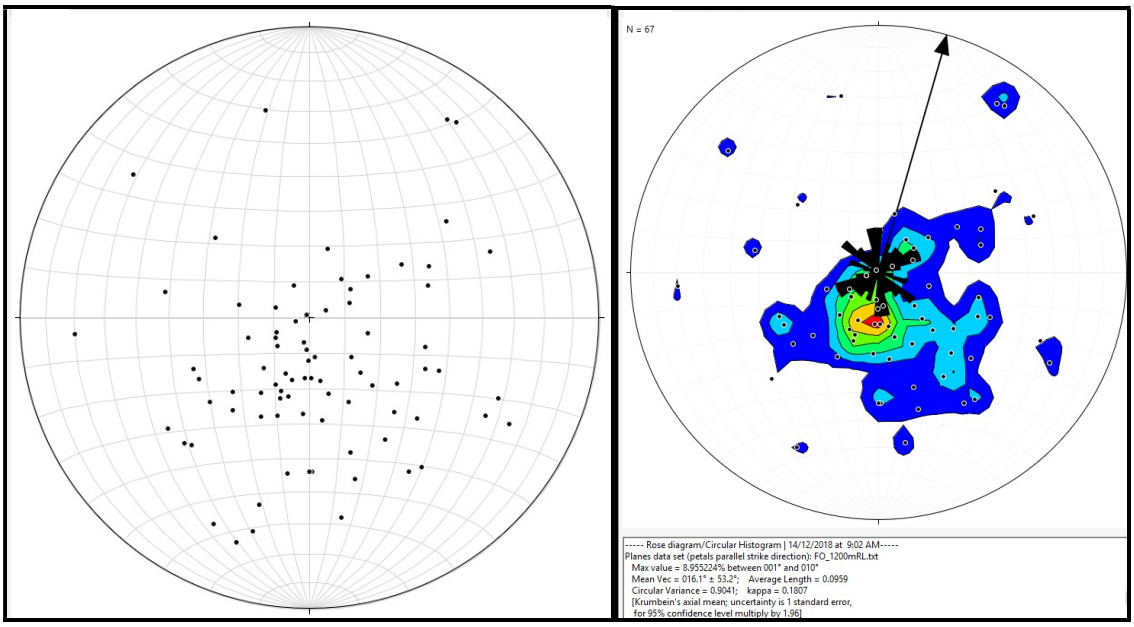


Figure 29. **Equal area lower hemisphere stereographic projection of foliations at mine level 1200mRL.**

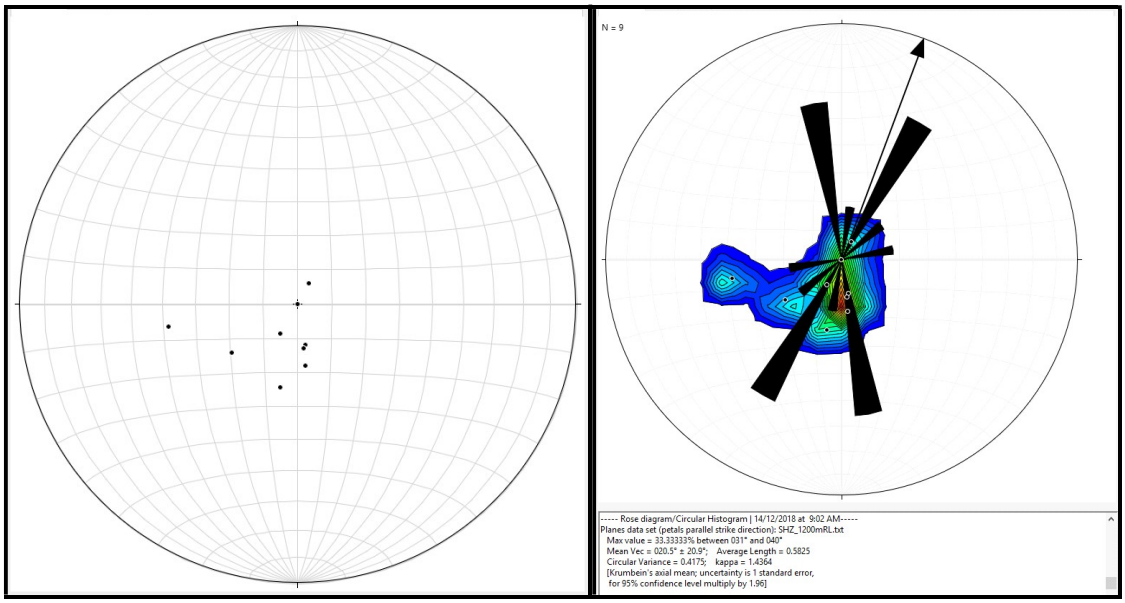


Figure 30. **Equal area lower hemisphere stereographic projection of shears at mine level 1200mRL.**

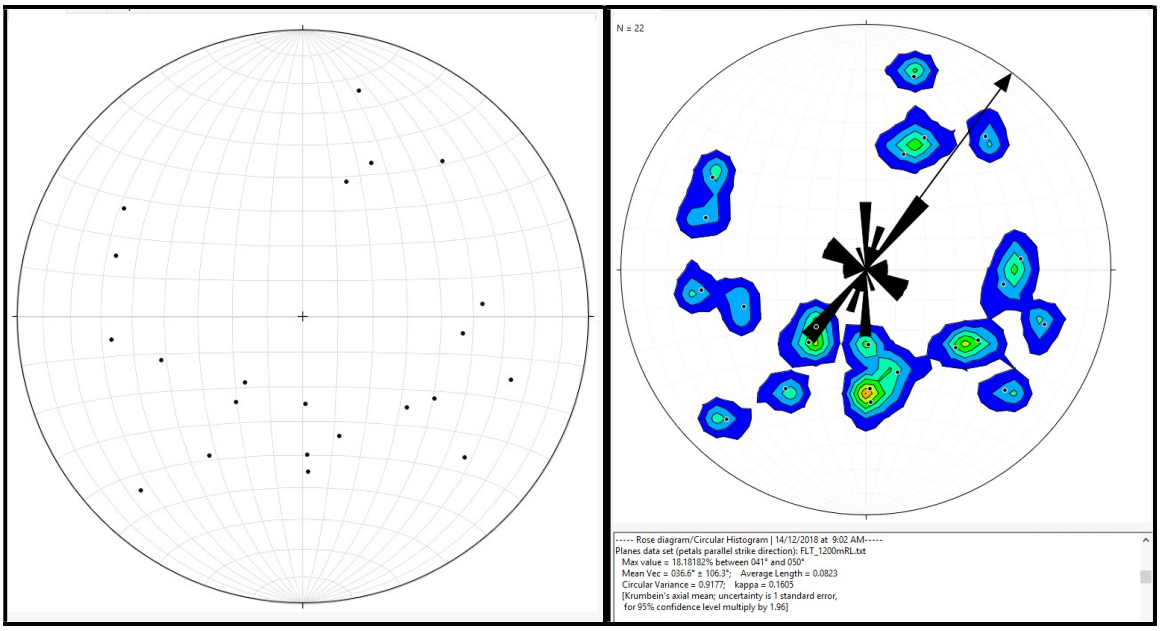


Figure 31. **Equal area lower hemisphere stereographic projection of faults at mine level 1200mRL.**

The vein structures (**Appendix V**) selected through the orebody for analysis and interpretation at mine level 1200mRL (**Figure 32**), show major structures striking NNE to NE related to the D3 event, crosscut by some secondary NW striking structures related to the D4 event.

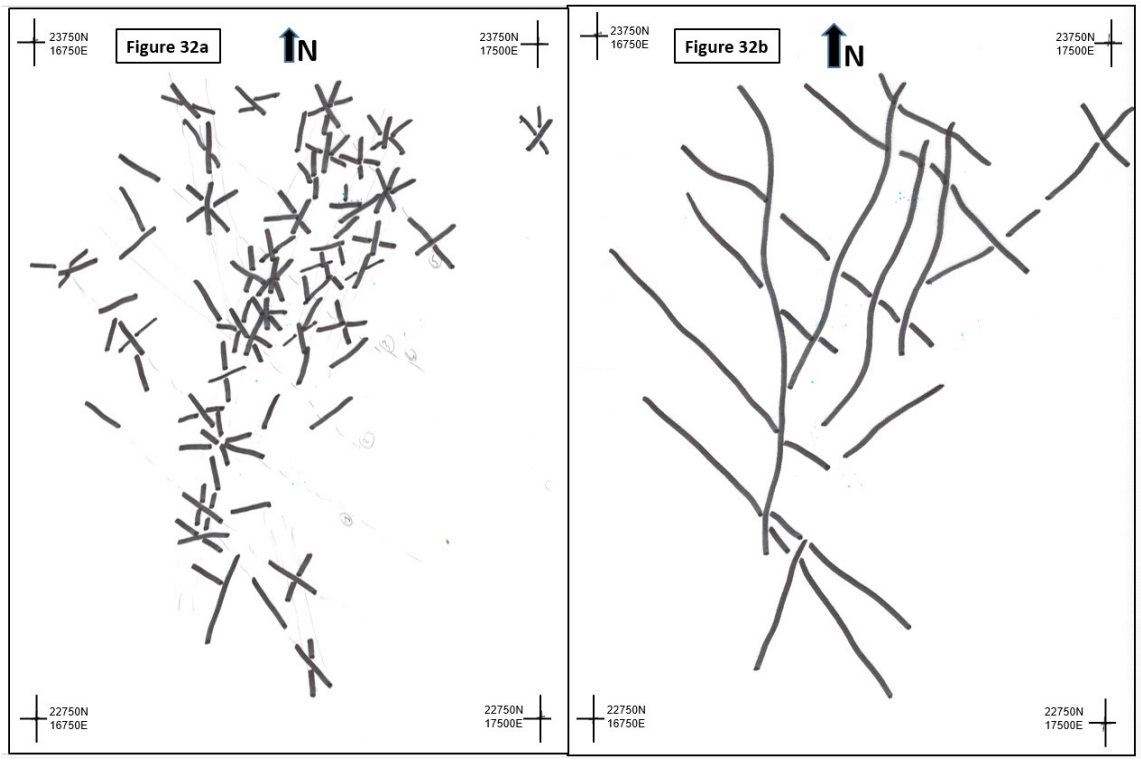


Figure 32. **Veins structures interpretation at mine level 1200mRL. (a). showing the mains trend identified from measurement. (b). showing the interpretation as lines form.**

The veins stereographic projection at mine level 1200mRL (**Figure 33**) plotted on lower projection of an equal-area stereonet (Schmidt projection), highlight the dominant NNE trending, W dipping structures (D3).

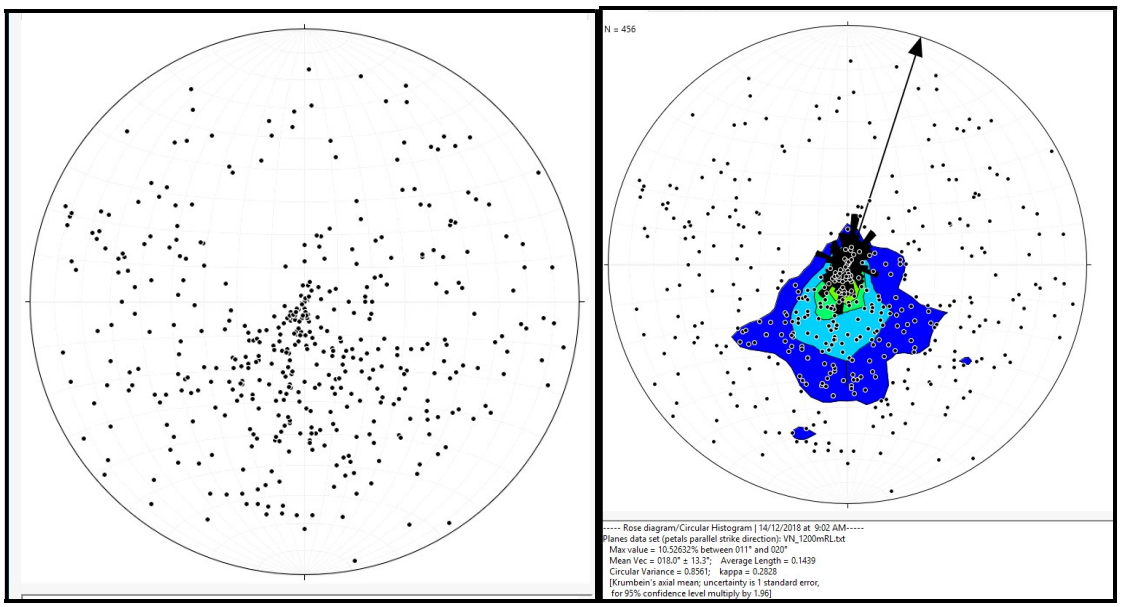


Figure 33. **Equal area lower hemisphere stereographic projection of veins at mine level 1200mRL.**

The structures interpretation at mine level 1200mRL from foliation, shears and faults (**Figure 28**) and from veins (**Figure 32**), show dominant NNE trending structures (D3), crosscut by some NW structures (D4). The stereonet plots of foliations, shears, faults (**Figure 29, Figure 30, and Figure 31)** and veins (**Figure 33**) at that level, confirm the general NNE striking, W dipping trend.

### 4.3.2 Structural analysis and interpretation at mine level 1100mRL

The foliations, shears and faults structures used for interpretation at level 1100mRL are showed in **Appendix III**. The assessment of the foliations, shears and faults and their interpretation at mine level 1100mRL (**Figure 34**) indicate NNE striking structures of D3 events and crosscut by some NW striking structures of D4 events.

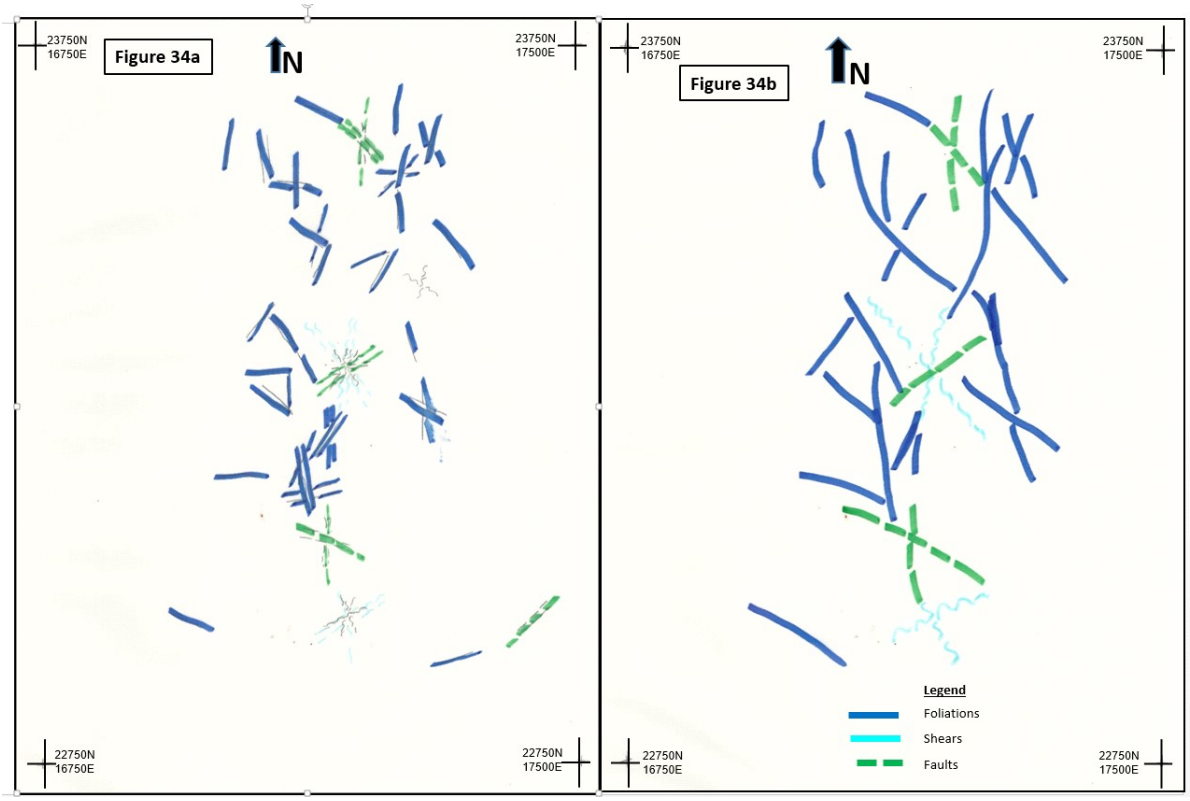


Figure 34. **Foliations/Shears/Faults interpretation at mine level 1100mRL. (a). showing the mains trend identified from measurement. (b). showing the interpretation as lines form.**

The stereographic projection of, foliation at mine level 1100mRL (**Figure 35**) and shears at mine level 1100mRL (**Figure 36**) plotted on lower projection of an equal-area stereonet (Schmidt projection) indicate generally N-S trending structures (D3) and steeply W dipping. The stereographic projection of faults at mine level 1100mRL (**Figure 37**) plotted on lower projection of an equal-area stereonet (Schmidt projection) are too few to be contoured and interpreted.

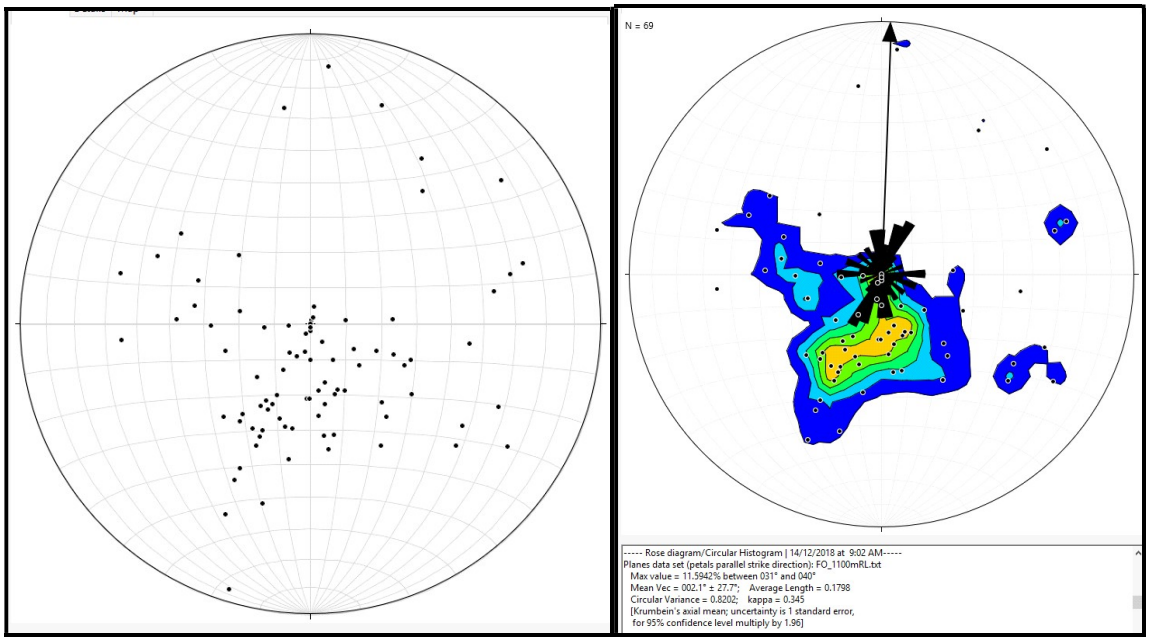


Figure 35. **Equal area lower hemisphere stereographic projection of foliations at mine level 1100mRL.**

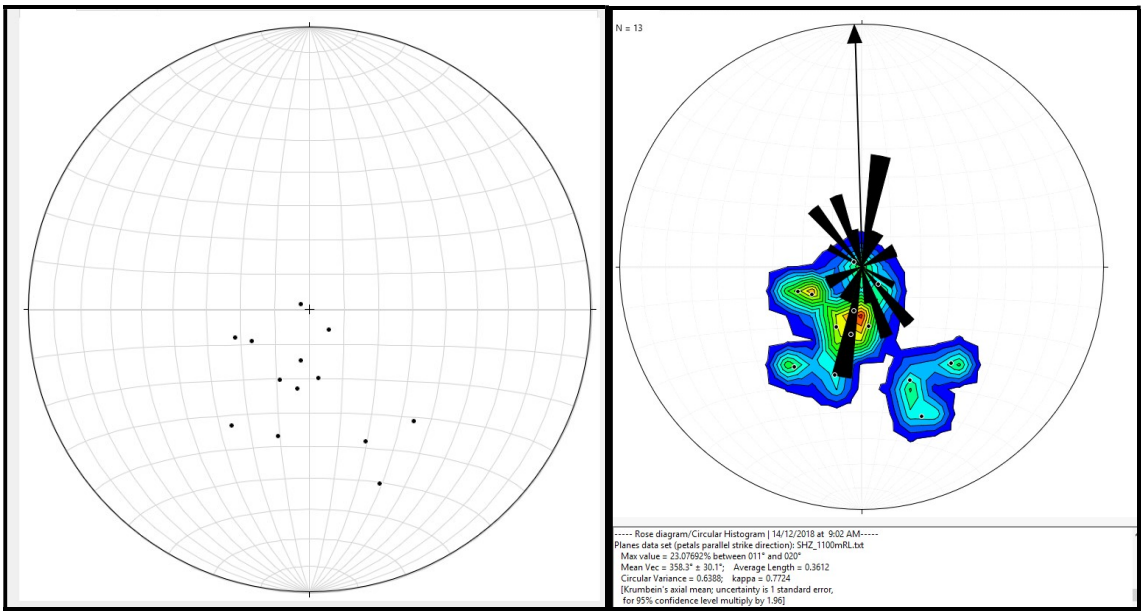


Figure 36. **Equal area lower hemisphere stereographic projection of shears at mine level 1100mRL.**

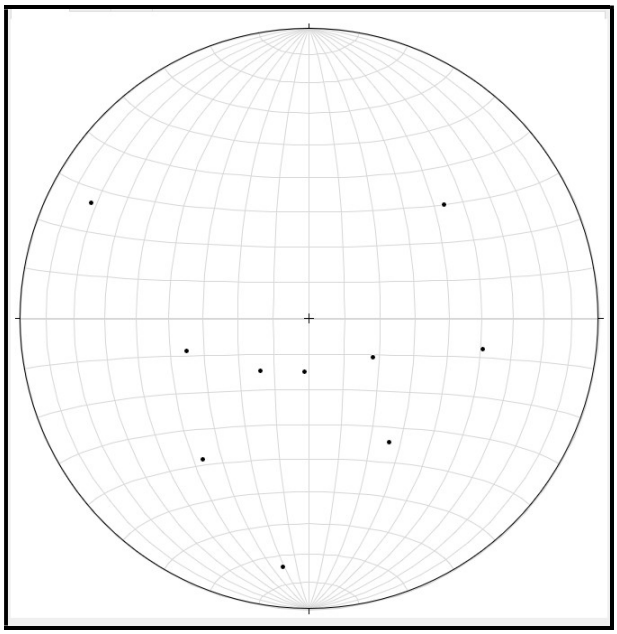

Figure 37. **Equal area lower hemisphere stereographic projection of faults at mine level 1100mRL.**

The vein structures interpretation at mine level 1100mRL (**Appendix VI**) and their analysis and interpretation (**Figure 38**) show major structures trending NE (D3) are crosscut by the secondary NW (D4) striking structures.

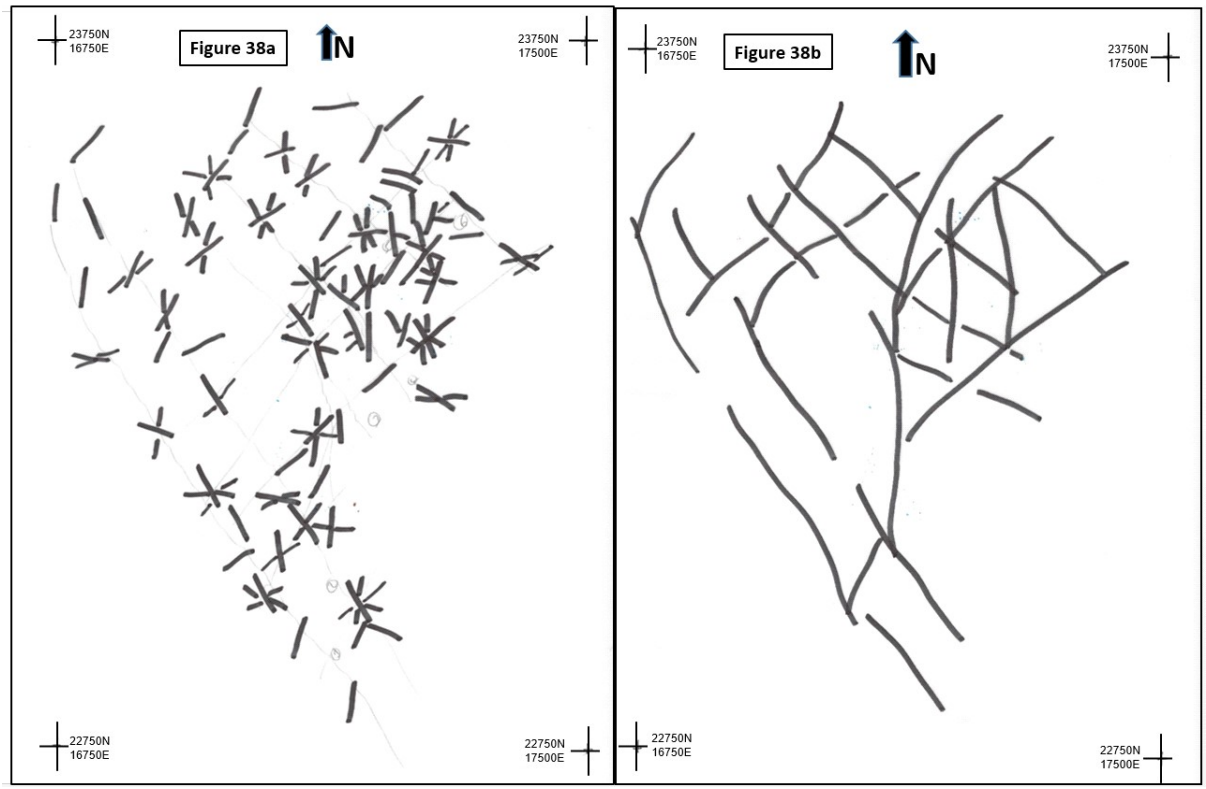


Figure 38. **Veins structures interpretation at mine level 1100mRL. (a). showing the mains trend identified from measurement. (b). showing the interpretation as lines form.**

The stereographic projection of veins at mine level 1100mRL (**Figure 39**) indicate generally NNE (D3) trending structures and W dipping.

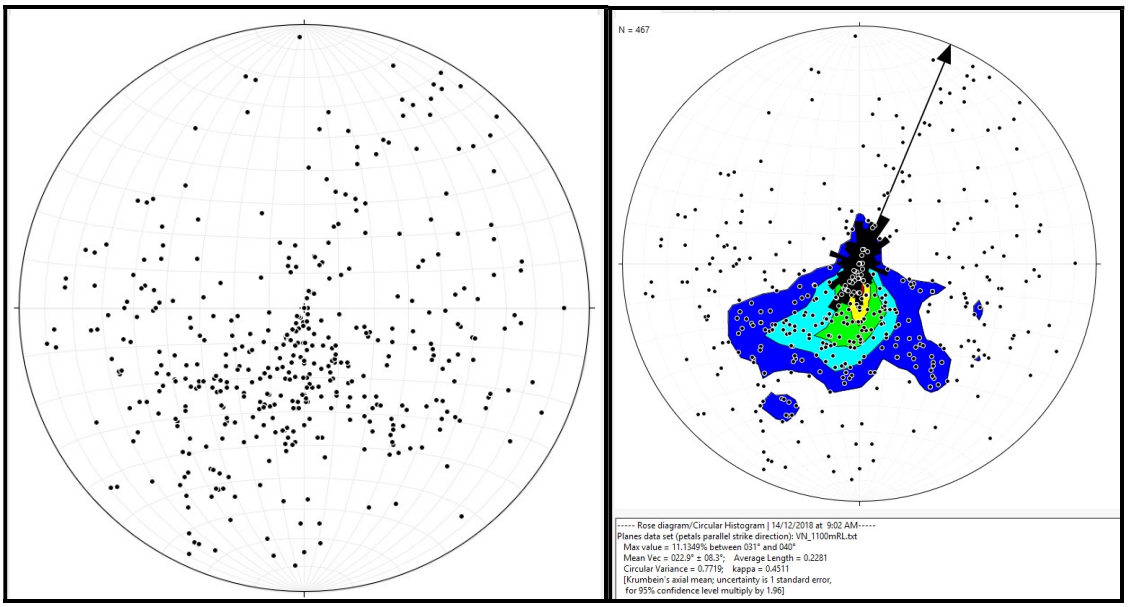


Figure 39. **Equal area lower hemisphere stereographic projection of veins at mine level 1100mRL.**

The foliation, shears and faults structures interpretation (**Figure 34**) and veins structures interpretation (**Figure 38**), at mine level 1100mRL, show generally a NNE (D3) trending structures crosscut by some NW (D4) structures. The stereonet plots of both foliations, shears, faults (**Figure 35, Figure 36, and Figure 37**) and veins at that mine level (**Figure 39**), also support that with general trend of N-S to NE (D3) and W dipping.

### 4.3.3 Structural analysis and interpretation at mine level 1000mRL

The foliations, shears and faults structures used for interpretation at mine level 1000mRL are showed in **Appendix IV**. The analysis of the foliations, shears and faults and their interpretation at mine level 1000mRL (**Figure 40**), indicate general trend of NNE structures (D3) and crosscut by the NW (D4) and E-W (D5) striking structures.

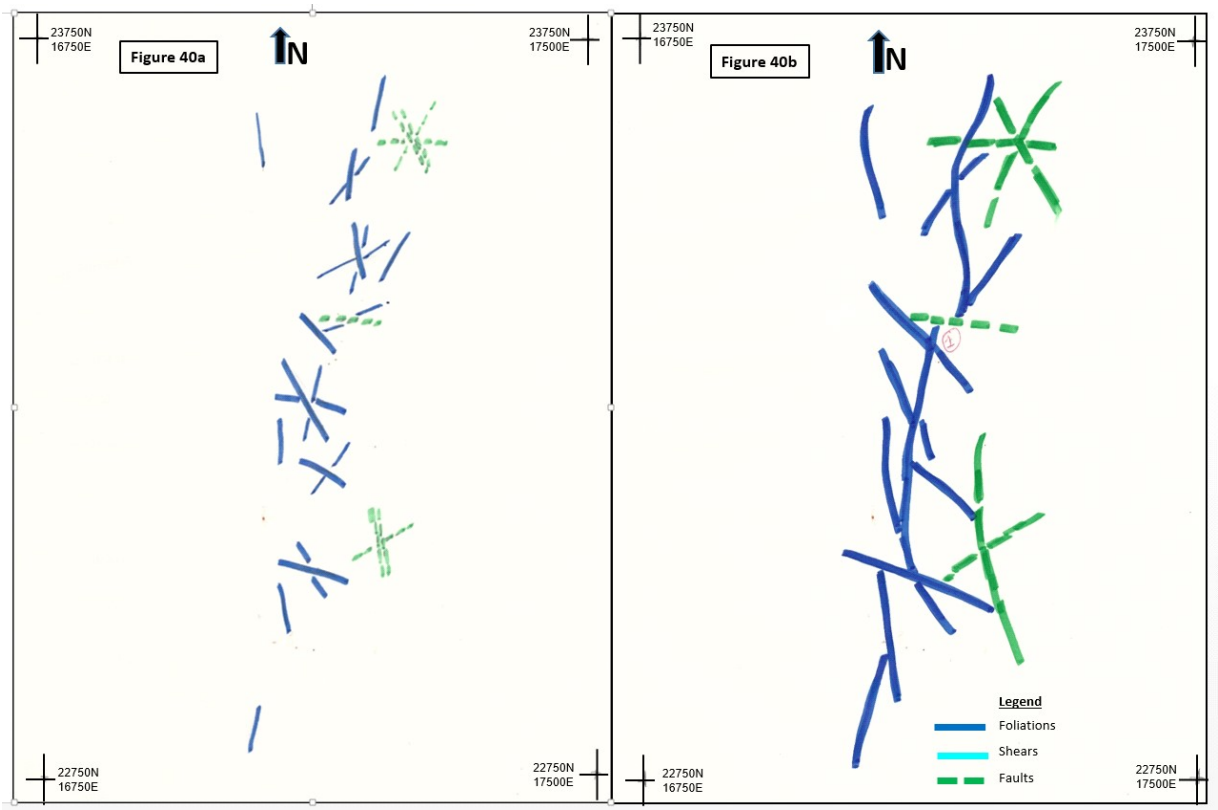


Figure 40. **Foliations/Shears/Faults interpretation at mine level 1000mRL. (a). showing the mains trend identified from measurement. (b). showing the interpretation as lines form.**

The stereographic projection of foliation at mine level 1000mRL (**Figure 41**) plotted on lower projection of an equal-area stereonet (Schmidt projection) indicate dominantly NNW trending structures (D4) and E dipping. The stereographic projection of faults at mine level 1000mRL (**Figure 42**) are too few to be contoured and interpreted. No shears data available for stereographic projection of shears at mine level 1000mRL.

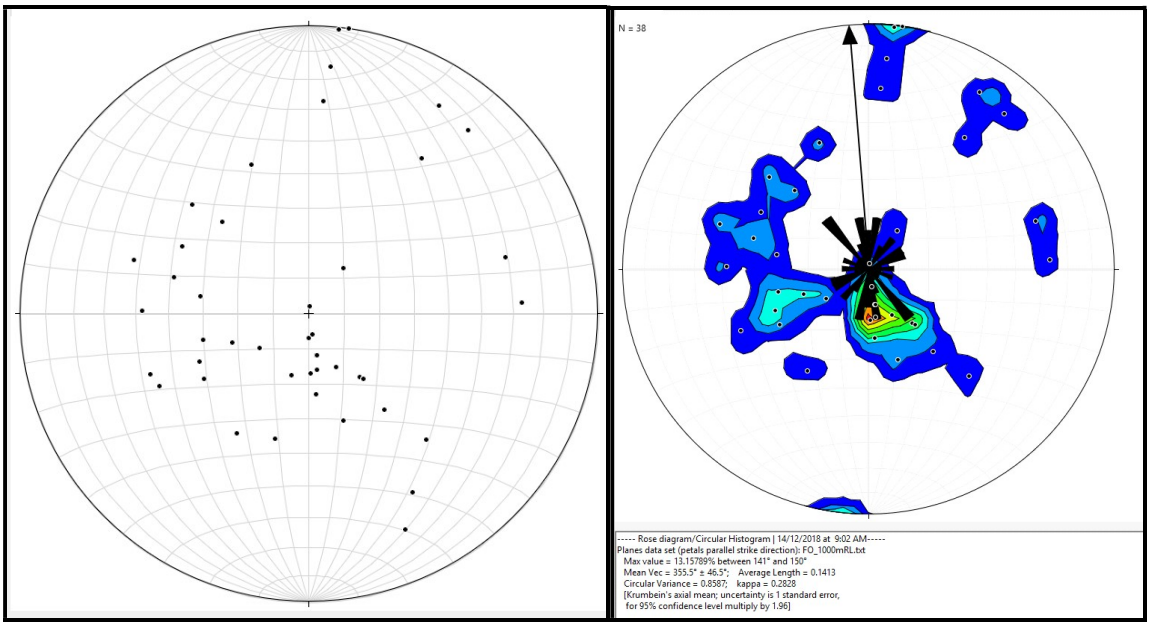


Figure 41. **Equal area lower hemisphere stereographic projection of foliations at mine level 1000mRL.**

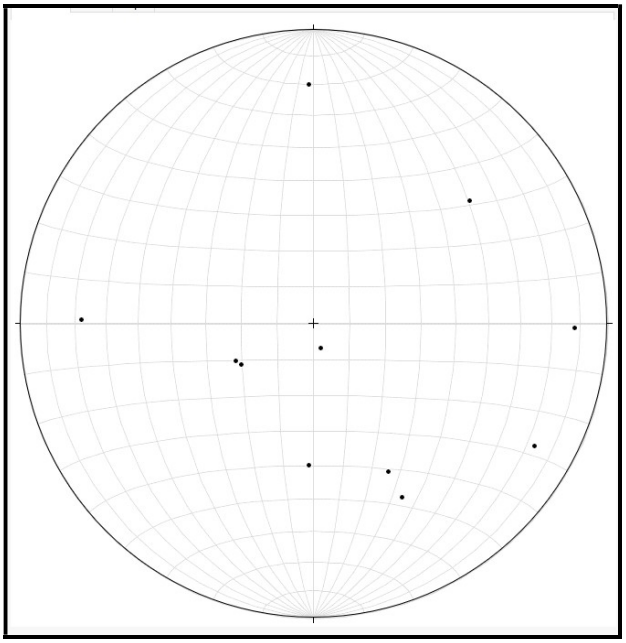

Figure 42. **Equal area lower hemisphere stereographic projection of faults at mine level 1000mRL.**

The vein structures selected through the orebody for interpretation at mine level 1000mRL are showed in **Appendix VII**. The analysis of the veins and their interpretation at mine level 1000mRL (**Figure 43**), show major structures striking NNE to NE (D3) are crosscut by the secondary NW striking structures (D4).

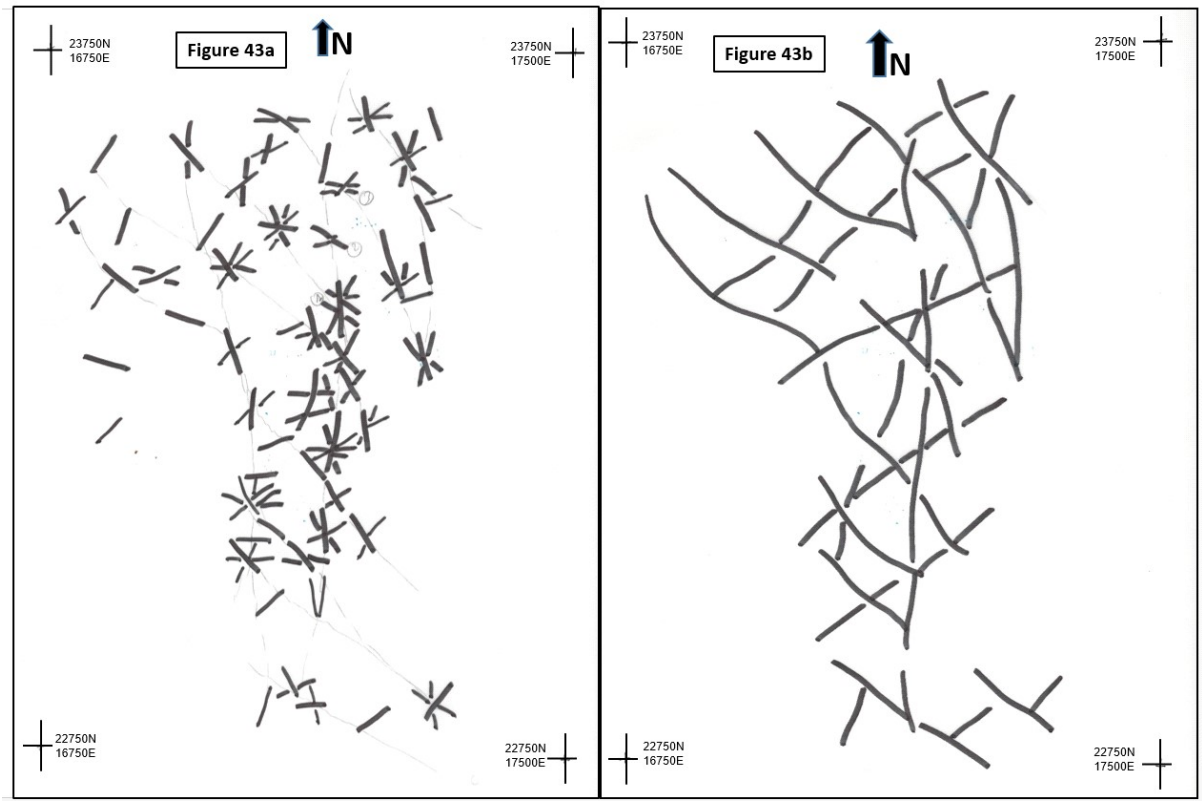


Figure 43. **Veins structures interpretation at mine level 1000mRL. (a). showing the mains trend identified from measurement. (b). showing the interpretation as lines form.**

The stereographic projection of veins at mine level 1000mRL (**Figure 44**) plotted on lower projection of an equal-area stereonet (Schmidt projection), indicate generally NNE trending structures (D3) and W dipping.

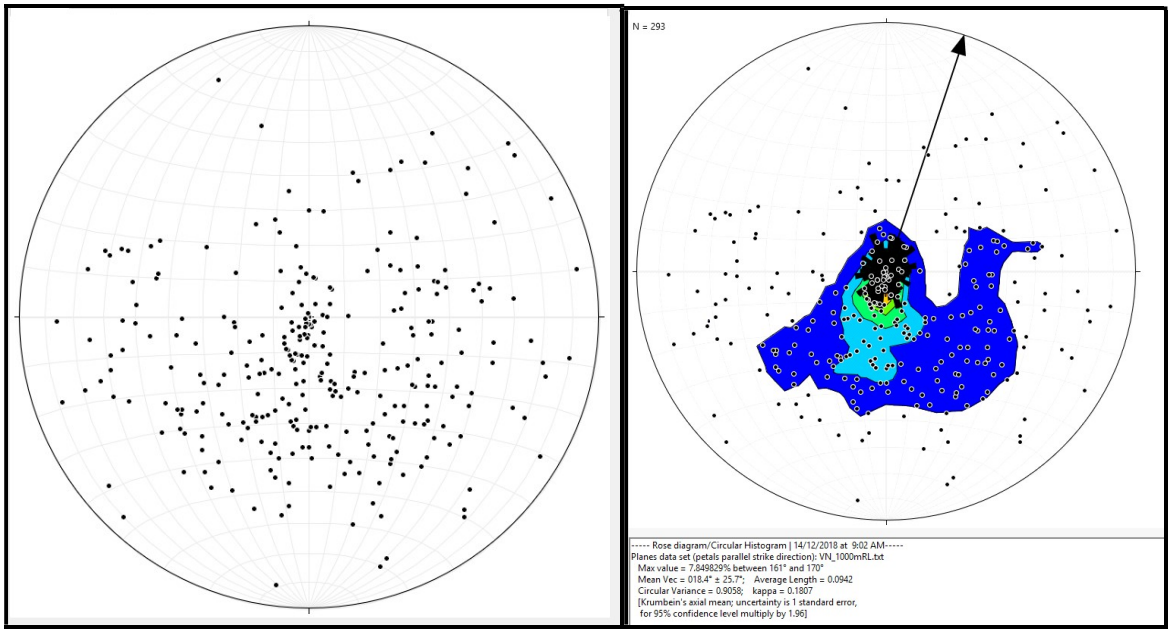


Figure 44. **Equal area lower hemisphere stereographic projection of veins at mine level 1000mRL.**

The structures interpretation at mine level 1100mRL from foliation, shears and faults (**Figure 34**) and from veins (**Figure 38**), show generally a NNE trending structures (D3) crosscut by some NW structures (D4). The stereonet plots of both foliations, shears, faults (**Figure 35, Figure 36, and Figure 37**) and veins at that level (**Figure 39**), rather show general trend of N-S and NE (D3) and W dipping.

### 4.3.4 Joints, Contacts and Fractures analysis and interpretation at mine levels, 1200mRL, 1100mRL and 1000mRL

The joints, contacts and fractures structures selected through the orebody for interpretation are too erratic to define preferential directions and could not help in this study (**Appendix VIII, Appendix IX** and **Appendix X**). This can be explained by the fact that the complex deformation history of Syama has produced an extremely complex array of joints and fractures that cannot be resolved with the available data. Similarly, the anastomosing nature and several generations of lamprophyre intrusion, coupled with alteration potentially obscuring intrusive contacts, make these measurements unreliable for interpretation. They have therefore been ignored.

The joints, contacts and fractures data plotted at the three levels are considered noisy and do not define recognisable preferential orientations. They have not been taken into account in this study to avoid confusing interpretations. Nevertheless, the stereographic projections has showed that they relatively follow the NNE trend.

The stereographic projects of joints, contacts and fractures measurements at mine level 1200mRL (**Figure 45**) plotted on lower projection of an equal-area stereonet (Schmidt projection), show a general NNE striking, W dipping trend.

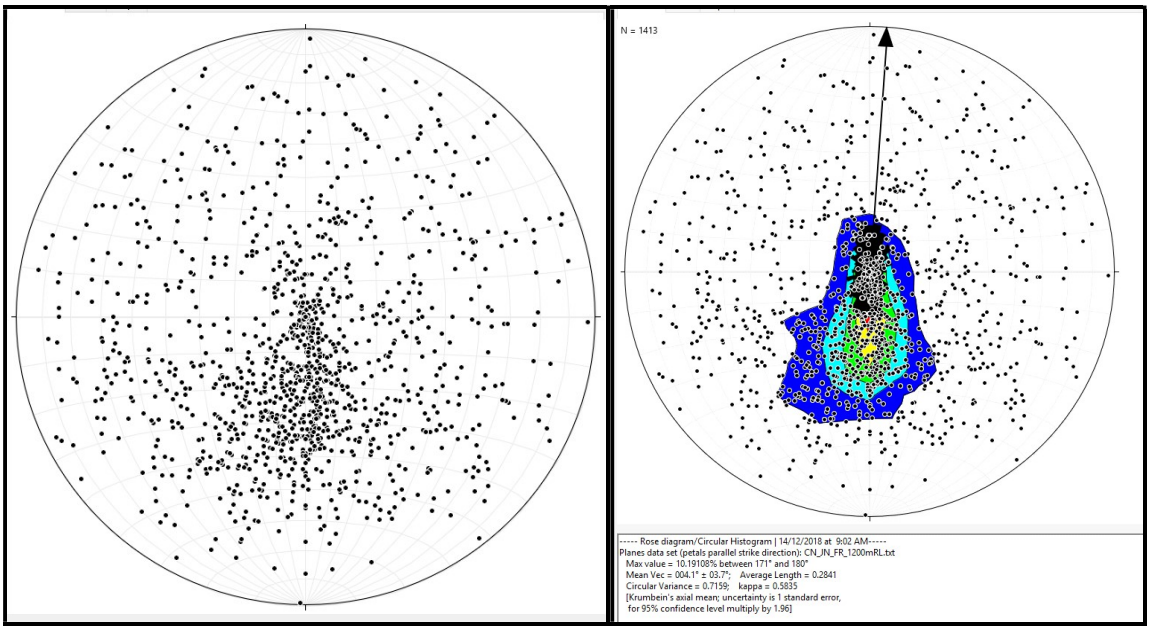


Figure 45. **Equal area lower hemisphere stereographic projection of Joints\contacts\fractures at mine level 1200mRL.**

The stereographic projections of joints, contacts and fractures at mine level 1100mRL (**Figure 46**) plotted on lower projection of an equal-area stereonet (Schmidt projection), show a general NNE striking, W dipping trend.

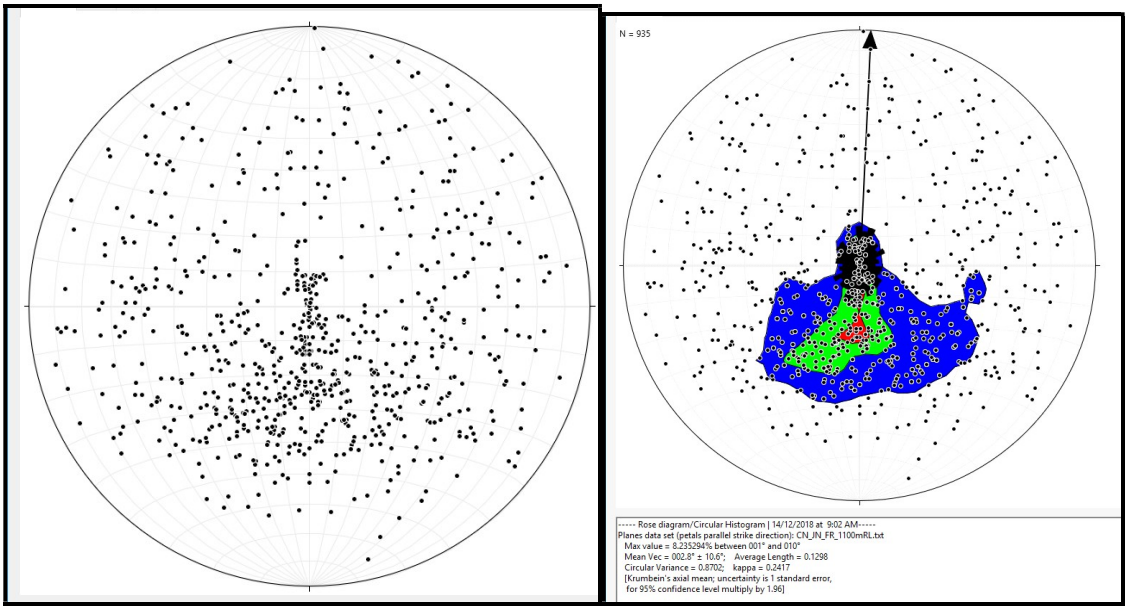


Figure 46. **Equal area lower hemisphere stereographic projection of Joints\contacts\fractures at mine level 110mRL.**

The stereographic projections of joints, contacts and fractures at mine level 1000mRL (**Figure 47**) plotted on lower projection of an equal-area stereonet (Schmidt projection) show general NNE striking and W dipping trend.

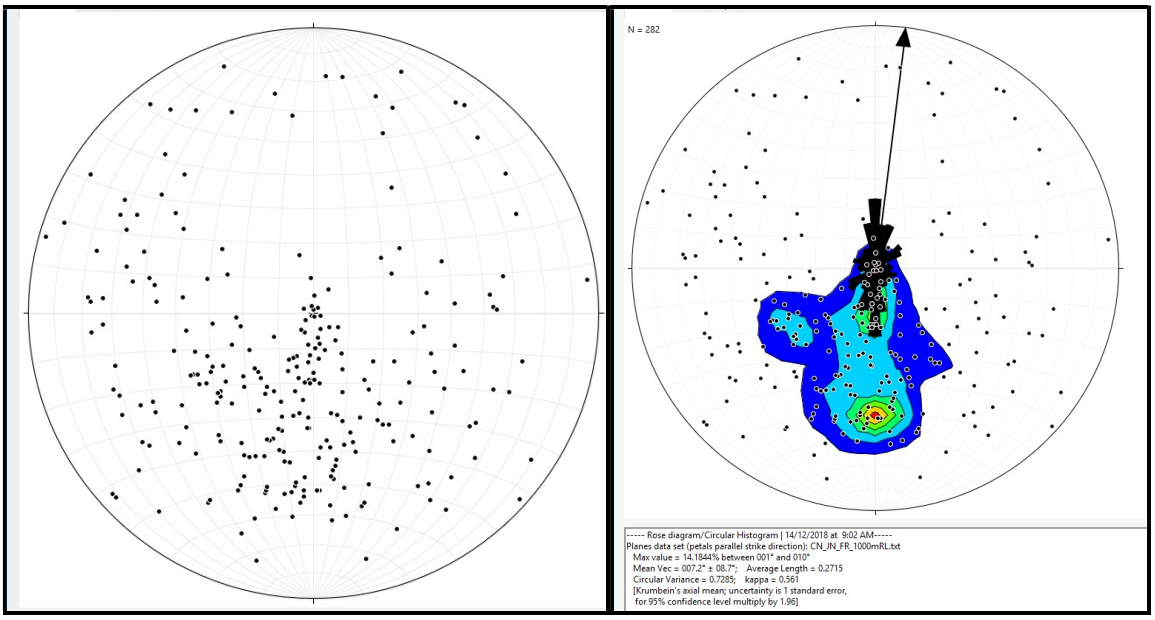


Figure 47. **Equal area lower hemisphere stereographic projection of Joints\contacts\fractures at mine level 1000mRL.**

## 4.4 Identification of high-grade shoot zones

The most recent Syama block model (Resolute, August 2017) has been plotted using Micromine and at each selected level corresponding high-grade zones have been printed out on A3 paper. The block model uses a 1g/t Au cut-off and has been colour coded as follows: between 1-3g/t Au (yellow), 3-5g/t Au (red) and greater than or equal to 5g/t Au (magenta). On the A3 printed paper, any ore block envelopes equal or above 5g/t Au have been contoured by hand as high-grade zones at each level of the selected structures (**Figure 48b, Figure 49b and Figure 50b**). The three chosen mine levels (1200mRL, 1100mRL and 1000mRL) are the most suitable levels to highlight higher grade blocks throughout the orebody. The images have been scanned by using A3 scanner printer. The raw block model images at each level are shown in Appendix **XI, Appendix XII** and **Appendix XII.**

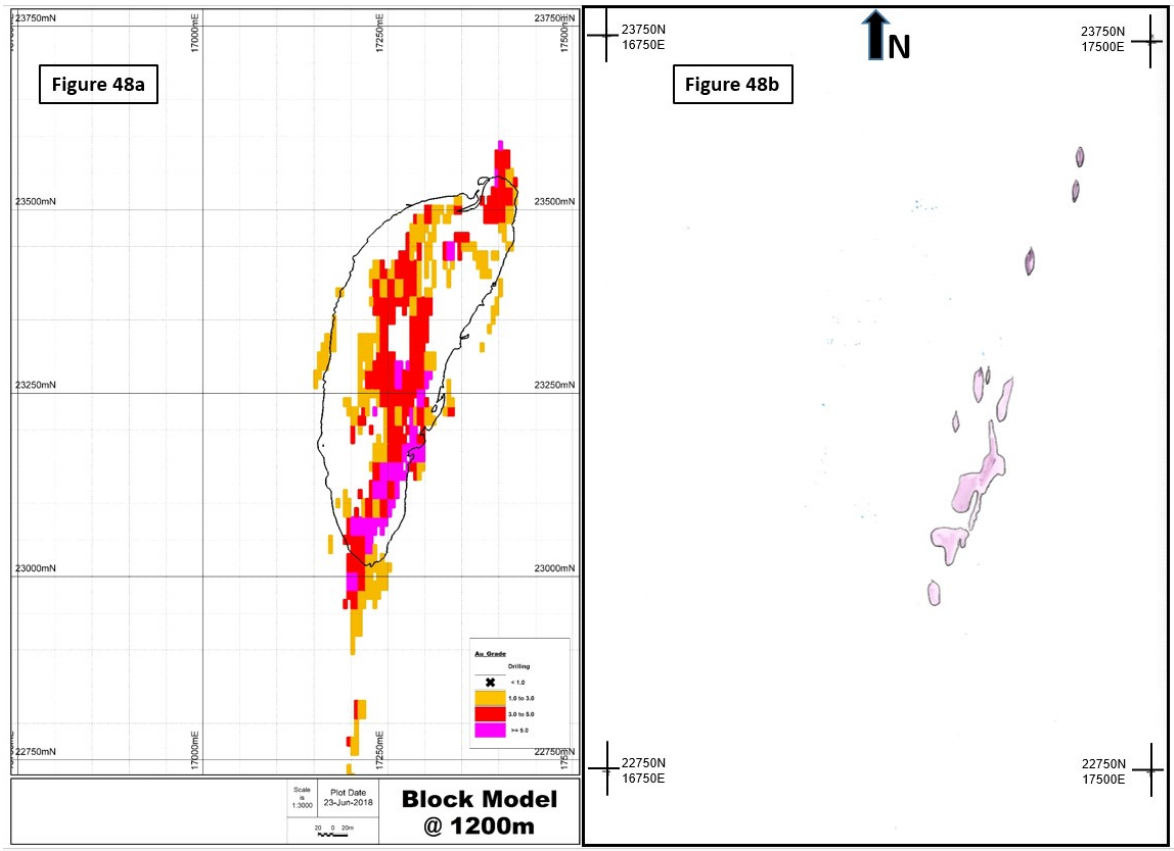


Figure 48. **(a). Ore Block Model with range of 1-3g/t Au, 3-5g/t Au and >5g/t Au at mine level 1200mRL. (b). Highest ore envelope zone equal or above 5g/t Au.**

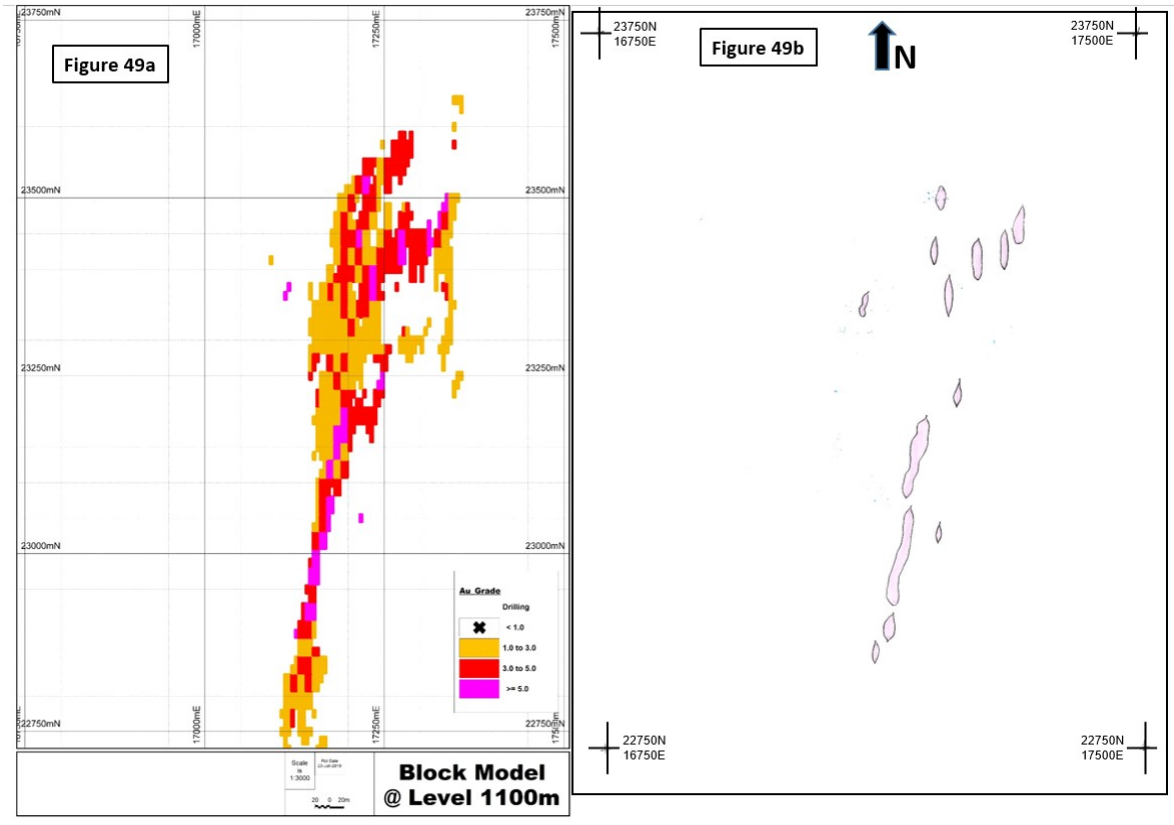


Figure 49. **(a). Ore Block Model with range of 1-3g/t Au, 3-5g/t Au and >5g/t Au at mine level 1100mRL. (b). Highest ore envelope zone equal or above 5g/t Au.**

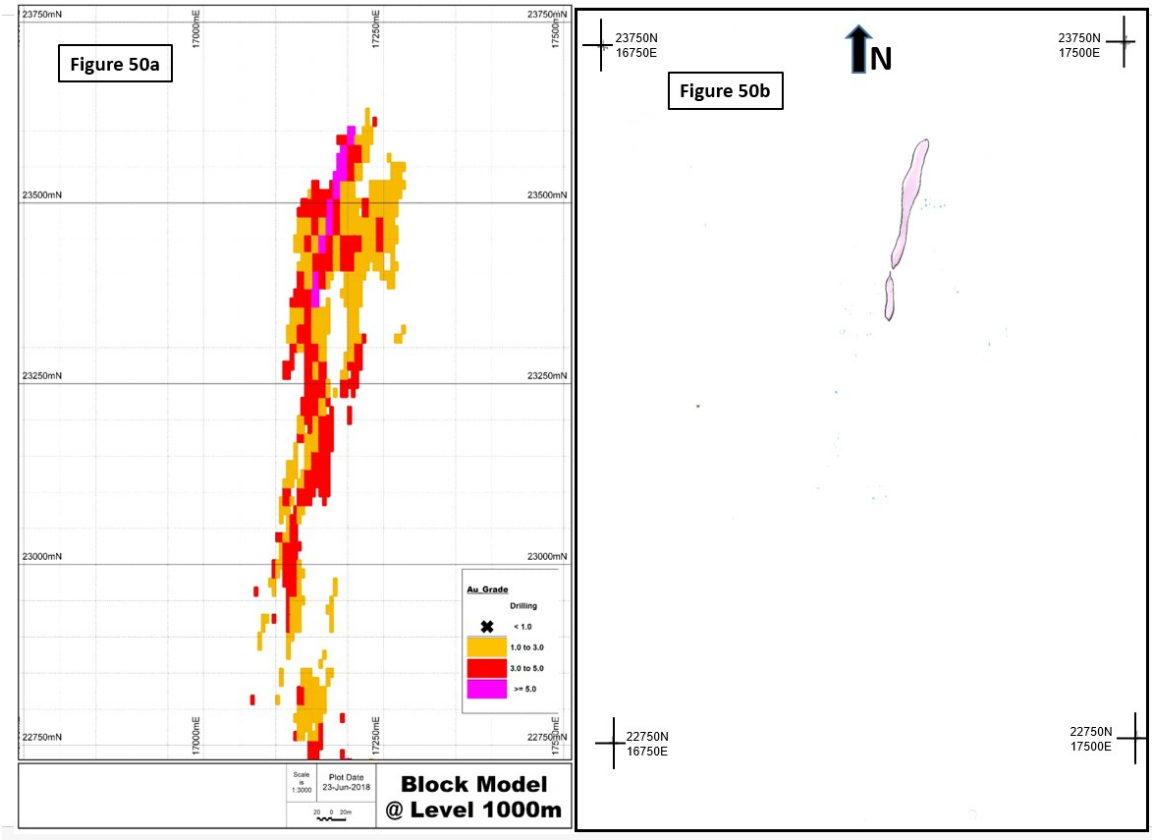


Figure 50. **(a). Ore Block Model with range of 1-3g/t Au, 3-5g/t Au and >5g/t Au at mine level 1000mRL. (b). Highest ore envelope zone equal or above 5g/t Au.**

## 4.5 Interpreted structures in relation to the location of the high-grade ore shoots at three mine levels.

### 4.5.1 At mine level 1200mRL.

At mine level 1200mRL, the foliation, shear and fault structures show six (6) high-grade ore shoot zones out of ten (10) that coincide with the intersection of interpreted NW (D4) structures and the NNE (D3) structures (**Figure 51**).

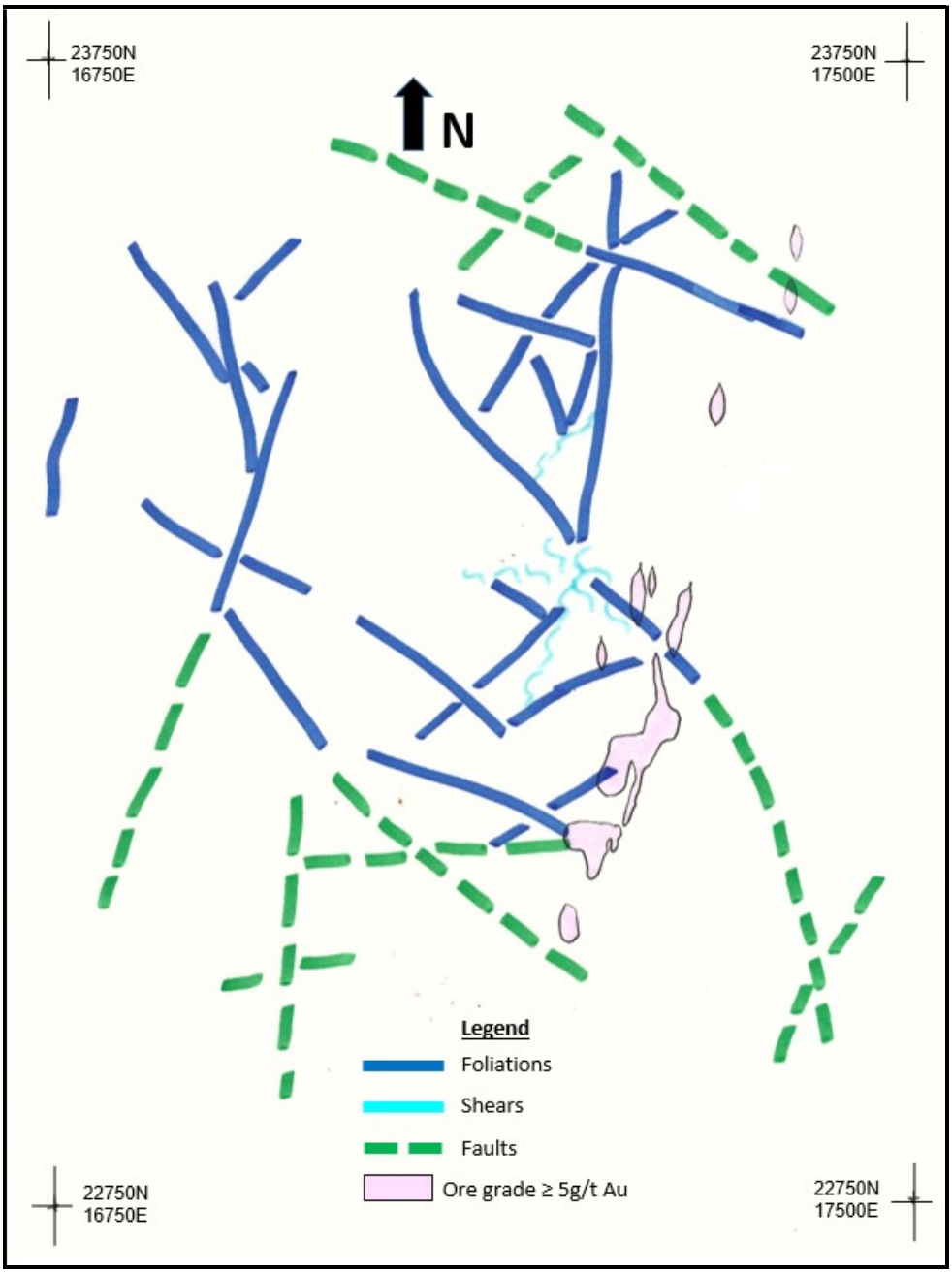


Figure 51. **High-grade ore equal or above 5g/t Au versus Foliation/Shears/Faults at mine level 1200mRL.**

At mine level 1200mRL, the vein structures interpretation are mainly offset from the mineralisation with only two (2) high-grade zones falling at structures intersection. However, when extrapolating these interpreted structures, they tend to have eight (8) high-grade ore shoot zones out of ten (10) coincide with the interpreted NW (D4) structures crossing the major NNE (D3) structures (**Figure 52**). This is explained by the fact that no structures were recorded in the highly mineralised zone, as at Syama, it is often completely broken.


Figure 52. **High-grade ore equal or above 5g/t Au versus Veins at mine level 1200mRL.**

### 4.5.2 At mine level 1100mRL

At mine level 1100mRL, the foliations, shears and faults structures show eight (8) high-grade ore shoot zones out of thirteen (13) that coincide with the intersection of interpreted NW (D4) structures and the major NNE (D3) structures (**Figure 53**).

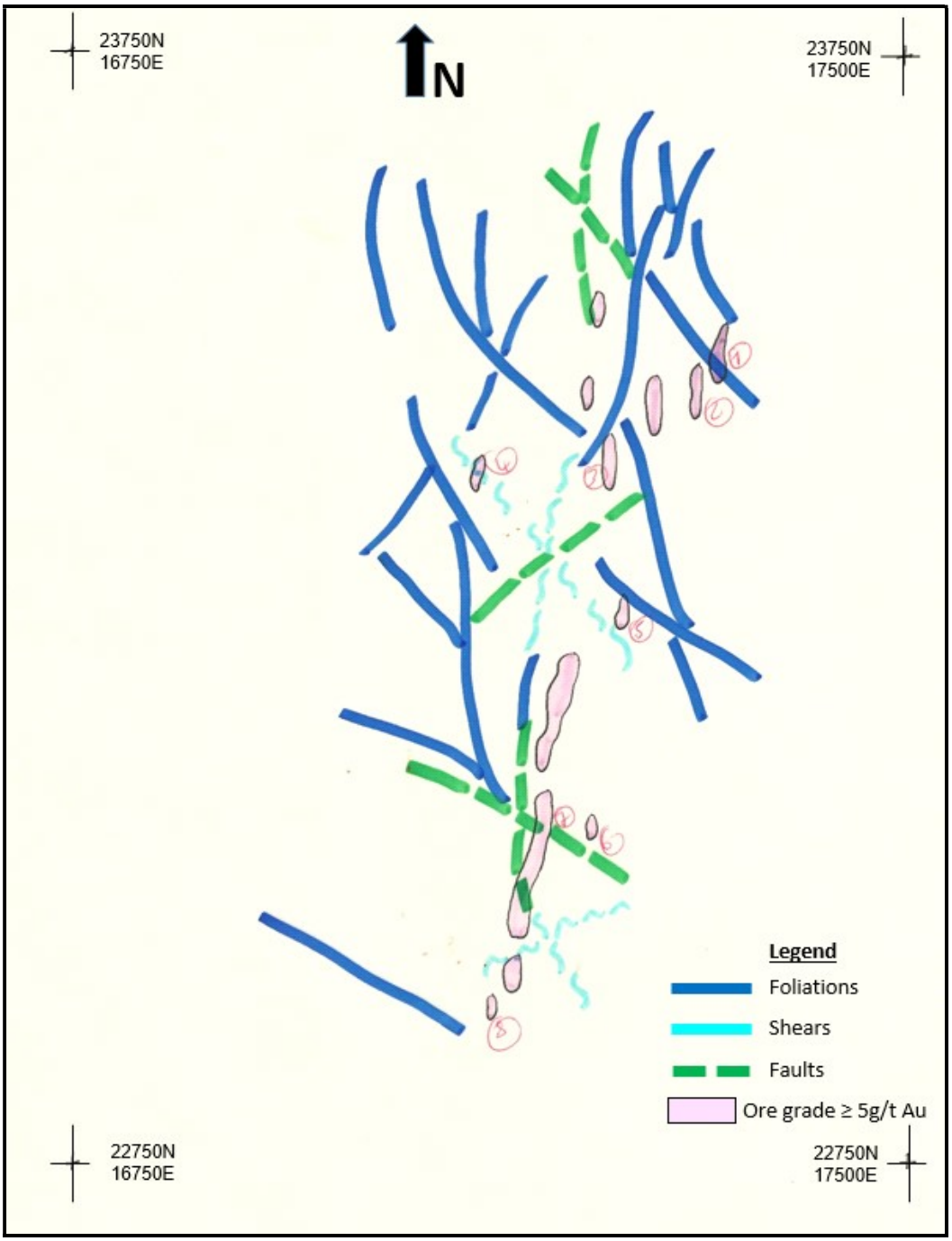


Figure 53. **High-grade ore equal or above 5g/t Au versus Foliation/Shears/Faults at mine level 1100mRL.**

At mine level 1100mRL, the veins structures show seven (7) of high-grade ore shoot zones out of thirteen (13) that coincide with the intersection of interpreted NW (D4) structures and the NNE (D3) structures (**Figure 54**).

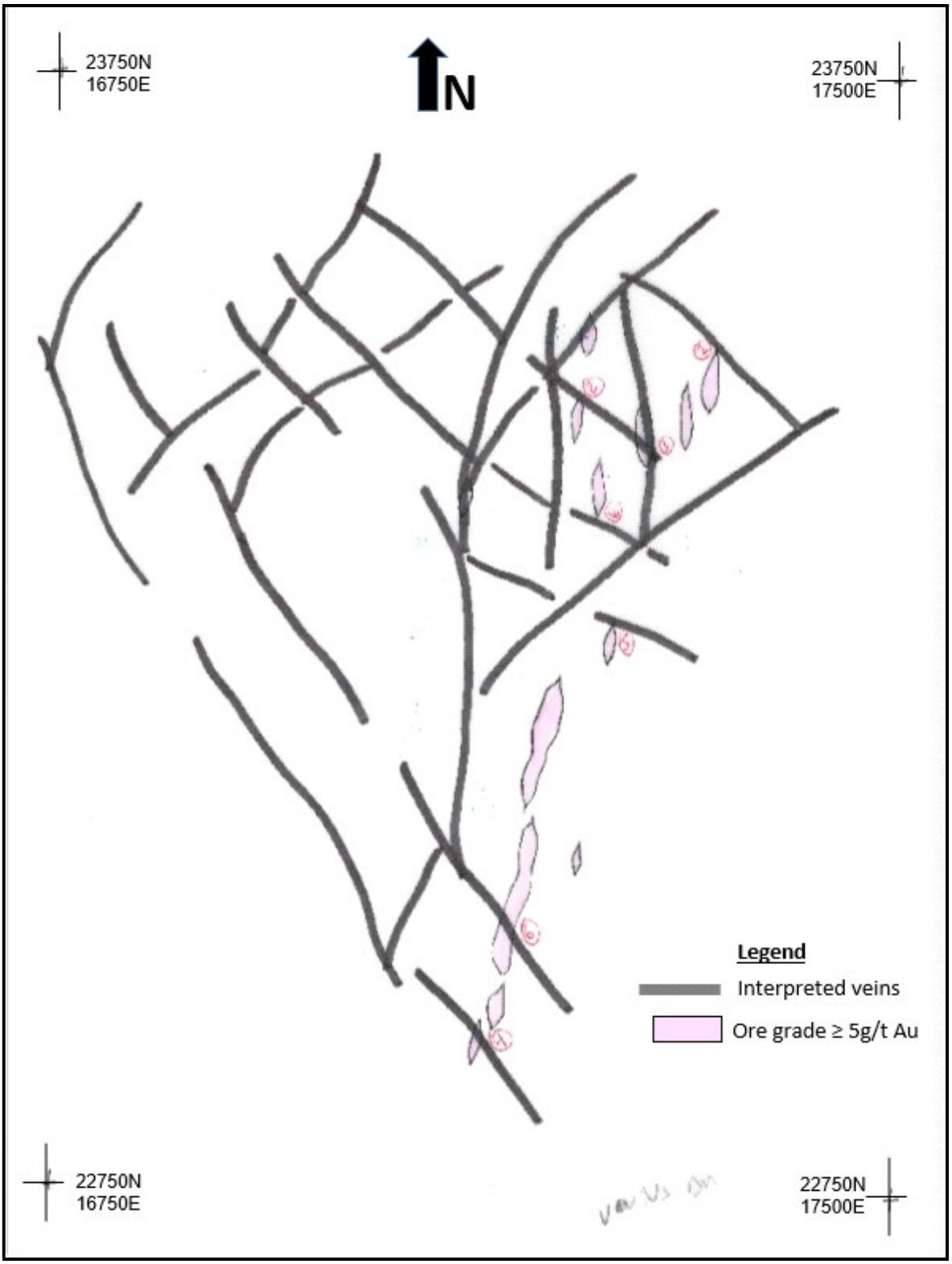


Figure 54. **High-grade ore equal or above 5g/t Au versus Veins at mine level 1100mRL.**

### 4.5.3 At mine level 1000mRL

At mine level 1000mRL, for the foliations, shears and faults structures, all the high-grade ore shoots coincide with the intersection of interpreted E-W (D5) structures and the major NNE (D3) structures (**Figure 55**). The NW interpreted structures do not fit in any high-grade mineralised envelop.

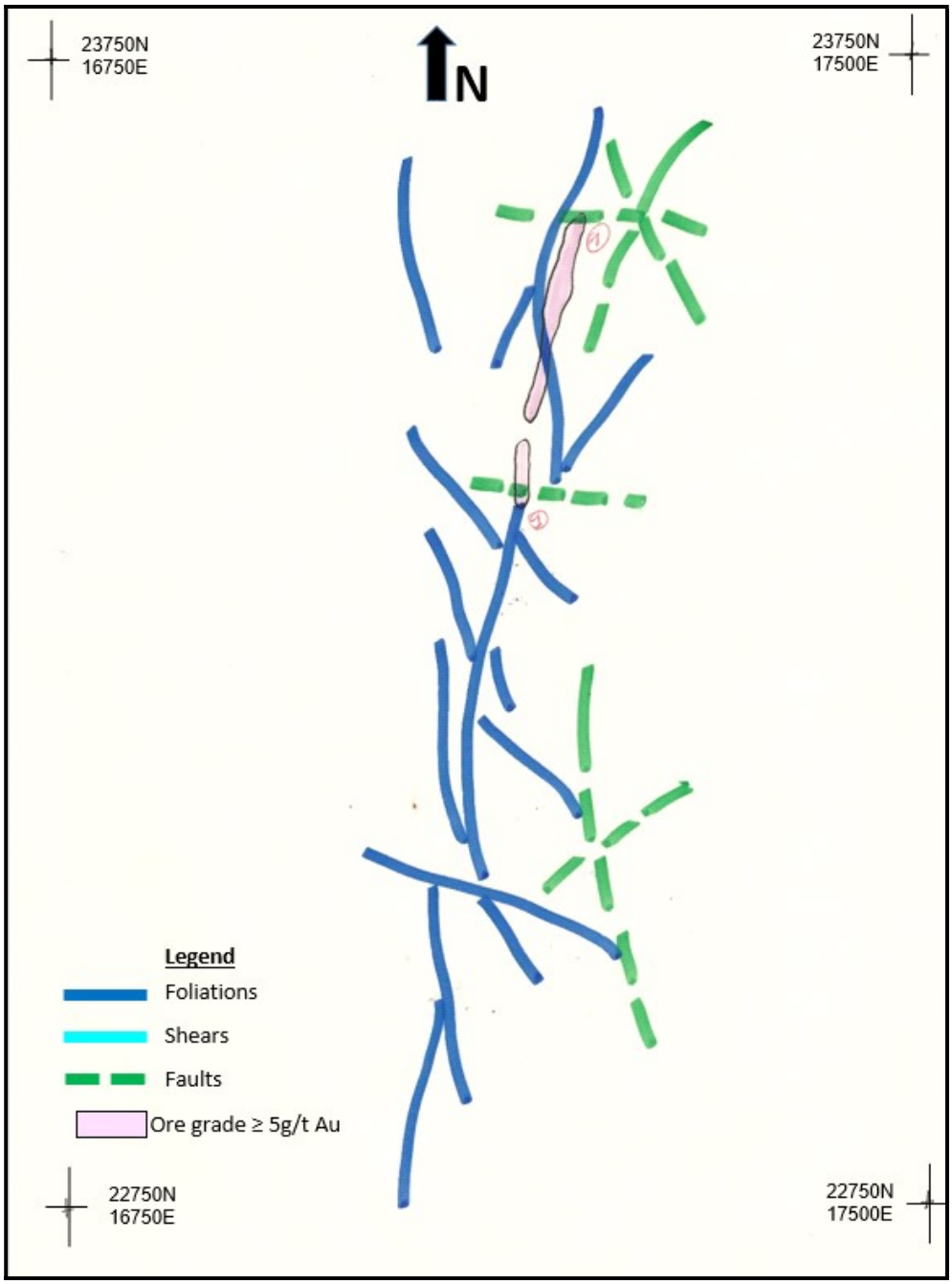


Figure 55. **High-grade ore equal or above 5g/t Au versus Foliation/Shears/Faults at mine level 1000mRL.**

At mine level 1000mRL, the veins structures show one (1) high-grade ore shoot zone out of two (2) that coincide with the intersection of interpreted NW (D4) structures and the major NNE (D3)structures (**Figure 56**).

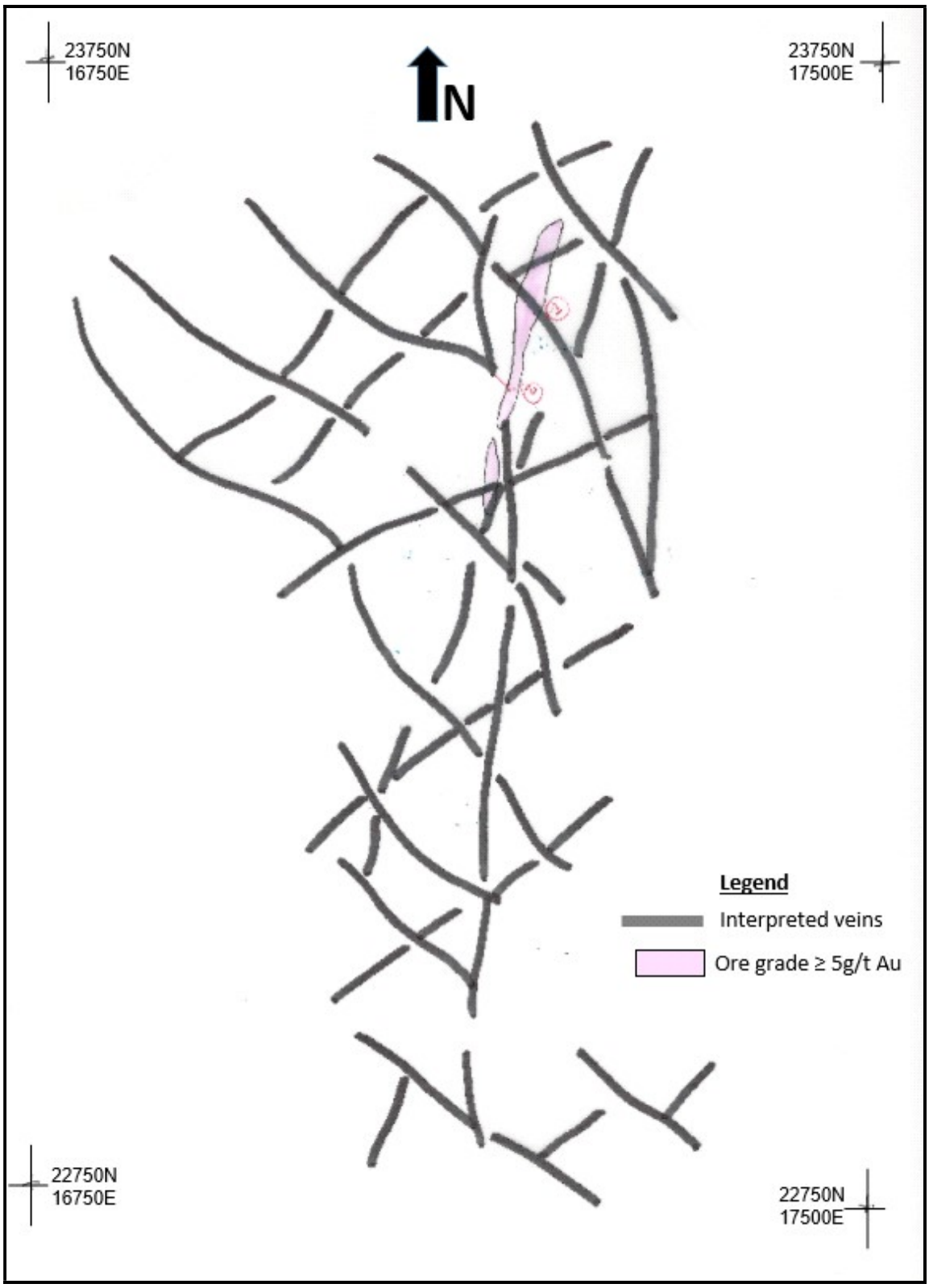


Figure 56. **High-grade ore equal or above 5g/t Au versus Veins at mine level 1000mRL.**

# Chapter 5. Discussion

The Syama gold deposit is a shear-zone hosted deposit type, grossly controlled by a NNE striking structural system. Deep drilling of the underground mineral resources and ore reserves, has intersected significant high grade-grade ore shoots that are believed to be located at the intersection of the dominant NNE striking structures and later, crosscutting NW structures. Understanding the relationship between the NNE and NW structures is seen as critical to effective drill targeting of high-grade shoots to increase underground resources and reserves at Syama.

The determination of relationships between high-grade ore shoots and NW structures in this study was conducted using two main types of structures; foliations, shears and faults, and veins. These structures were selected across the Syama orebody, plotted using Micromine and interpreted with tracing paper.

## 5.1 Foliation, shear and fault structures

The stereonet analysis of foliation, shear and fault structures exhibit variable orientations, but confirm a dominant NNE striking, W dipping trend (D3), crosscut by a later (D4) NW trend. The stereographic analysis of foliation, shear and fault orientation also highlights the dominant D3, NNE striking, W dipping trending structures, consistent with the overall Syama structural trend.

## 5.2 Quartz vein structures

Quartz vein interpretation showed highly variable orientations, which is consistent with the mineralisation located within intense stockwork or breccia zones that are the main focus for the high-grade gold mineralisation at Syama. The stereographic analysis of vein orientations again highlights the dominant D3, NNE striking, W dipping trending structures, consistent with the overall Syama structural trend. The vein structures also show some E-W structures that are late (D5) deformation event and are mainly barren of gold mineralisation.

## 5.3 Structural intersections and high-grade ore shoots

Structural analysis and interpretation of the foliations, shears and faults at the three levels through the Syama orebody indicate that some of the high gold grade shoots are located at the intersection of the dominant NNE structural trend and a secondary, later NW structural trend. This is also supported by structural analysis of veins associated with high-grade mineralisation. The later NW structures may have played a role in reactivating earlier NNE structures and allowed more hydrothermal fluids to flow and upgrade gold mineralisation at these intersections. These crosscutting structural zones often resulted in completely broken features, with high-grade mineralisation hosted in zones of brecciation and intense stockwork or sheeted vein sets.

The dominant NNE trend from stereographic plots is believed to be reflecting D3 deformation, with the NW trend related to the D4 deformation event. The E-W structures are related to the late D5 deformation event. Earlier workers, (Olson et al., 1992), believed the NW structures to be also D3, but there is significant evidence that the NW structures often offset the NNE set and are therefore later (McCuaig, 2004).

The actual measured structures are often outside of the orebody area, as the ore zone is usually highly broken, and it is impossible to measure any structural features. The interpretation of structures has therefore been in these cases extrapolated through the orebody area to be able to link them with the orebody. The Syama structural database is a large data set that has been collected by various geologists from the different companies over the life of the mine. The NW striking faults are subparallel to the drilling direction and subsequently some of these structures were not properly recorded. Therefore the findings of this study need to be applied with caution.

# Chapter 6. Conclusion

This study has investigated the hypothesis that high-grade ore shoots at Syama are focussed at the intersection zones of the major NNE and secondary NW structures.

The structural analysis and interpretation of the structures in this study has confirmed the location of high-grade ore shoots at the intersection of NNE structures that are attributed to the D3 deformation event, with the NW structures attributed to the D4 deformation event.

The results of this study suggest the timing of the NW structures contradicts an early study by Olson et al., 1992, who stated that the NW structures were coeval with the D3 NNE structures, but is consistent with later views that the NW structures are later, corresponding to the D4 event (McCuaig, 2004), and have played a role in reactivating the D3 NNE structures and upgrading gold mineralisation.

In conclusion, the interpretation of the structures against the high-grade gold shoot zones at Syama show that the NNE faults are D3 and co-genetic with the main mineralising event. These structures were reactivated during D4 when the NW structures were active. The NW structures have allowed for further mineralising fluids to flow through the reactivated D3 faults, upgrading the gold grade at their intersections. The E-W structures are believed to be late and related to D5.

Ongoing exploration should target the intersections of the NNE and NW structures, both at Syama and elsewhere in the belt, as potential sites of high-grade ore to increase resources and reserves.

# *References*


Allibone, A., McCuaig, C., Harris, D., Etheridge, M.A., Munroe, S., and Byrne, D., 2002, Structural controls on gold mineralisation at the Ashanti gold deposit, Obuasi, Ghana: *Economic Geology,* Special Publication 9, p. 65–93.

Allmendinger, R. W., Cardozo, N. C., and Fisher, D., 2013, Structural Geology Algorithms: Vectors & Tensors: Cambridge, England, Cambridge University Press, 289 p.

Ballo, I., Hein, K.A.A., Guindo, B., Sanogo, L., Ouologuem, Y., Daou, G., and Traore, A., 2016, The Syama and Tabakoroni goldfields, Mali: *Ore Geology Reviews*, v. 78, p. 578–585.

Bentley, P.N., Venter, L., Moolman, R., Henry, G., Heidstra, P., and Reading, D., 2000. Geological review, gold target prioritisation and recommendations for future exploration work. Syama Exploration Permits Randgold Resources Ltd. internal report, unpublished.

Beeson, J., Kas De Luca., Ian Neilson., Matt Noble., John Standing., Scott Halley., and Doug Mason., 2007. The geological campaign, Syama, Mali. Confidential Report to Resolute Mining Limited, March 2007. 99 pp.

Béziat, D., Siebenaller, L., Salvi, S., and Chevalier, P., 2016, A weathered skarn-type mineralisation in Ivory Coast: The Ity gold deposit: *Ore Geology Reviews*, v. 78, p. 724–730.

Cardozo, N., and Allmendinger, R. W., 2013, Spherical projections with OSXStereonet: Computers & Geosciences, v. 51, no. 0, p. 193-205.

Cox, S. F., Knackstedt, M.A., and Brrown, J., 2001. Principles of Structural Control on Permeability and Fluid Flow in Hydrothermal Systems. *Economic Geology*, v. 14, p. 1-24.

Craig Johnson., Ben McCormack., Ian Neilson., and Jon Standing., 2014. Syama North Geological Campaign 2014. 87pp.

Denis Fougerouse., Steven Micklethwaite., Stanislav Ulrich., John Miller., Bélinda Godel., David T. Adams., and McCuaig. T. Campbell., 2017. Evidence for two stages of mineralisation in the West Africa's largest Gold deposit: Obuassi, Ghana. *Economic Geology*, v. 112, p. 3-22.

Feybesse, J.L., Billa, M., Guerrot, C., Duguey, E., Lescuyer, J.L., Milesi, J.-P., and Bouchot, V., 2006, The Paleoproterozoic Ghanaian province: Geodynamic model and ore controls, including regional stress modeling: *Precambrian Research*, v. 149, p. 149–196.

Goldfarb, R.J., Baker T., Dube B., Groves D.I., Hart C.J.R., Gosselin P., 2005, Distribution, Character, and Genesis of Gold Deposits in Metamorphic Terranes. *Economic Geology,* 100th Anniversary Volume, 407-450.

Goldfarb, R.J., Anne-Sylvie André-Mayer., Simon M. Jowitt., and Gavin M. Mudd., 2017. West Africa, The world's Premier Paleoproterozoic gold Province. *Economic Geology*, v. 112, p. 123-143.

Hanssen, E., Diakite, K., Mullins, M., 1997. The Syama District exploration history, geology setting, and gold mineralisation. Unpublished Report to BHP, 1997.

Harbidge, P., 2001. Syama closure geology report. Unpublished report to Randgold Resources, 17-06-01, 26p.

Jessel, M.W., Begg, C. G., and Miller, S. M., 2016. The geophysical signatures of the West African Craton. *Precambrian Research*, v. 217, p. 3–24.

Kušnir, I., 1999. Gold in Mali. Acta Montan. Slovaca Ročnik 4, p.311–318.

Lawrence, D.M., Treloar, P.J., Rankin, A.H., Harbidge, P., and Holliday, J., 2013a, The geology and mineralogy of the Loulo mining district, Mali, West Africa: Evidence for two distinct styles of orogenic gold mineralisation: *Economic Geology*, v. 108, p. 199–227.

Lawrence, D.M., Treloar, P.J., Rankin, A.H., Boyce, A., and Harbidge, P., 2013b, A fluid inclusion and stable isotope study at the Loulo mining district, Mali, West Africa: Implications for multifluid sources in the generation of orogenic gold deposits: *Economic Geology*, v. 108, p. 229–257.

Lawrence, D.M., Lambert-Smith, J.S., and Treloar, P.J., 2016, A review of gold mineralisation in Mali, in Bouabdellah, M., and Slack, J.F., eds., Mineral deposits of North Africa: *Mineral Resource Reviews*, Switzerland, Springer International Publishing, p. 327–351.

Lawrence, D.M., A.H. Allibone., Chang.Z., Meffre.S., Lambert-Smith J.S., and. Treloar.P.J., 2017. The Tongon Au Deposit, Northern Côte d'Ivoire: An Example of Paleoproterozoic Au Skarn Mineralisation. *Economic Geology*, v. 112, pp. 1571–1593.

Lebrun. E., John Miller., Nicolas Thébaud., Stanislav Ulrich., and McCuaig .T. Campbell., 2017. Structural Controls on an Orogenic Gold Systems, the World-Class Siguiri Gold District, Siguiri Basin, West Africa. *Economic Geology*, v. 112, p. 73–98.

Le Mignot Elodie., Luc Siebenaller., Didier Béziat., Anne-Sylvie André-Mayer., Laurie Reisberg., Stefano Salvi., Germán Velasquez., Catherine Zimmermann., Athanase Naré., and Guy Francesch., 2017. The Paleoproterozoic Copper-Gold Deposits of the Gaoua District, Burkina Faso: Superposition of Orogenic Gold on a Porphyry Copper Occurrence?. *Economic Geology*, v. 112, pp. 99–122

Le Mignot, E., Reisberg, L., André-Mayer, A.-S., Bourassa, Y., Fontaine, A., and Miller, J., 2017b, Re-Os geochronological evidence for multiple Paleoproterozoic gold events at the scale of the West African craton: *Economic Geology*, v. 112, p. 145–168.

Milesi, J.P., Ledru, P., Feybesse, J.L., Dommanget, A., and Marcoux, E., 1992, Early Proterozoic ore deposits and tectonics of the Birimian orogenic belt, West Africa: *Precambrian Research*, v. 58, p. 305–344.

McCuaig, T. C., 2004. Structural Review of the Syama Gold Deposit, Mali. Unpublished Report to Resolute Mining, March, 2004.

McCuaig, T. C., 2005. Comments on controls on mineralisation in the Syama belt, Mali. Unpublished report prepared for Resolute Mining by SRK Consulting, March 2005. SRK Project Number RES001, 30 pp.

Olsen, S.F., Diakite, K., Ott, L., Guindo, A., Ford, C.R.B., Winer, N., Hanssen, E., Bradley, R., Pohl, D., 1992. Regional setting, structure, and descriptive geology of the Middle Proterozoic Syama gold deposit, Mali, West Africa. *Economic Geology*. v. 87, 310–331.

Otto R., Richard Fry., and Earl. A., 2014. Syama underground pre-feasibility study. Unpublished Report to Resolute Mining 2014. 250pp.

Peucat, J.-J., Capdevila, R., Drareni, A., Mahdjoub, Y., and Kahoui, M., 2005, The Eglab massif in the West African Craton (Algeria), an original segment of the Eburnean orogenic belt: petrology, geochemistry and geochronology: *Precambrian Research*, v. 136, p. 309–352.

Robert and Poulsen (2001). Vein Formation and Deformation in Greenstone Gold Deposits. *Economic Geology*. v. 14, p. 111–155.

Standing, J., 2005. Geological and structural mapping in the Syama–Finkolo prospect area, Mali, West Africa. Confidential Report by Jigsaw Geoscience Pty Ltd to Resolute Mining Limited, April 2005 (29 pp.).

Standing, J., 2007. Report and recommendations from the geological campaign — Syama-Mali. Confidential Report to Resolute Mining Limited by Jigsaw Geoscience Pty Ltd, March 2007 (99 pp.).

Traoré Yollande Dasso., Luc Siebenaller., Stefano Salvi., Didier Béziat., and Mamadou Lamine Bouaré., 2016. Progressive Gold Mineralisation along the Syama corridor, southern Mali (West Africa), *Ore Geology Reviews*, v. 78, p. 586–598.

Treloar, P.J., Lawrence, D.M., Senghor, D., Boyce, A., and Harbidge, P., 2015, The Massawa gold deposit, eastern Senegal, West Africa: An orogenic gold deposit sourced from magmatically derived fluids? *Geological Society London* Special Publication 393, p. 135–160.

West African Exploration Initiative (2016). stage3.

Perseus Mining Limited (2018). Annual report 2018. Retrieved from **http://www.perseusmining.com**.

Resolute Mining Limited (2018). Quarterly Activities Report 2018. Retrieved from **http://www.rml.com.au**.

# *Appendices*

***Appendix I: Structures codes and legend using in Micromine for plotting***

| Structures_Codes | Description | Structure_colour |
|---|---|---|
| F0 | Foliation (undif.) | FO |
| F1 | Weak Foliation | F1 |
| F2 | Moderate Foliation | F2 |
| F3 | Strong Foliation | F3 |
| FAP | Foliation - Axial Plane | FAP |
| MYL | Mylonite | MYL |
| SHZ | Shear Zone | SHZ |
| FLT | Fault | FLT |
| VMX | Vein - Massive | VMX |
| VEX | Vein - Extensional | VEX |
| VPTG | Vein - Ptygmatic | VPTG |
| VLM | Vein - Laminated | VLM |
| VNT | Vein (undif.) | VN |
| VNT | Veinlet | VNT |
| VSW | Vein - Stockwork | VSW |
| BX | Breccia (undif.) | BX |
| CN | Contact | CN |
| FR | Fracture | FR |
| FR1 | Weak Fracture Intensity | FR1 |
| FR2 | Moderate Fracture Intensity | FR2 |
| FR3 | High Fracture Intensity | FR3 |
| JN | Jointing | JN |
| J1 | Weak Joint Intensity | J1 |
| J2 | Moderate Joint Intensity | J2 |
| J3 | High Joint Intensity | J3 |
| FCL | Cleavage | FCL |
| LM | Lineation - Mineral Elongation | LM |
| LS | Lineation - Striation | LS |
| S0 | Bedding | SO |
| S1 | Bedding - Lamination | S1 |
| SF | Bedding - Thin | SF |
| SGD | Graded Bedding | SGD |
| NR | Not Recorded | NR |

*Appendix II: Foliations/Shears/Faults at level 1200mRL*

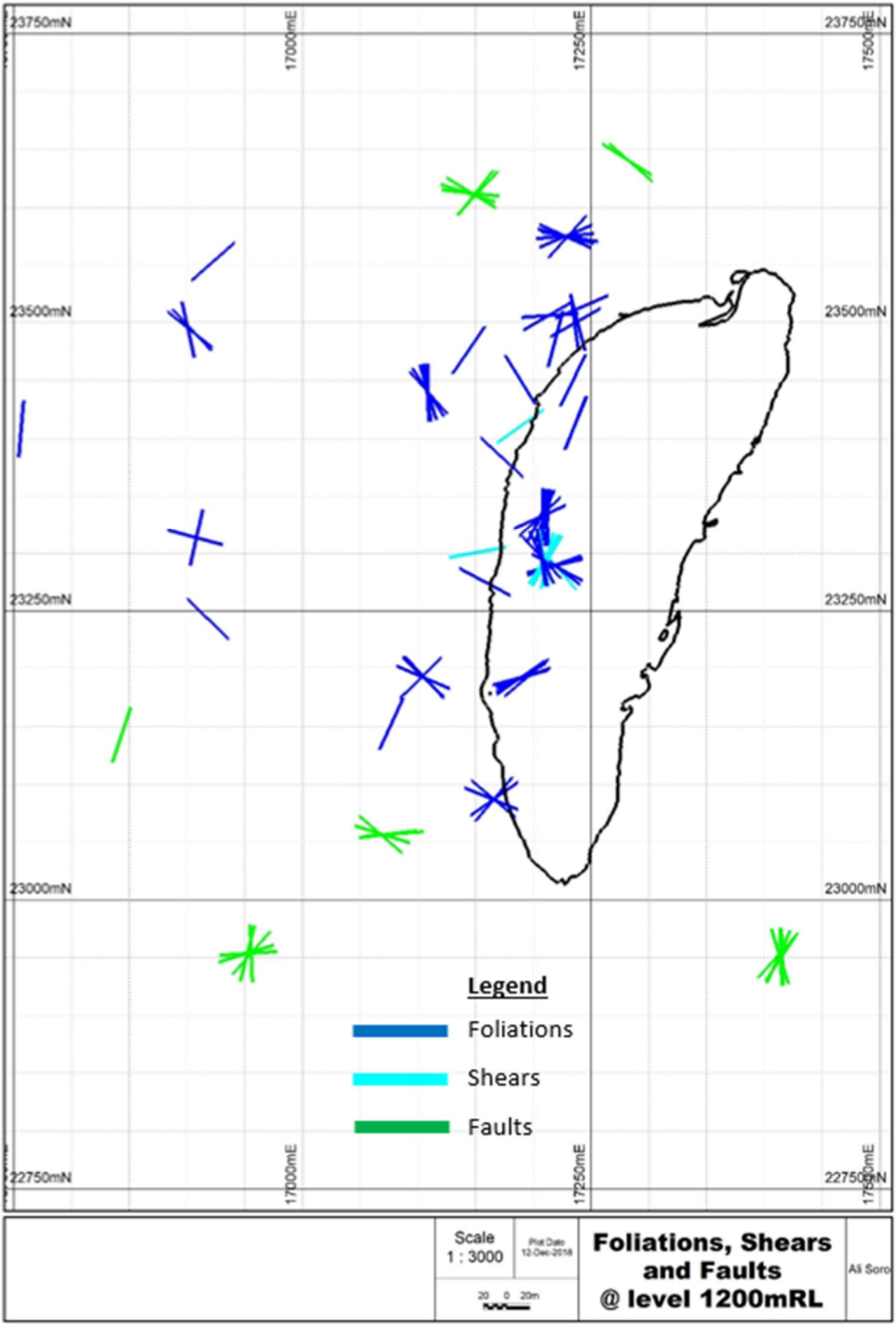

*Appendix III: Foliations/Shears/Faults at level 1100mRL*

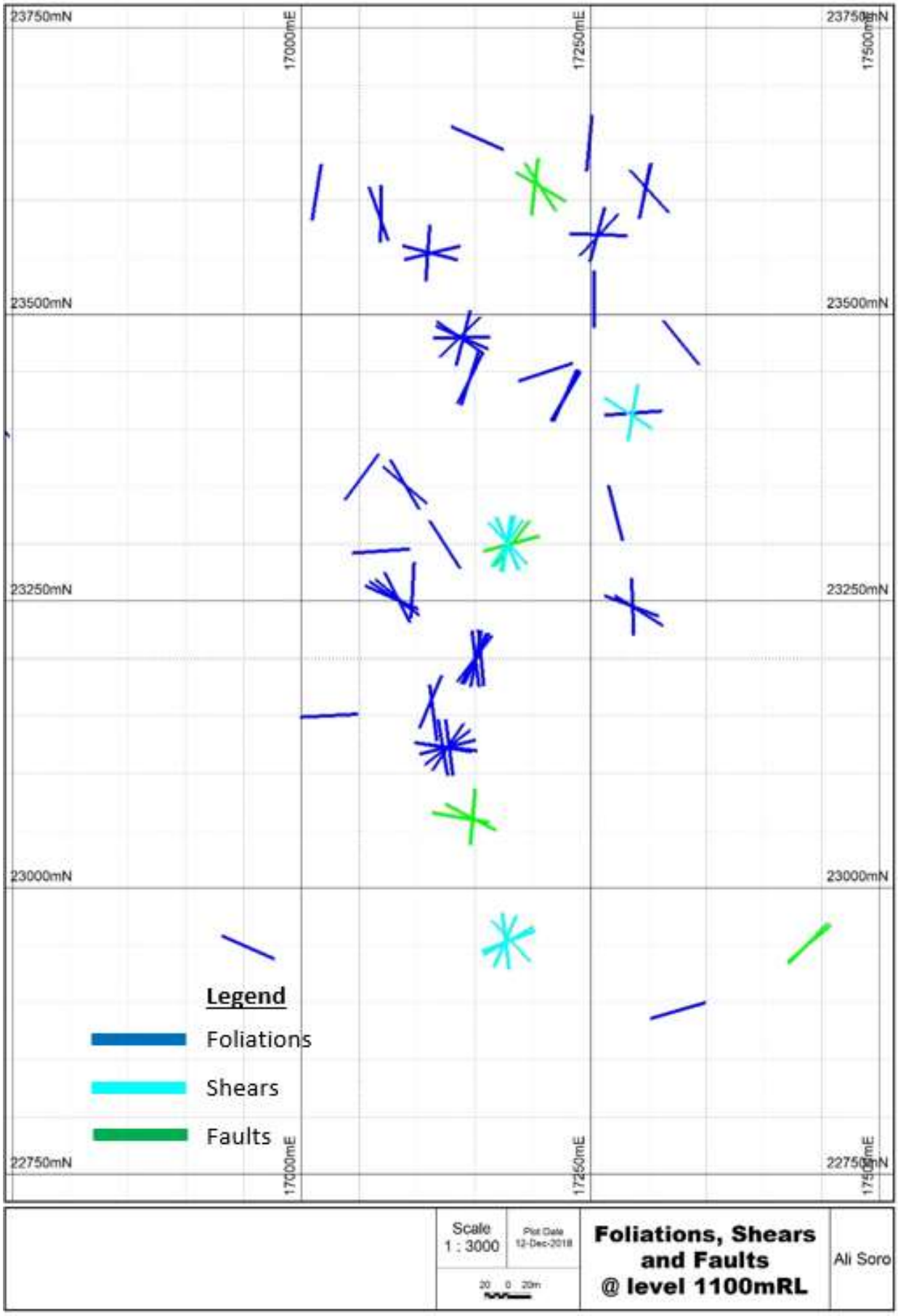

*Appendix IV: Foliations/Shears/Faults at level 1000mRL*

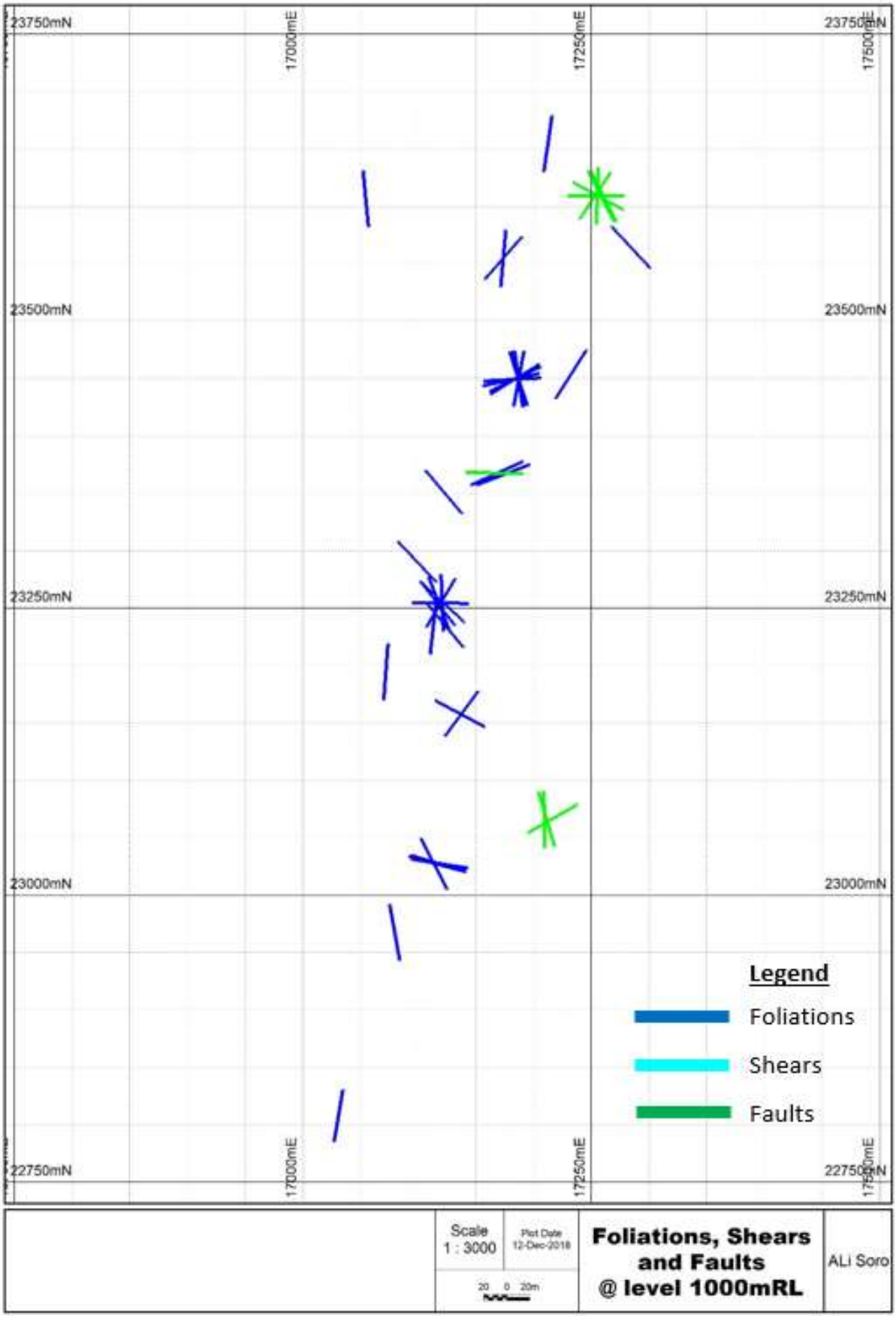

*Appendix V: Vein at level 1200mRL*

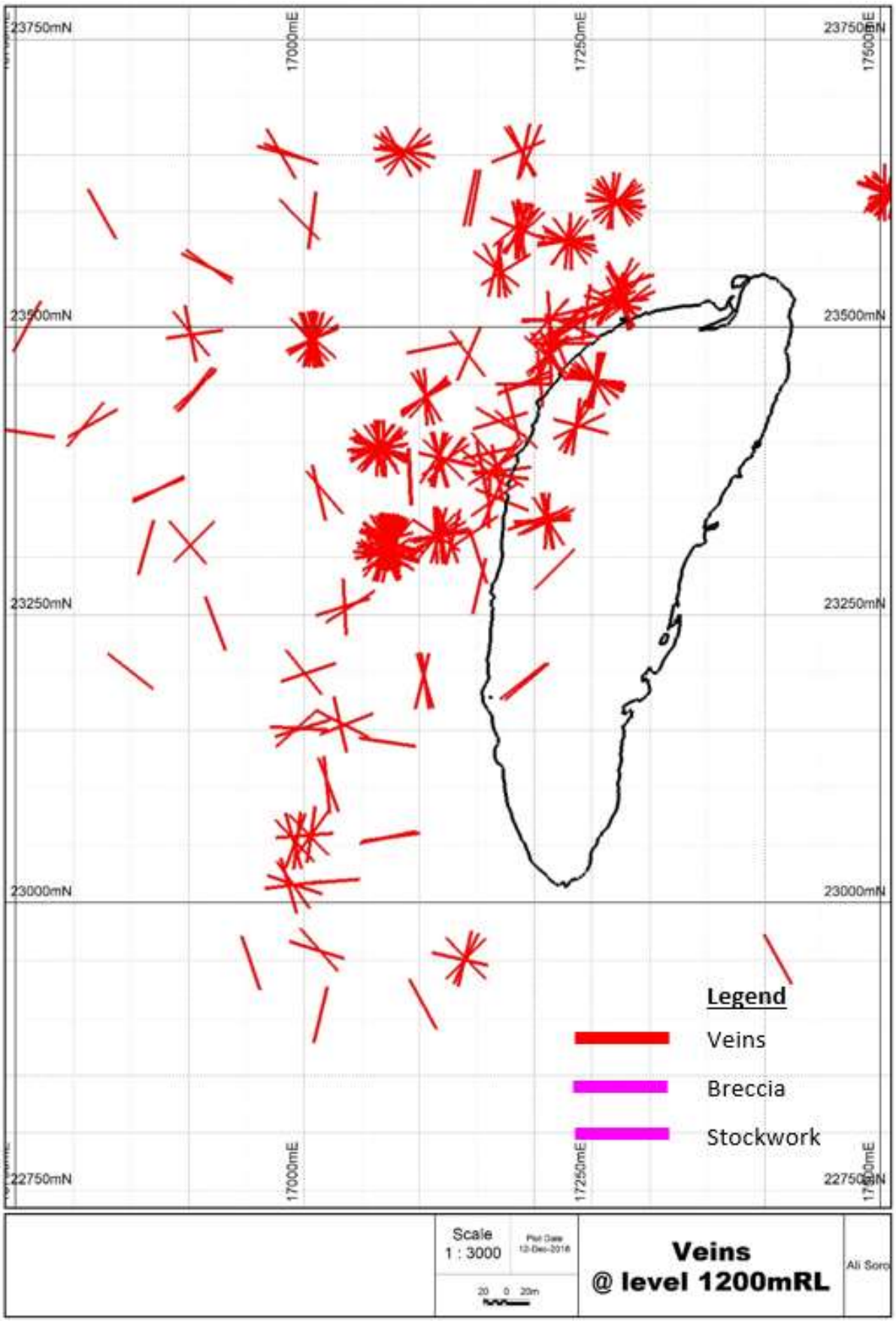

*Appendix VI: Veins at level 1100mRL*

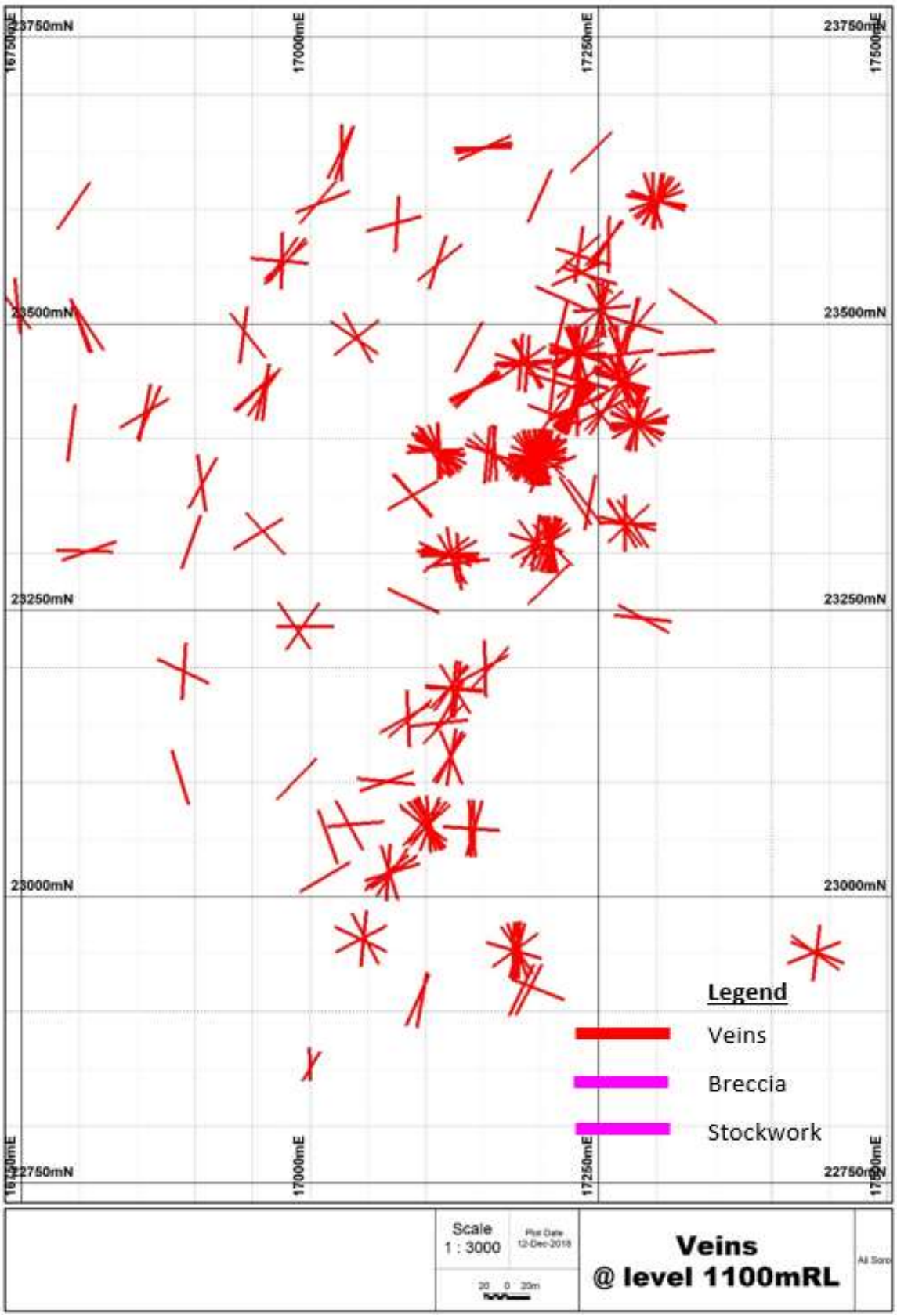

*Appendix VII: Veins at level 1000mRL*

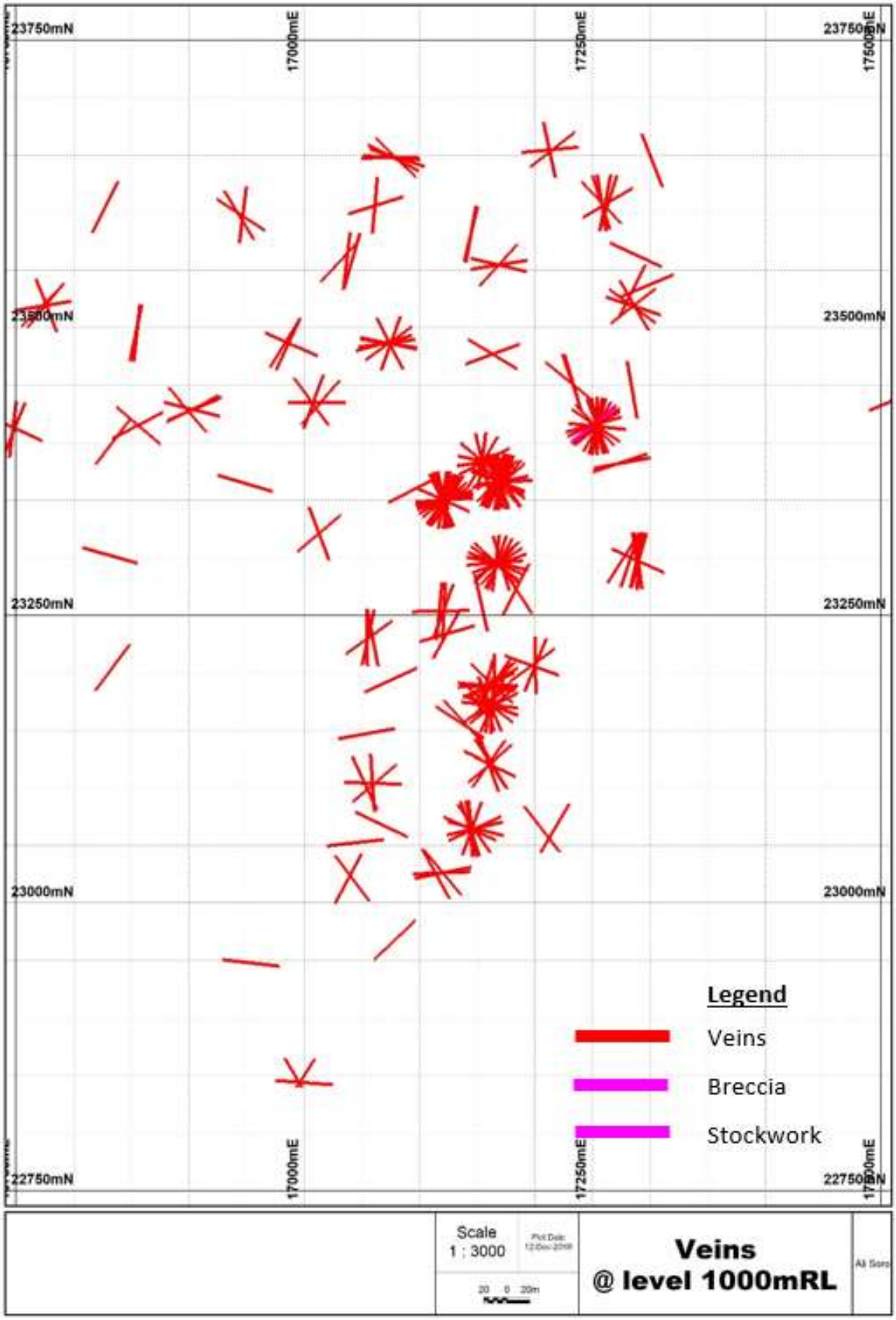

*Appendix VIII: Joints/Contacts/Fractures at level 1200mRL*

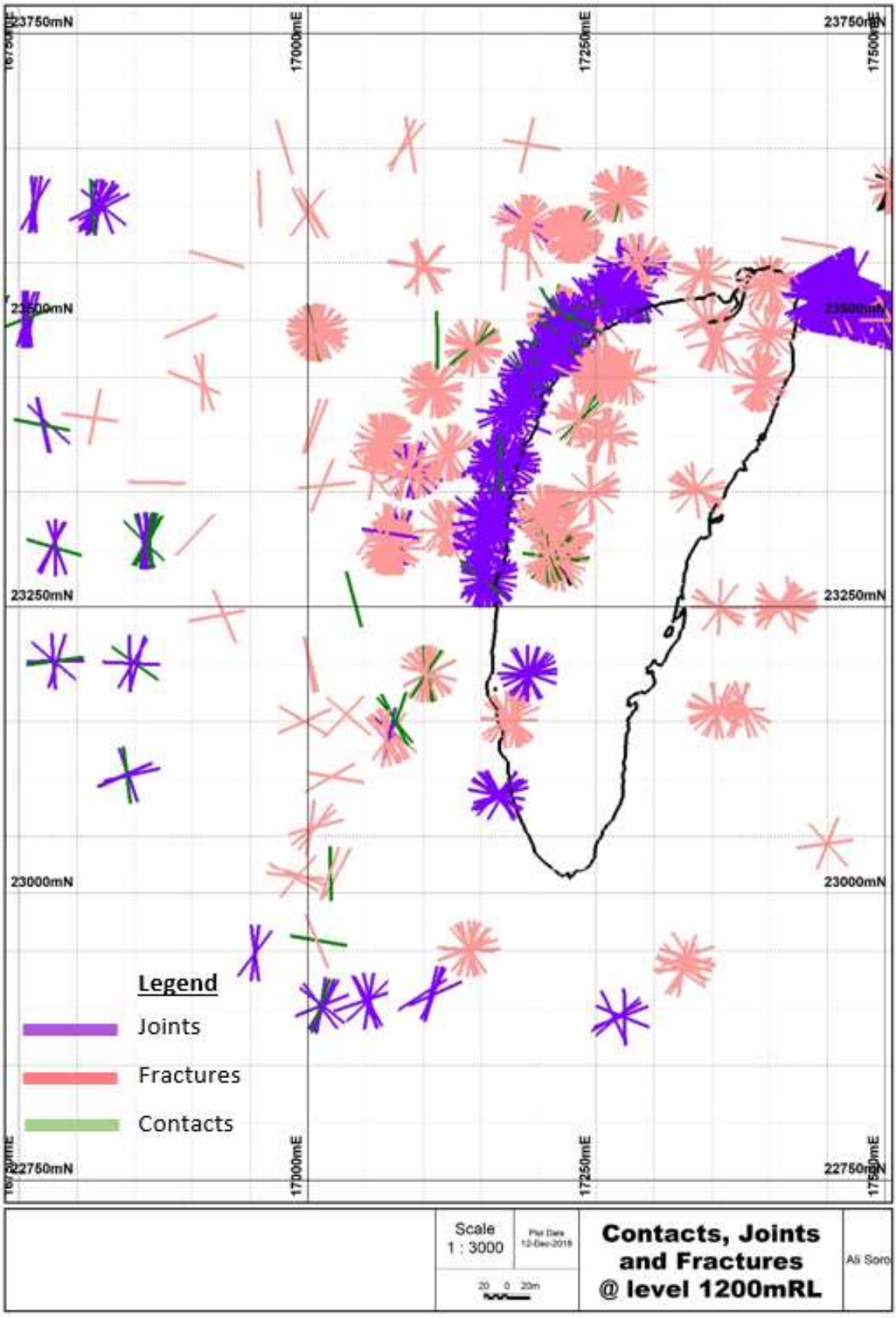

*Appendix IX: Joints/Contacts/Fractures at level 1100mRL*

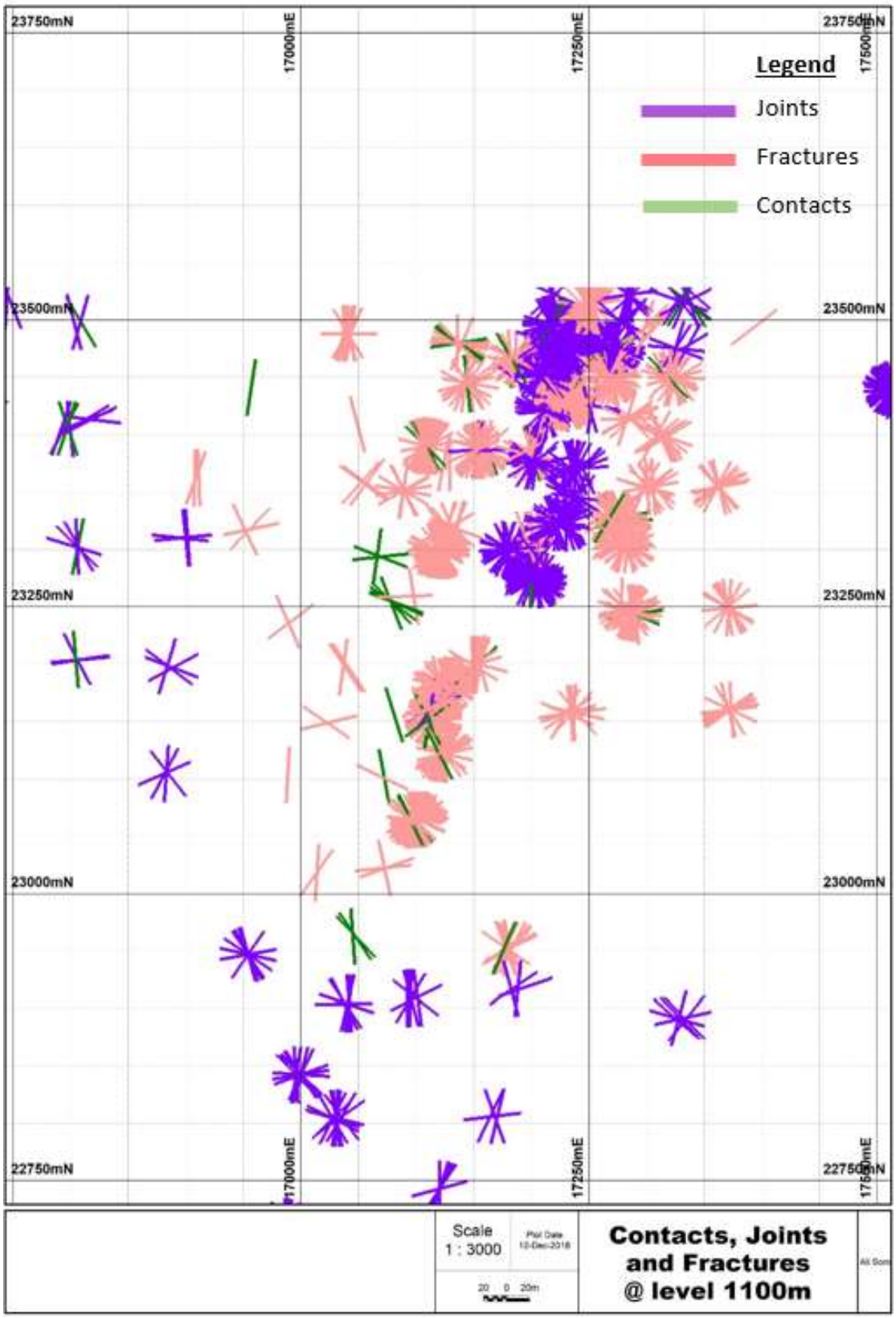

*Appendix X: Joints/Contacts/Fractures at level 1000mRL*

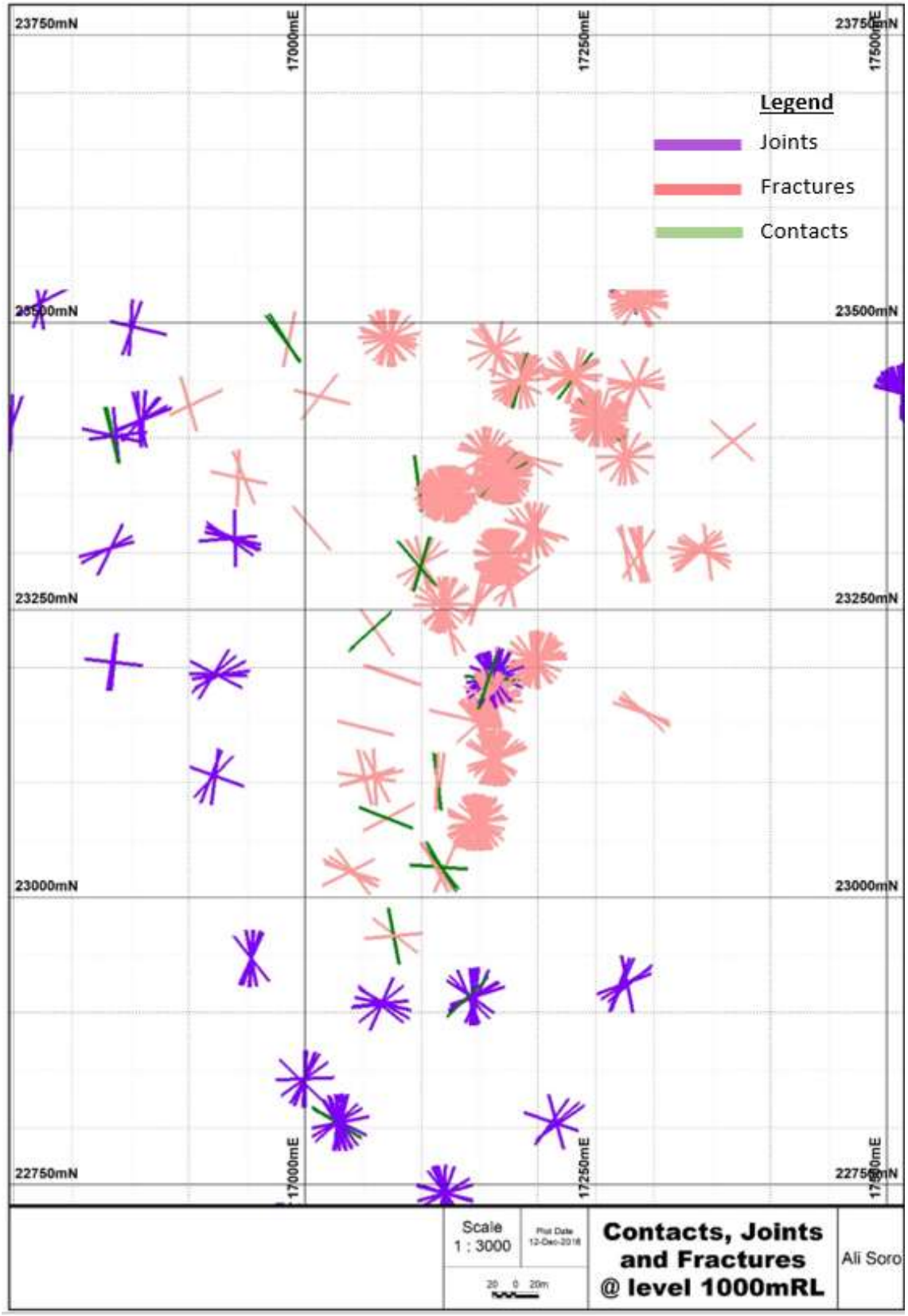

*Appendix XI: Block Model at level 1200mRL*

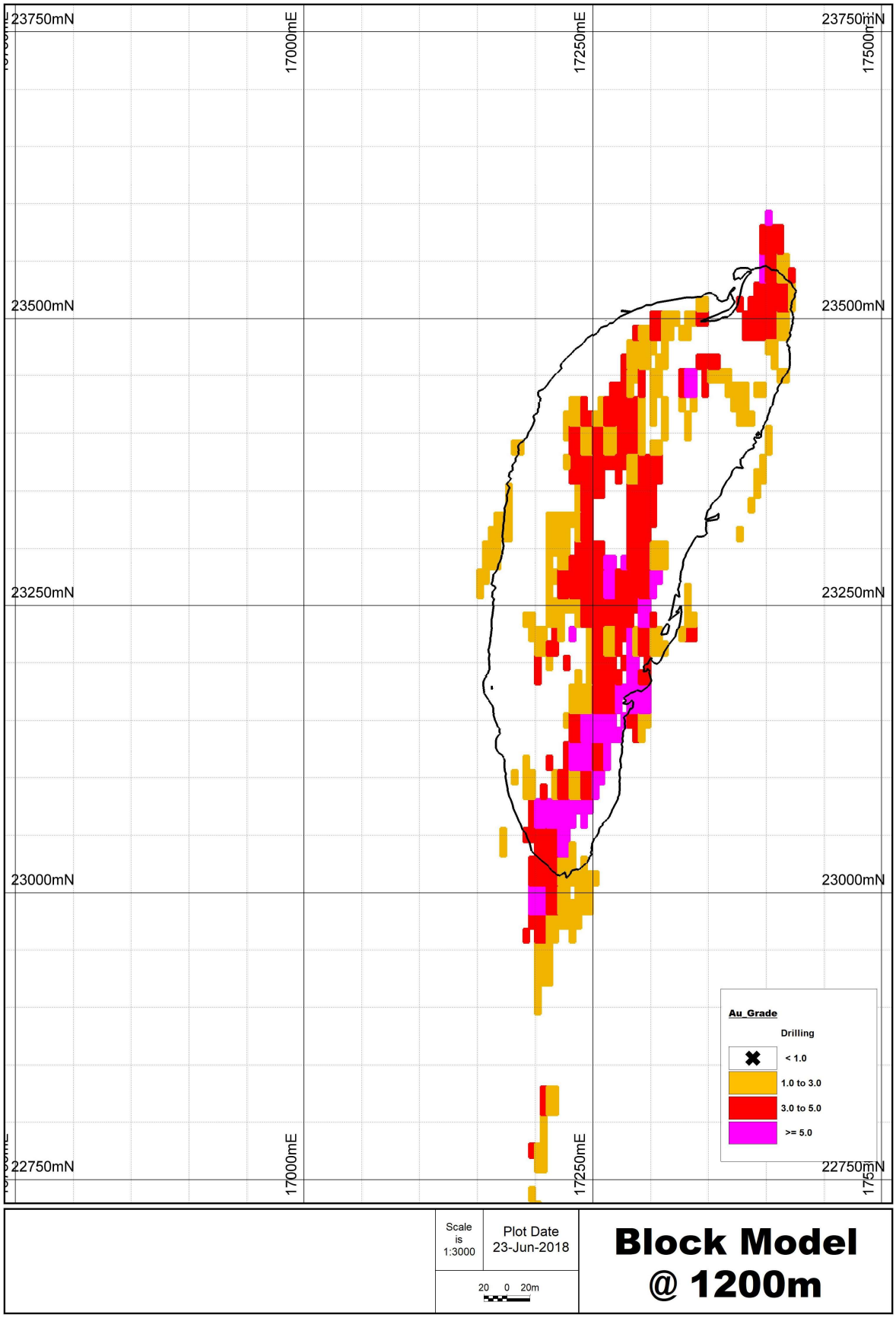

*Appendix XII: Block Model at level 1100mRL*

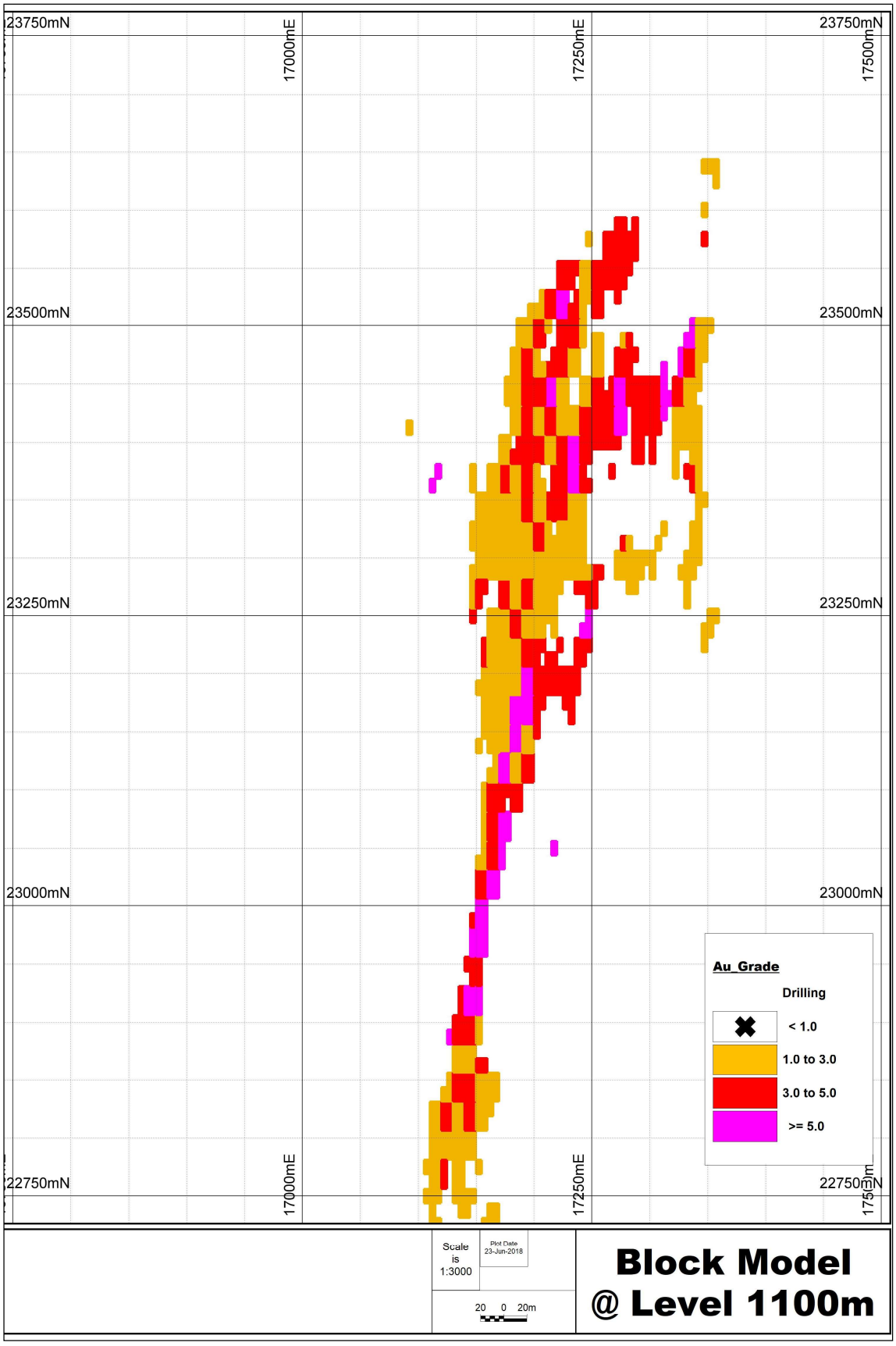

*Appendix XIII: Block Model at level 1000mRL*